SPATIAL DISTRIBUTION OF POROSITY IN EOCENE CARBONATE RESERVOIR UPPER INDUS BASIN PAKISTAN

BY

IHTERAM UL HAQ

M.PHIL GEOPHYSICS

(2020-2022)

DEPARTMENT OF EARTH SCIENCES

QUAID-I-AZAM UNIVERSITY ISLAMABAD, PAKISTAN

CERTIFICATE

It is certified that ***Mr. Ihteram Ul Haq*** **s/o** ***Dr. Hussain Ahmad*** enrolled under registration number 02112013011, carried out the research work in this dissertation under my supervision and accepted in its present form by the department of Earth Sciences, Quaid-i-Azam university Islamabad, as satisfying the requirement for the award of M.Phil degree in Geophysics.

RECOMMENDED BY

Dr. Aamir Ali _____

Associate professor / Supervisor

External examiner _____

Dr. Aamir Ali _____

Chairman

DEPARTMENT OF EARTH SCIENCE

QUAID-I-AZAM UNIVERSITY

ISLAMABAD

DEDICATION

This thesis work is dedicated to my father, Dr. Hussain Ahmad, who has been a constant source of support and encouragement during the challenges of this research. This work is also dedicated to my deceased mother, who have always loved me unconditionally and whose good examples have taught me to work hard for the things that I aspire to achieve.

Acknowledgement

I would like to acknowledge Higher Education Commission (HEC) for providing me scholarship for a financial support during my M.Phil studies. It has been an honor to be the recipient of the indigenous HEC Fata and Balochistan Scholarship and I am indebted to the donors in providing me complete academic freedom in this research.

The completion of this research could not have been possible without the due diligence and expertise of **Dr. Aamir Ali**, my beloved thesis supervisor. I express my sincere appreciation to my supervisor for his guidance in the preparation of this thesis and his assistance in any way that I may have asked.

A debt of gratitude is also owed to my friend Mr. Yawar Amin (Phd student) for his continuous help throughout my research work.

I also acknowledged the efforts and prayer of my father Dr. Hussain Ahmad for his support and sacrifices throughout the study.

IHTERAM UL HAQ

2020-2022

List of Figures

List of Tables

ABSTRACT

Porosity is the most important factor in evaluating reservoirs. Porosity extraction from seismic data is an extremely difficult task that is subject to ambiguity for a variety of reasons. For the extraction of porosity from seismic data, seismic inversion is used. The main theme of this research project is to show the spatial distribution of total and effective porosity at the reservoir level and also to compare the results of Model-based and Sparse-spike inversion. Further aim of evaluating the reservoir porosity used in this dissertation is the seismic attributes. The amplitude, shape, and position of a seismic waveform are commonly described by seismic attributes. The attributes considered in this dissertation are limited to fracture identification, orientation, and intensity of the fracture at reservoir level.

In this research, 3D seismic data were firstly used to mark horizon with the help of synthetic seismogram then time and depth contour map of the Chorgali and Sakessar formation were generated which confirm that time and depth is increasing towards NW and decreasing towards SW. Well log data of Balkassar OXY-1 well was used to calculate porosities and other reservoir properties of the Chorgali and Sakessar formation of Balkassar area, Pakistan's Upper Indus basin. No zone for Hydrocarbon accumulation is present in the Chorgali and Sakessar formation, only a small zone of 3m between 2424 to 2427 were marked at Chorgali level containing 44% hydrocarbon and 56% water saturation with a total porosity of 27% and effective porosity of 25%.

To examine the fracture density and orientation as well as the hydrocarbon saturation, the fracture attributes were applied to a Chorgali and Sakessar level. According to the attribute results, there is a very little fracture density at the Chorgali and Sakessar levels, where the OXY-1 well is drilled, and there is a considerable density of fractures at the Chorgali level to the South-East of the OXY-1 well.

The well log data and the interpreted horizon were then used in Model-based and Sparse-spike inversion to better visualize the seismic data in the form of acoustic impedance. Acoustic impedances were very high at the location of the well OXY-1 but adjacent areas to the south west on the same inline 90 but cross line 266 shows from the result of both Model-based and Sparse-spike inversion that it has a very low impedance. however, when compared the results of both method, Model-based were more pronounced than the result of the Sparse-spike inversion.

A geostatistical method was applied to extract the total and effective porosity from the acoustic impedance derived from both the Model-based and Sparse-spike inversion. After this slices of

porosities were created to check the spatial distribution of porosities at Chorgali and Sakessar level. This spatial distribution of porosity also suggested that that there is very low porosity zone at both Chorgali and Sakessar level where the OXY-1 well is drilled the high porosity zone is exactly to the SW of the well Balkassar OXY-1 on the same inline 90 but cross line 266 at Chorgali level. Low acoustic impedance models were constructed using well-log data. The use of well-log data allows for the calibration of reservoir porosity with inverted acoustic impedance. The spatial porosity distribution within the Chorgali and Sakessar formation is accurately estimated by the results of Model-based inversion and Sparse-spike inversion. Following post stack inversion, the total and effective porosity at Chorgali level is 11% and 9%, compared to 4% and 2% at Sakessar level respectively. Porosity values predicted from the seismic data via Probabilistic Neural network were in good agreement with the porosity derived from the well log data.

The methodology used in this dissertation can be applied to a similar basin in Asia and across Pakistan having same geology and structural setting.

CHAPTER 1

INTRODUCTION

A well-known method for better understanding and visualizing the hydrocarbon-bearing zone in the subsurface is known as seismic reservoir characterization. Characterizing a reservoir entail estimating important reservoir characteristics such porosity, permeability, the upper and lower boundaries of the reservoir, as well as the lateral and vertical extent of those boundaries, heterogeneity, and the type and volume of subsurface fluids (Bacon et al., 2007).

Reservoir properties are typically estimated using seismic and well-log data at various scales of investigation (Hearts et al., 2002). We can more effectively connect seismic, well log and core data to field observations by using interpolations and other geostatistical techniques, which enhances our comprehension of the regional geology (Mukerji et al., 2001).

Acoustic impedance is retrieved from seismic reflection profiles and 3D volumes using seismic inversion techniques, along with spatial distribution of depositional facies, local petrophysical characteristics, and different reservoir properties (Angeleri and Carpi, 1982).

Seismic, well log and inversion data are then integrated to identify the various physical parameters (such as porosity and lithological information) of significant reservoir intervals (Landa et al., 2000).

An enhanced seismic resolution is one of seismic inversion's advantages (Delaplanche et al., 1982) as a result of layer-oriented impedance's more precise restrictions for reservoir models and improved seismic interpretation (Ashcroft, 2011). The primary inversion methods for post-stack data are Model-based and Sparse-spike inversion and these inversion types are based on different algorithm (Silva et al., 2004).

For post-stack inversion to maintain the amplitude and phase with a greater signal-to-noise ratio, post-stack data and the appropriate processing techniques are needed (Simm and Bacon, 2014).

The filtered low frequencies must be incorporated in the inversion result which were removed during processing. It's also important to consider the fact that absorption prevents higher frequencies from being recorded. Resolving thin beds and determining local elastic parameters may be challenging due to the lack of higher and lower frequencies in post-stack seismic data. Because the Post stack data is a bandlimited (Zhang et al., 2012). Although the use of Post stack inversion techniques is growing for a number of geophysical and geological studies, they do have certain inherent limitations (Verma et al., 2018).

Around the world, the methodology used in seismic inversion are frequently used for the determination of reservoir parameters and acoustic impedance (Alavi, 2004). The techniques used in Seismic inversion for the identification of hydrocarbon bearing strata is used in a number of Asian basins (Karbalaali et al., 2013). Due to the Indus basin's potential for hydrocarbons, substantial research has been done on it since 1930's (De Terra et al., 1936).
Chorgali and Sakessar are the known reservoir of this region, however significant variation in properties of Chorgali and Sakessar has been noted in this region.
Post stack seismic inversion and wireline log data were carried out to understand and depict reservoir property of the Eocene carbonate reservoir (Chorgali limestone and Sakessar limestone) of Balkassar oil field Upper Indus basin, Potwar plateau Pakistan. Post-stack inversion offers an acceptable approximation of the acoustic impedance and permits the spatial distribution of essential petrophysical parameters that are available at well sites. The property includes total porosity and effective porosity. Geostatistical connections between seismic and well calculated reservoir parameters helps to make this distribution easier and these relations are in the range of seismic resolution.
The spatial distribution of porosity obtained through seismic data demonstrates a nice matching at the wells site and reveals a no significant reservoir bearing hydrocarbon possibility for Eocene carbonates in the research area (porosity in the range of 6–12 percent).
The main objective of this research is to check the spatial distribution of porosity at reservoir scale using limited data sets. Seismic 3D data and wireline log data provided by the DGPC is used to accomplish this dissertation. The constraints of seismic techniques, i.e., seismic resolution, the algorithm which is applied during data processing, limitations of seismic inversion method itself, and the seismic signature of the local geology are some of the uncertainties related with porosity assessment. The limited well data utilized to validate the inversion method serves as the only control points. The outcomes so produced are open to debate and critique, but when compared to other procedures, the inversion process I present in this dissertation yields the best outcomes. Seismic data integrated with well log data was used to map key seismic stratigraphic horizons of the Balkassar block of Upper Indus Basin. In this dissertation, only one well's well log data (OXY-1) and seismic 3D data were used to finish the inversion process. Gamma ray log, Resistivity log, Caliper log, Density log, and acoustic logs were all included in the well-log data. Well-log data were used to document the spatial variability of the main reservoir interval and to link seismic with well information.

A geo-statistical link between acoustic impedance and porosity was also checked at the well site. Thus, in this work, reservoir porosity is extracted using Model-based post-stack impedance and Sparse-spike post-stack impedance as 'external' attributes.

Further aim of this research is to evaluate of the reservoir property with the help of seismic attributes. Petroleum exploration and production are using seismic attributes more frequently, and they are now part of the seismic interpretation method. The seismic attributes is divided into structural attributes and stratigraphic attributes (Brown, 2001).

Amplitude data is the basic form of seismic data, but seismic attributes can show properties that are difficult to perceive in amplitude data alone. Seismic attributes describe the position, amplitude and shape of the waveform. Seismic attributes can be used to discover prospects, find and improve faults and fracture sets to reveal structural history, and even provide direct hydrocarbon indications by extracting information from seismic data that would otherwise be concealed in the data (Burnett et al., 2003). The attributes were applied to Chorgali and Sakessar horizon to see the spatial distribution of the fracture density and the orientation.

The methodology that is tested in this region will be useful for the characterization of reservoirs bearing hydrocarbon in a variety of basins across Pakistan and in other regions of the world that have geological settings that are comparable.

1.1 Main objectives of the research work

General objective of dissertation is as follows,

1. Seismic data interpretation for the identification of horizons of interest.
2. Petrophysical analysis to find the important properties of the reservoir and for the identification of the zone of interest.
3. Fracture corridor modeling by applying the attributes to see the orientation, shape and density of the fracture at reservoir level.
4. Seismic post stack inversion is performed to identify rock properties (acoustic impedance, effective and total porosity,) and the porosity derived from petrophysics were used in geostatistical analysis to extract porosity from the seismic for checking the extent of porosity on whole seismic cube that is the spatial distribution of porosity.

1.2 Introduction to the research area

The geological location of the study area is in the Upper Indus basin Potwar plateau while geographically it is located in Punjab province Pakistan. The field is located in southwestern part of the Islamabad nearly at the distance of 105 km in Chakwal district. The geological

location of the study area is middle part of the Potwar basin which is the northern part of the Upper Indus basin. The geographical coordinates of the study area are Latitude 72.320 – 72.470 E and Longitude 32.510 – 33.020 N.

Geographically Balkassar shares borders with Kalar Khar in south, towards east with the city of Chakwal, towards west lies city of the Thalagang. This area is lying in foreland fold and thrust belt of Himalayan region which is located at appendage of the famous Soan syncline (Hassany and Saleem, 2001). The detailed tectonic map of Northern Pakistan with Balkassar area in the red color (Figure 1.1).

1.3 Data set used for the accomplishment of this dissertation

The 3D seismic cube, which consists of 118 inline and 72 cross lines, was the source of the data used in this study and for well log analysis Balkassar OXY-1 well was used to extract petrophysical information from the well.

The seismic and well log data is correlated using the synthetic seismogram for the improved reservoir characterization. The provided 3D seismic data and well log data by DGPC is listed in Table 1.1, 1.2. but due the limitation of the data all important logs were present in the Balkassar OXY-1 and the remaining two were useless, so I chose only OXY -1 throughout my dissertation.

Table 1.1: Well data used for this research work, with a well name, total depth, and status of the well.

Well name	Total Depth (m)	Status of the well
Balkassar OXY-1	**3129 m**	**Abandoned oil well**
Balkassar 07	**2567 m**	**Developmental oil well**
Balkassar 1A	**2712 m**	**Developmental oil well**

Table 1.2: Seismic 3D data used in this research work, with line name, starting points, ending points and the total number of inline and crossline

Line name	Starts	Ends	Total number Lines
Inline	**72**	**189**	**118**
Cross line	**260**	**331**	**72**

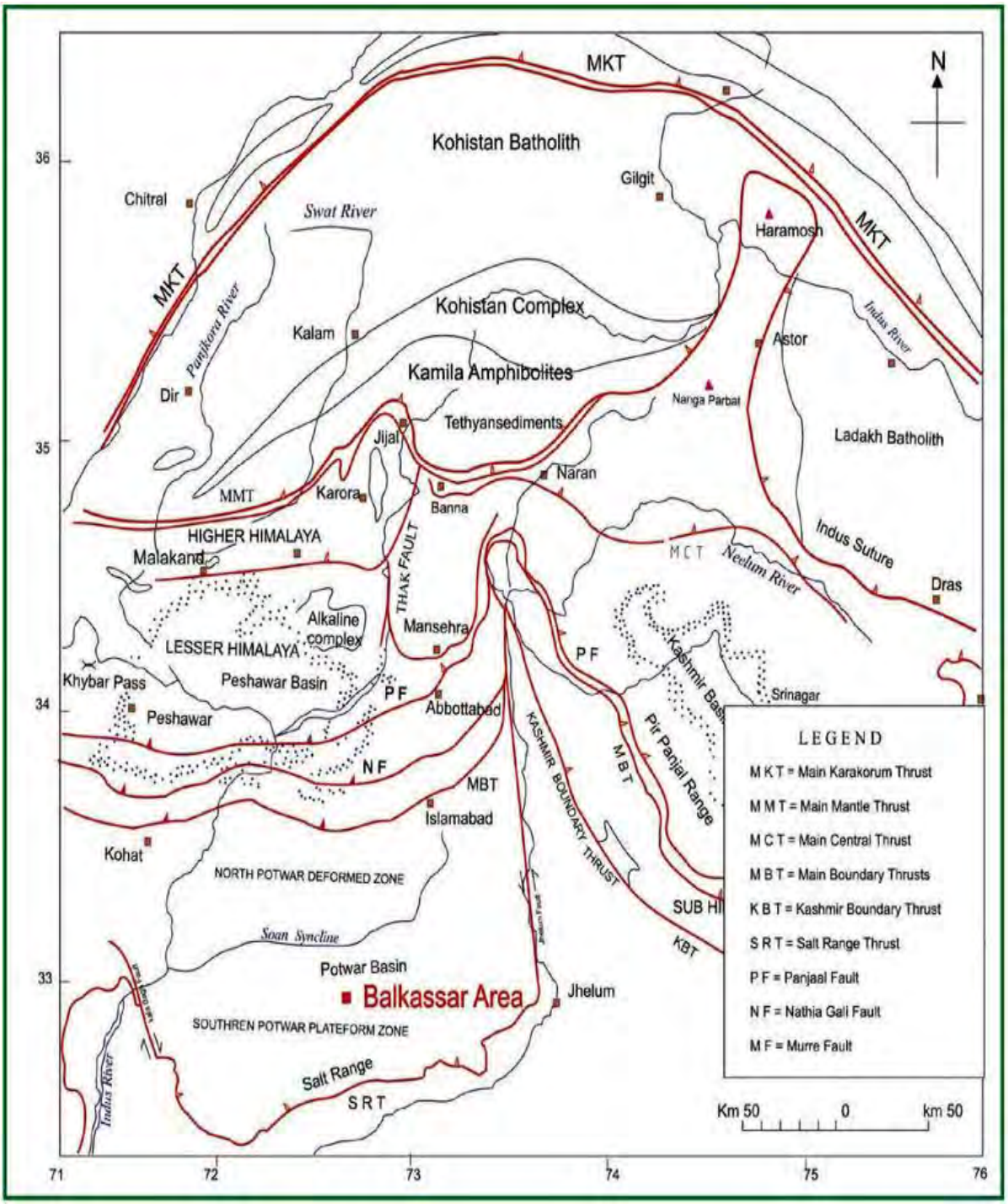

Figure 1.1 Tectonic map of Northern Pakistan showing Balkassar area in the red in between the salt range and soan syncline, salt range lies to the south of the Balkassar area while the soan syncline lies to the north of the Balkassar area (Ghazanfar, 1993) .

1.4 Complete Thesis organization

- This research work is divided into 7 chapter. the first chapter include the complete introduction of the whole research area with background knowledge and provided data set.
- The 2nd chapter is about the structural and stratigraphic style of the Balkassar area and Potwar sub basin to understand the background knowledge of the seismic data interpretation.
- The 3rd chapter include the complete seismic data interpretation to understand the petroleum system in study area and to mark the stratigraphic horizon for the hydrocarbon accumulation and for inversion analysis.
- The 4th chapter is about the petrophysical analysis to extract the reservoir rock properties.
- The 5th chapter is about the application of attributes for fracture characterization and to see the orientation and density of fracture in the reservoir.
- The 6th is about the seismic Post stack inversion for deriving the physical properties of rock from the 3D seismic data.
- The 7th chapter is about the spatial distribution of porosity to better visualize the porosity of sparse well location to the whole seismic cube.

CHAPTER 2

GEOLOGY OF THE RESEARCH AREA

2.1 Introduction

Knowledge of geology and tectonic of the area is very important for a seismic interpretation specialist. Sometimes different lithology of the rocks may have similar signature which is very difficult for the seismic interpretation specialist to make difference between these similar signatures and to deal with these complexities, an interpreter must have a strong knowledge of the geology, stratigraphy, structure and tectonic of the research area.

The research area is in the Upper Indus basin and the Indus basin is located to the western side of India, and it is the northwestern region of Pakistan and extends to an area of about 873,000 square kilometers (Wander et al., 2004). From the northern side Indus basin is bounded by main mantle thrust, Indian shield to the eastern side and southern side of the Indus basin in covered by Indus offshore while the western side of the Indus basin is coincided with Bela Muslim Bagh. The tectonic study also provides the evidence of some basement highs over the plane platform area that acts as dividers (Ahmed et al., 1998).

Indus basin is the major basin of Pakistan which is further divided into Upper, Central, and Southern Indus basin.

Upper Indus basin consists of the northern part of KPK and the Punjab province including the Potwar and the Kohat basins. Sedimentation in the Kohat-potwar basin began in the Precambrian and lasted until the Pleistocene. Three major unconformities in the area are Ordovician to Carboniferous, Mesozoic to late Permian and Eocene to Oligocene. Salt Range formation which overlain metamorphic rocks reported as the oldest sedimentary rocks in the Kohat-Potwar Basin. The Upper Indus basin is located in Northern Pakistan and is separated by the Sargodha High from the Lower Indus basin. The northern and eastern boundaries coincide with the Main Boundary Thrust (MBT). The western boundary of the basin is marked by the uplift of pre-Eocene sediments that are eastward directed and are thrusting to the west of Bannu.

The central and southern part of the Indus basin is collectively known as the Lower Indus basin. This part consists of Suleiman fold and thrust belt, Karachi embayment, Badin region, Kandhkot high and the Jacobabad high (Kadri, 1995).

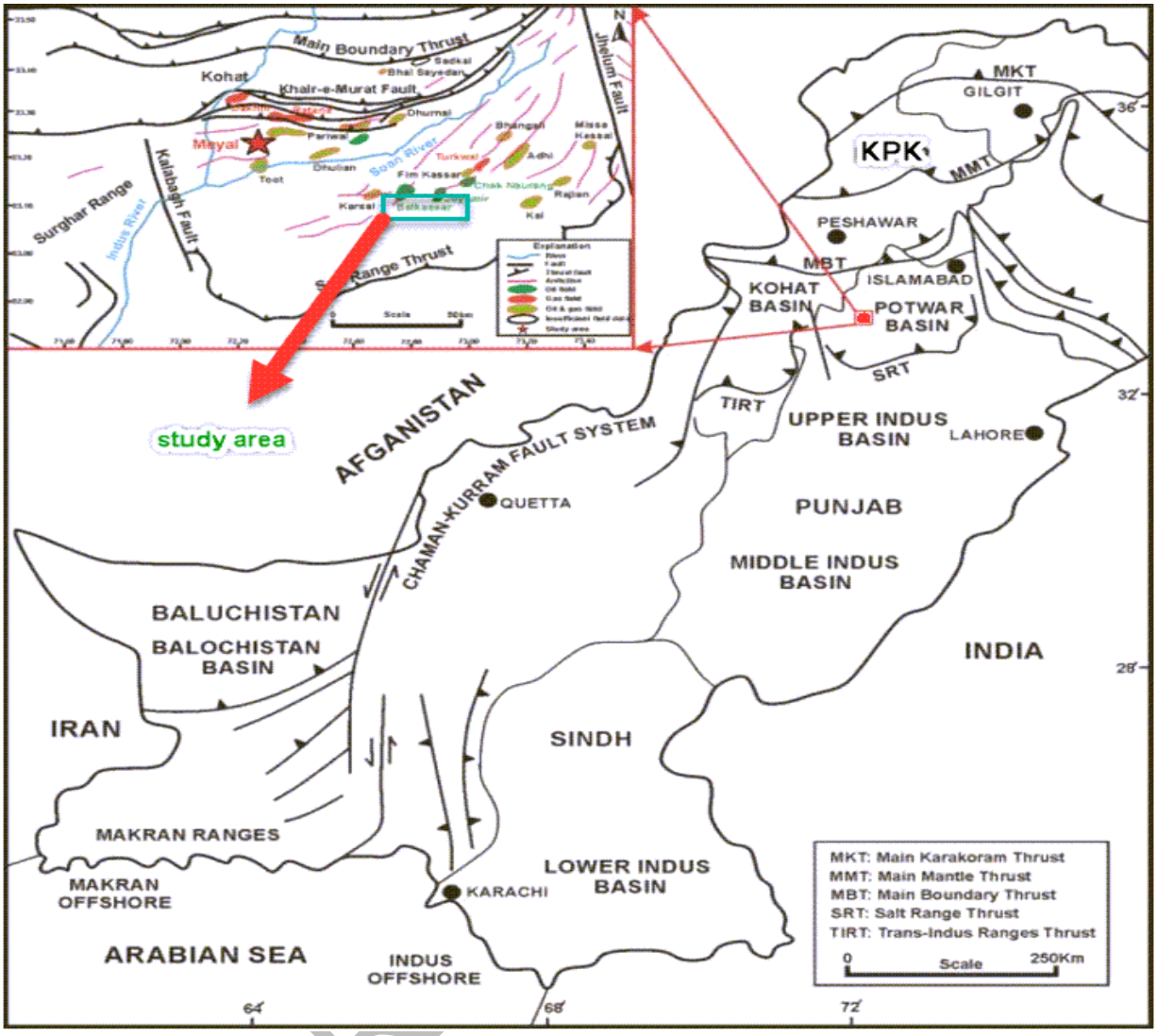

Figure 2.1 Generalized tectonic map and Sedimentary Basins of Pakistan (Farah et al., 2003). The red rectangle show the tectonic framework of the Potwar Basin where green rectangle indicates the location of the study area.

2.2 Geological setting of the research area

The research area i.e., Balkassar area is in Upper Indus basin, Potwar plateau. Potwar plateau is the northwestern part of Himalayan Mountain ranges (Kemal, 1991). Potwar plateau has an undulating topography comprises of the series of the parallel ridges, regionally extended valleys having normally E-W trend.

The Potwar basin is covered thickly by the molasse sediments of the Miocene to Pleistocene. While on the southern side tertiary sequence is also exposed (Shami and Baig, 2003). The northern most part is highly deformed zone called the Northern Potwar Deformed Zone

(NPDZ). All these zones are bounded by the foreland verging faults pop-up zones created by the transform movements.

NPDZ is connected to a Soan syncline having northward dipping plane to the south while having the steeply dipping northern limb along the NPDZ. The western part comprised the series of the east west trending broad and gently fold. While on the eastern side the structural style changes suddenly occur and we get a tight fold, anticline, and the broad syncline. Axial zone of the mostly anticline dip steeply and the overturned (Pennock et al., 1998).

The thrust wedge has been transported in the southward direction as a coherent slab with higher internal deformation with in the central and the western Potwar sub-basin (Baker et al, 1998). On the eastern side of the Potwar, the deformation is very small and having the telescopic features due to the enhancement of the basal traction and the faults cut up section causing the pop-up zones, faults, fold and the triangular structures is 24km extended region (Peencock et al., 1989). The tectonic structures of the Potwar basin is the thin skinned because there is very less involvement of the basement (Kazmi and Jan 1997).

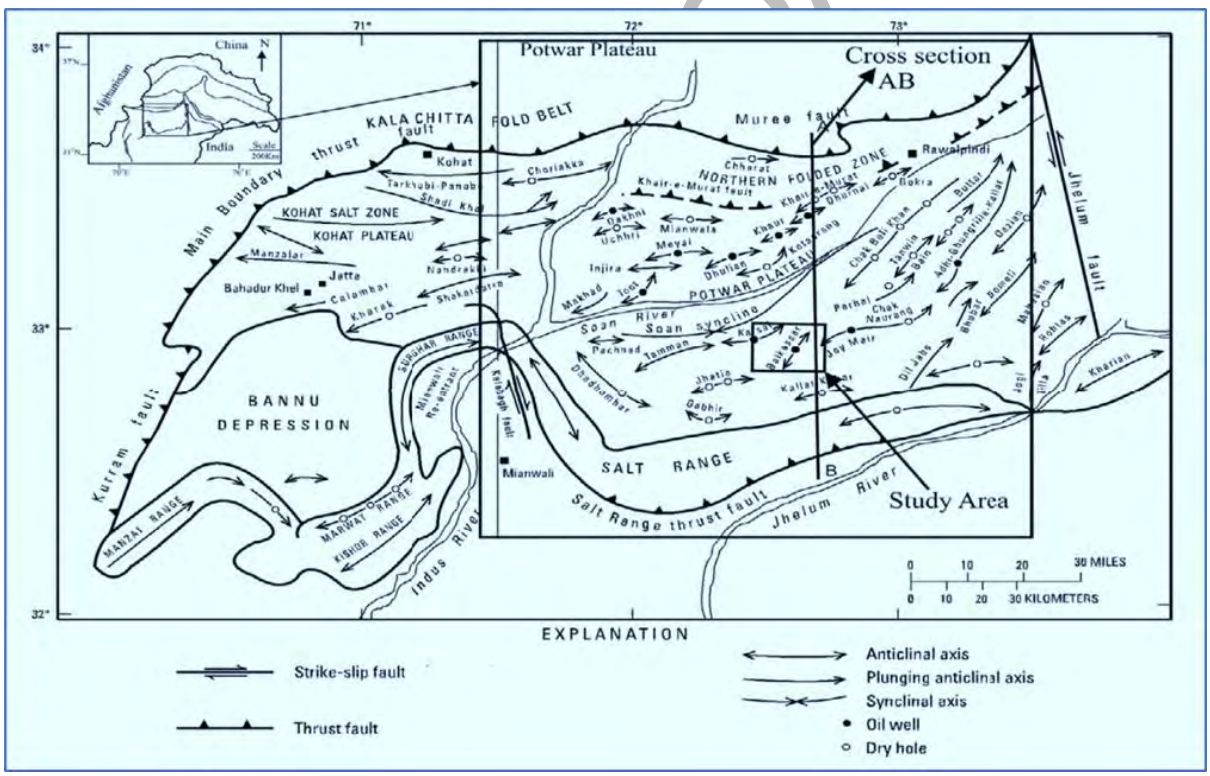

Figure 2.2 Structural map showing different tectonic divisions and major structures of Potwar sub-basin (Shami, 1998; Zahid et al., 2014).

The study area balkassar shown in the rectangle has a several structural tectonic sub-division. like kharsel fault in the North, Joy Mair thrust fault in the east, and two fault in the west Jatai and Ghabbir and in the south kalar kahar fault and salt range thrust. Hence the area is located in a tectonically intense compression region.

2.3 Stratigraphy of the research area

The stratigraphic section of the Balkassar area is divided into three parts by three unconformities. But these unconformities cannot be seen on the seismic data due to the complex pushing of tectonic forces. These unconformities can be encountered into the age of Mesozoic to Oligocene and Ordovician age to Carboniferous (Masood et al., 2017). The unconformities can be seen in the Figure 2.3. The Potwar basin is loaded with thick sheet of the Infra-Cambrian sedimentary Evaporates which are overlain by the thin sheet of the Miocene to Pliocene molasses stores (Ahmad et al., 2008). This entire section is seriously twisted many time due to the tectonic movement of Himalayan orogeny from Pliocene to middle Pleistocene time (Davis et al., 1937).

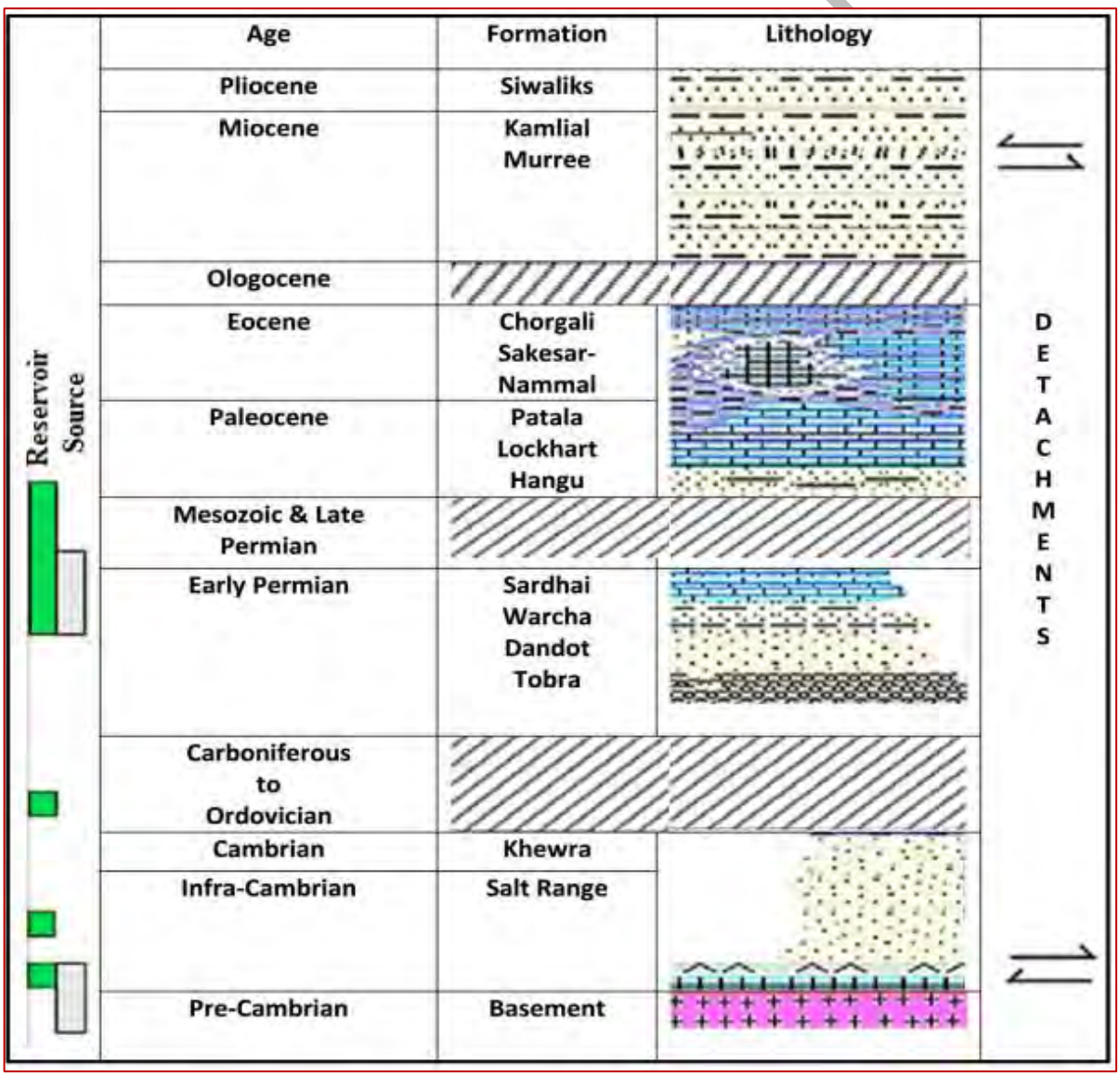

Figure 2.3 Stratigraphic column showing age, formation and lithology of the study area (Masood et al., 2017).

2.4 Petroleum system of the study area

According to the USGS there are several different separate petroleum systems are existing in Potwar Sub-Basin (Wandrey et al., 2001).

(i) Source Rocks

There are many source rocks in the study area. Patala shale of Paleocene with the organic content of (0.5-3.5%) (Khan et al., 1986) is main source rock in the Potwar basin. Jutana, Khussak and Kewra formation also act as source rocks in the study area with organic content of 27 to 26% (Shami and Baig, 2003). Lockhart limestone having suitable amount of the organic matter is also act as the fair source rocks in this area (Kadri, 1995)

(ii) Reservoir Rocks

The different reservoir rocks are encountered in Potwar area while drilling but in the Balkassar area the fractured carbonates of Chorgali formation is the main reservoir in the study area. The different reservoir of the study area Potwar basin is listed in Figure 2.3. Amb and the Wargal formation in the Dhurnal field. Khewra sandstone with porosity (10-12) %, Tobra, Dandot and Warcha formation at Adhi field.

(iii) Seal Rock

Shale of the Chorgali formation is acting as a seal Rock in the Balkassar oil field. The other seal rocks are the Shale and the clay stone of the Murree formation. This provides the efficient lateral seal in the salt range Potwar-Foreland basin (SRPFB) (Shami and Baig, 2003).

Table 2.1 Stratigraphic column of Balkassar OXY-01 well (Shami 1998; Zahid et al., 2014)

Age	Formation	Lithology	Environment of Deposition	Top (m)	Thickness
Pliocene	Nagri	Sandstone	Fluvial	0	478.82
Miocene	Chinji	Sandstone and Clay	Fluvial	478.8	929.29
Miocene	Kamlial	Sandstone	Fluvial	1408.1	106.68
Unconformity					
Miocene	Murree	Sandstone	Fluvial	1514.8	906.74
Eocene	Chorgali	Limestone and Shale	Marine	2421.5	45.72
Eocene	Sakesar	Limestone	Marine	2467.2	135.63
Paleocene	Patala	Shale	Shallow marine to lagoon	2602.9	21.34
Paleocene	Lockhart	Limestone	Shallow marine	2624.2	35.05
Paleocene	Hangu	Sandstone	Shallow marine	2659.3	27.34
Unconformity					
Early Permian	Sardhai	Clays	Lacustrine to shallow marine	2686.7	109.72
Early Permian	Warcha	Sandstone	Fluvial to lagoon	2796.4	143.73
Early Permian	Dandot	Sandstone	Shallow marine	2938.1	60.96
Early Permian	Tobra	Conglomerate	Glacial to Fluvial	2999.1	51.8
Unconformity					
Early Cambrian	Khewra	Sandstone	Shallow marine	3050.9	78.33
Pre-Cambrian	Salt Range	Evaporates, marl	Marine hypersaline	3129.2	0.77

CHAPTER 3

SEISMIC INTERPRETATION

3.1 Introduction

Seismic interpretation is to know about the geology of the earth subsurface, interpretation of seismic data become profitable when you have a better understanding of the geology of the subsurface, to turn the irregular recorded travel times into a meaningful subsurface model, the influence of an unstable geology setting is minimized along the profile. This is important for the certainty of the target horizon's depth geometry (Dobrin and Savit, 1976).

The structural analysis and stratigraphic analysis are the two fundamental methods for interpreting seismic data (Keary and Brooks, 1991). Indication of the structural traps in the subsurface of the earth bearing hydrocarbons is the main goal of structural interpretation of seismic data. Time and depth structural maps are generated, to get an idea about the geometry of selected reflection events.

In stratigraphic interpretation the seismic section is divided into a sequence of reflections which is genetically related in a sedimentary sequence. The main objective of interpretation in this chapter was merely focused on time and depth mapping of targeted horizons and to evaluate the structural configuration of the research area.

All the information which is gathered during the exploration process must be characterized in seismic data interpretation. 3D seismic data having quite higher resolution as compared to 2D because the essence of 3D technique is an actual data gathering tracked by processing and interpretation of 3D seismic volume that is not followed in 2D (Soroor, 2010). 3D survey has a strong capability to clearly express the problem of field assessment, production, exploration, and development (Tegland, 1977). 3D seismic is quite powerful delineation tool, highly costive and generally wells cost quite higher. The success of the well is directly related with the quality of structural interpretation of 3D survey (Aurn hammer and Tonnies, 2005).

Seismic data interpretation for the hydrocarbon exploration has two approaches. One is called the qualitative and second is the quantitative approach. Any technique can be adopted according to the geology and stratigraphy of the area (Sheriff, 1998). Use of the seismic data in the improvement of hydrocarbon field has become vigorous, practically when maturity is obtained by the field and hydrocarbon pocket started to be exhausted (Bacon et al., 2007).

The first step of this research is to interpret 3D seismic data for the identification of stratigraphic intercept, mark and map important stratigraphic boundaries and the stratigraphic horizon.

The 2nd step is to calculate the reservoir property from the well logs analysis. which will be discussed in detail in chapter 4. In the 3rd step the interpreted seismic data was used to apply the attributes for fracture corridors modeling. The 4th step is about to apply the inversion technique on the interpreted data (which will be discussed in detail in chapter 6) such as Model-based and Sparse-spike inversion, to identify and quantify the high porosity zone in the Sakessar and Chorgali Formation of Balkassar oil field, Upper Indus basin, Potwar plateau.

The 5th step includes the spatial distribution of porosity to see the predicted porosity on a large scale at the whole seismic cube. Hence it is concluded that this chapter is very important for the accomplishment of this dissertation.

3.2 Workflow used in interpretation

Seismic data interpretation cannot be completed without doing the following steps.

Firstly, the navigation data of seismic lines is loaded then the SEG-Y and well data is loaded to generate the base map. With the help of the well data synthetic seismogram is generated. The horizon marking, gridding and the time and depth contouring is the main objective of seismic data interpretation. Once the horizon is marked then apply gridding to the data, after this, the time contouring map is generated and then this time contouring map is transformed into the depth contouring map.

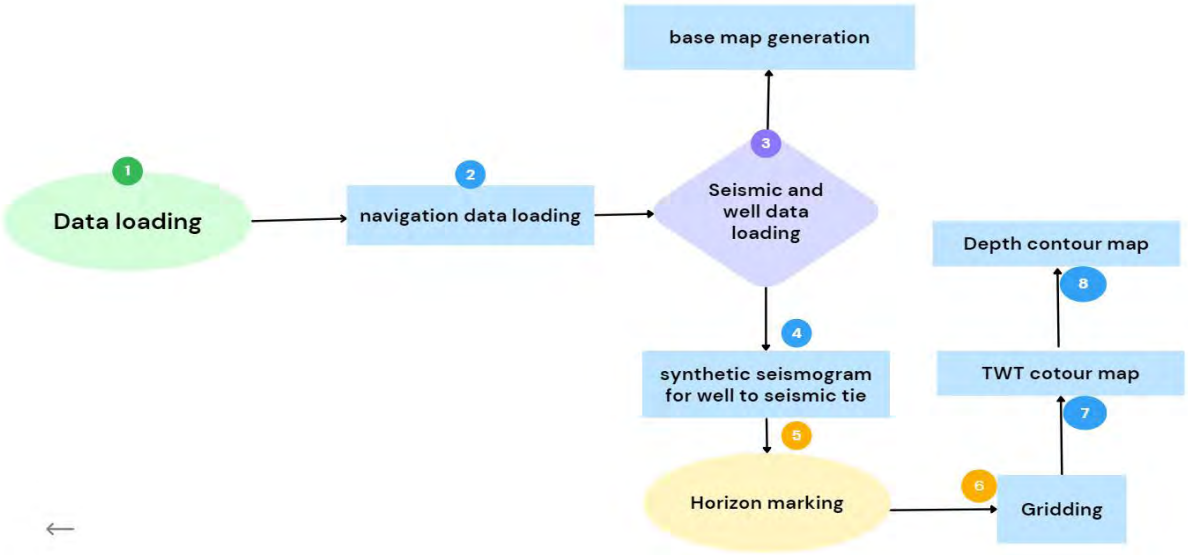

Figure 3.1 The flow chart used in seismic data interpretation started from the data loading to a depth contour mapping.

3.2.1 Base Map of the seismic lines in the study area

Base map depicts the extension and location of the seismic lines, well sites, concession boundaries and seismic survey shot points. It is prepared after loading the navigation data, seismic and well data in (IHS kingdom suit 2020) software. The 3D base map of seismic lines and the well are shown in different symbols is prepared.

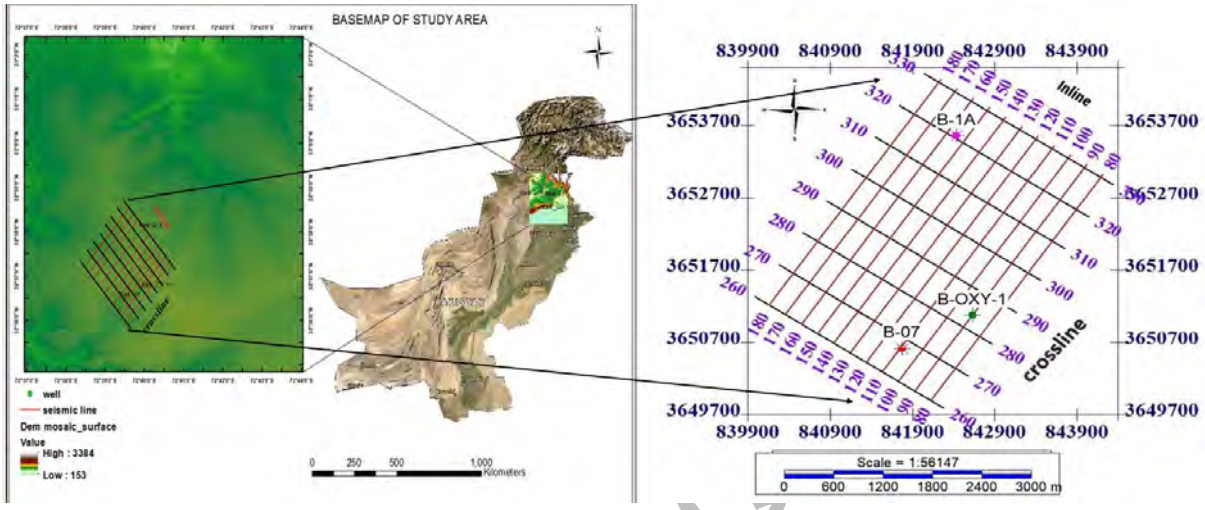

Figure 3.2 3D base map of the study area with the DEM image on the left. The red lines displayed in direction N-E and S-W this Shows inline from 80 to 180 while the black lines displayed N-W and S-E are the cross lines from 260 to 330. The well Balkassar OXY-1 is shown on the map on inline 90 and cross line 284. And Balkassar 07 is also shown with a red dot on inline 110 while Balkassar 1A in shown on map with a magneta color dot on cross line 320.

3.2.2 Generation of synthetic seismogram for well to seismic tie

The synthetic seismogram is very helpful for linking the down hole geology with seismic data because horizon is a direct relation between the observed lithology and the seismic reflection pattern (Copper et al., 2004).

Strong control over the subsurface map leads us towards the correctness of the map. This control can be enhanced by the correlation of well with seismic data. There are several approaches for this correlation but the most famous and suitable is the displaying of the synthetic seismogram to the seismic line for well to seismic tie.

The synthetic seismogram is generated from the well Balkassar OXY-01 shown in Figure 3.3 by the following steps.

1. Loading of the well data and the formation tops.

2. Opening the SYN-PAK modeling and selecting the desired well logs from the selected well.
3. Calculate the velocity from sonic log by inverting this.
4. Load Time depth chart in the software.
5. Acoustic impedance log was derived from the product of density and velocity log.
6. AI was then used to compute the reflection coefficient.
7. Then took the Gamma ray log as reference.
8. After all the above steps the convolution of reflection coefficient and the source wavelet gives the synthetic trace.
9. Now this synthetic trace will be displayed on the seismic section for the correlation of seismic to well tie.

The synthetic seismogram is linked to the seismic inline 90 at the well location, demonstrating that the synthetic model and the seismic interpretation of the horizon are identical.

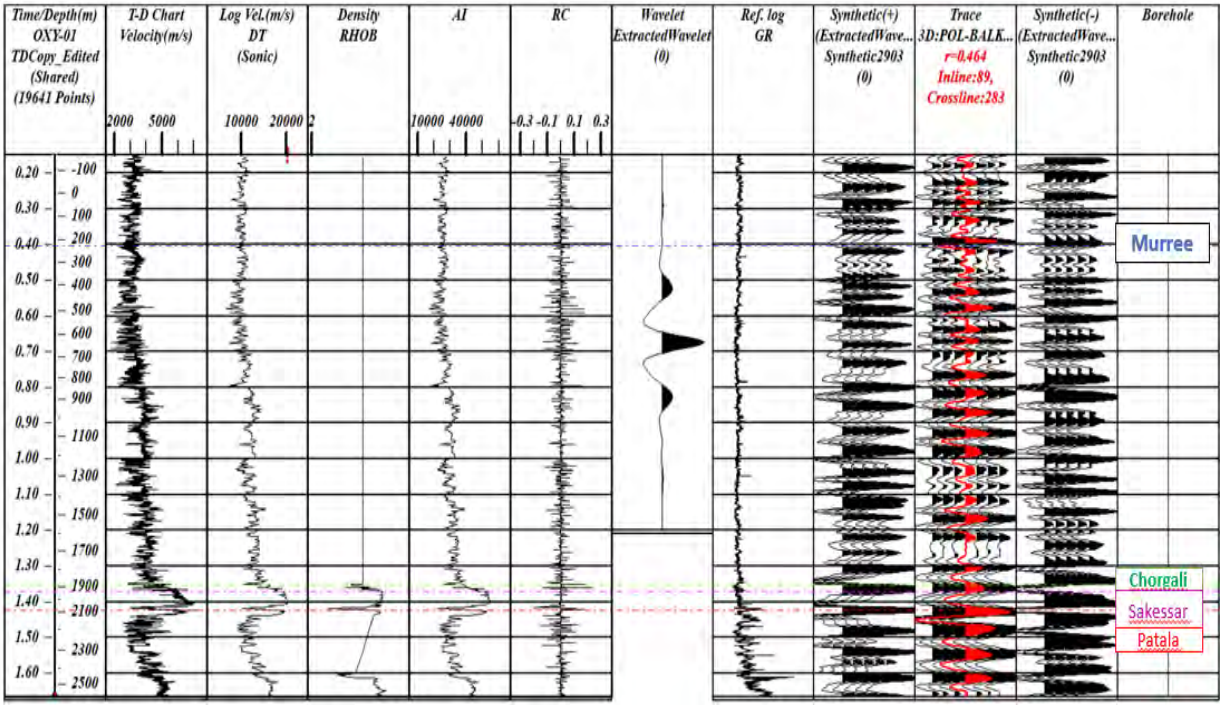

Figure 3.3 Synthetic seismogram of Balkassar OXY-1 on inline 90 and cross line 284 with a correlation coefficient of 0.464. Doted lines are the formation tops of Murree, Chorgali, Sakessar and Patala at time 0.41, 1.36, 1.37 and 1.42 respectively.

3.2.3 Interpretation of 3D seismic lines (horizon marking).

Line-by-line interpretation was the foundation of early 3-D interpretation systems. Modern 3D interpretation methods rely on volume visualization and amplitude manipulation inside the

image volume to highlight important structural and stratigraphic characteristics.

The Figure 3.4 is a seismic 3D section which is visualized in 2D for interpretation purpose. The synthetic seismogram Figure 3.3 which was generated on inline 90 and cross line 284 are nicely matching with the horizon of the seismic section. This synthetic seismogram is used for the interpretation of the horizon marking and the synthetic seismogram is displayed on seismic section as shown in Figure 3.4. There is no faults marked at reservoir level on 3D seismic data because the data contain information just below the crest of the balkassar anticline.

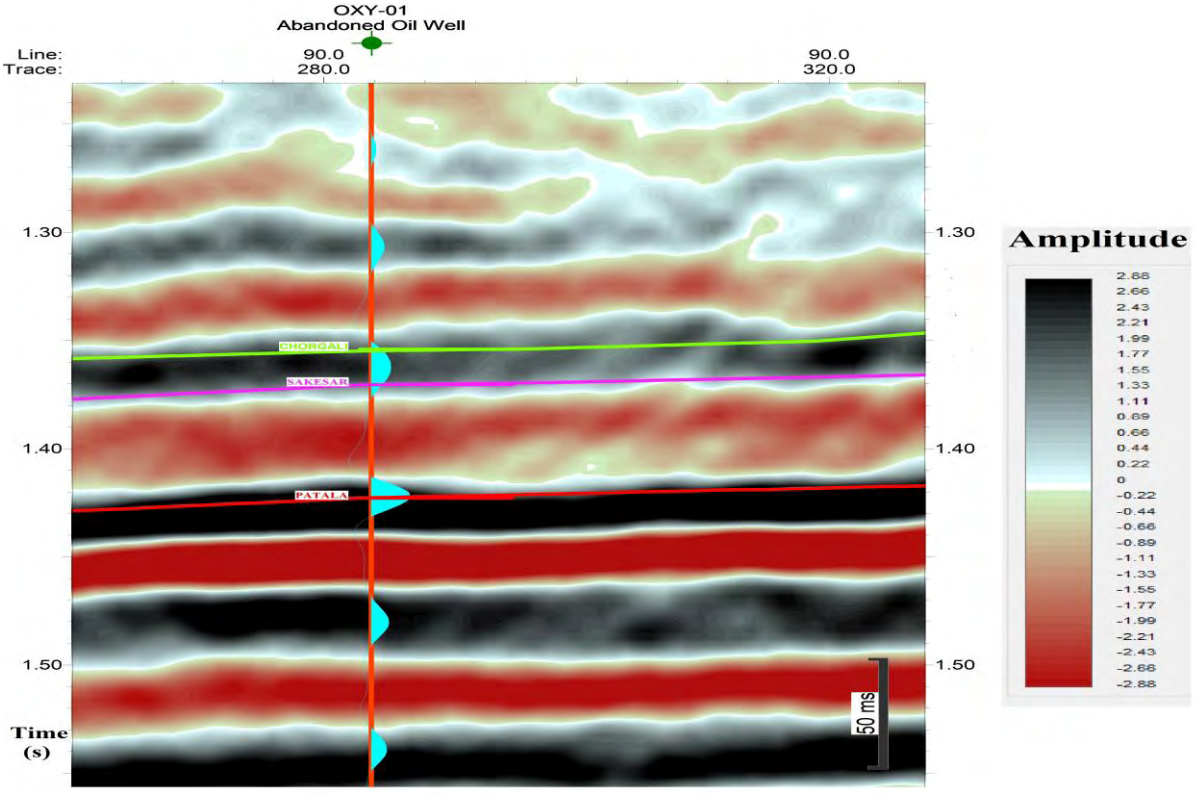

Figure 3.4 Seismic data interpretation with cyan color synthetic seismogram, green color line is the Chorgali horizon and magneta color line is the Sakessar horizon while the red line is the Patala horizon.

3.2.4 Seismic Gridding

After passing from all the above steps the next step is the generation of grids which is necessary for the contour maps generation. Grids give the variation in different geophysical quantities on full base map in time, depth, and amplitude units etc. Basically, grid is the extrapolation of the seismic data at blank spaces among the different seismic survey lines where data is most acquired. The grids constructed for the reservoir rocks Chorgali and Sakessar in time and depth unit. Different colors in the grids showing the time and depth variation along the structure. The discussion related to this time variation will be discussed in detail in section 3.2.5.

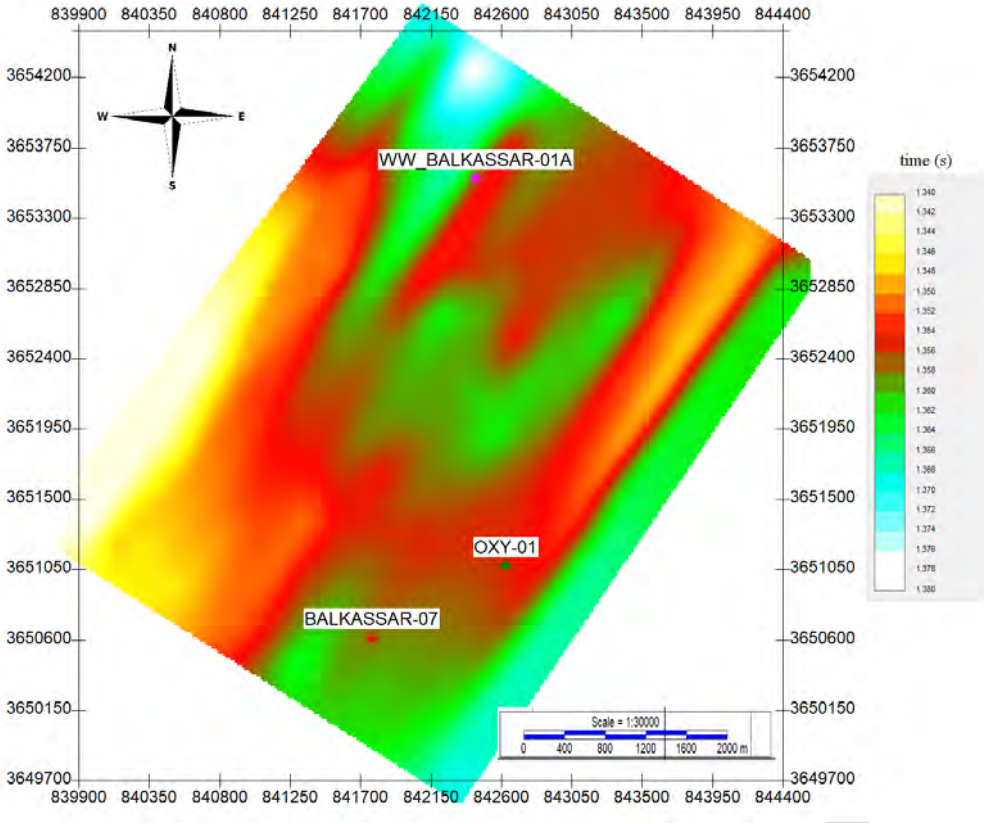

Figure 3.5 Time grid map of Chorgali formation

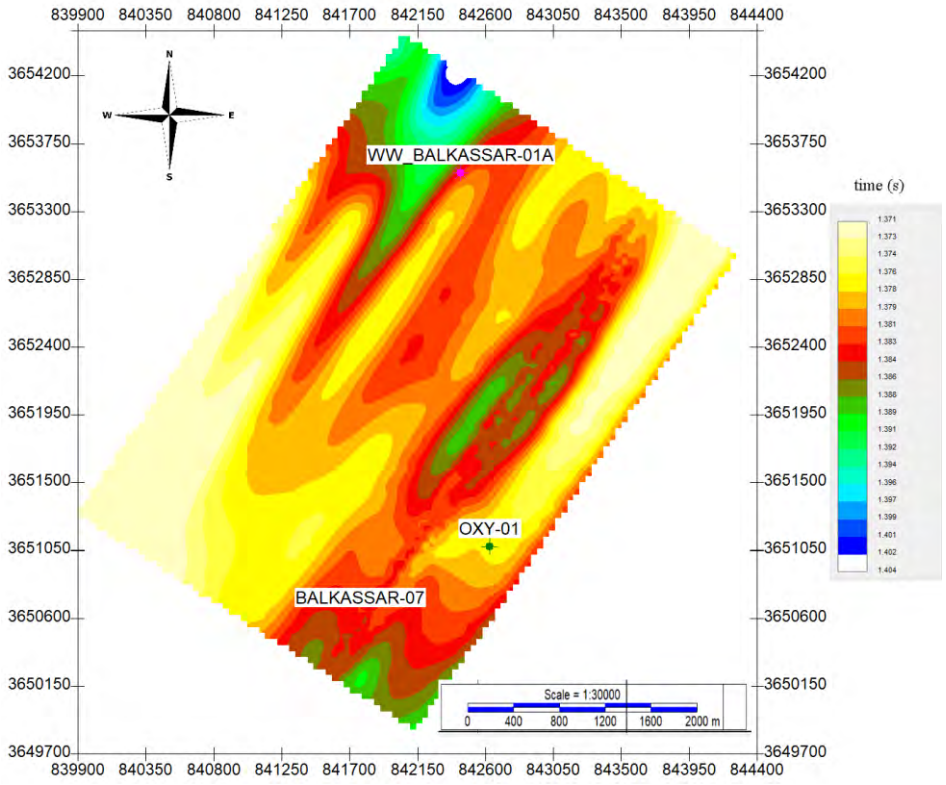

Figure 3.6 Time grid map of Sakessar formation

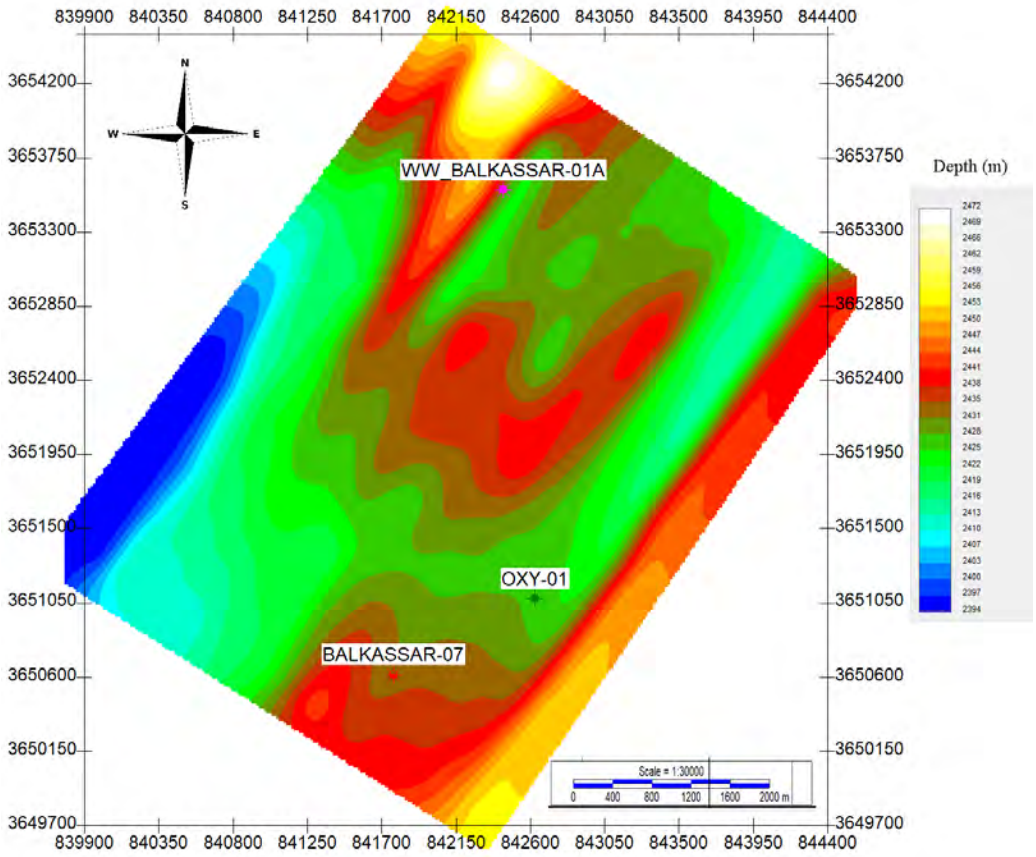

Figure 3.7 Depth grid map of Chorgali formation

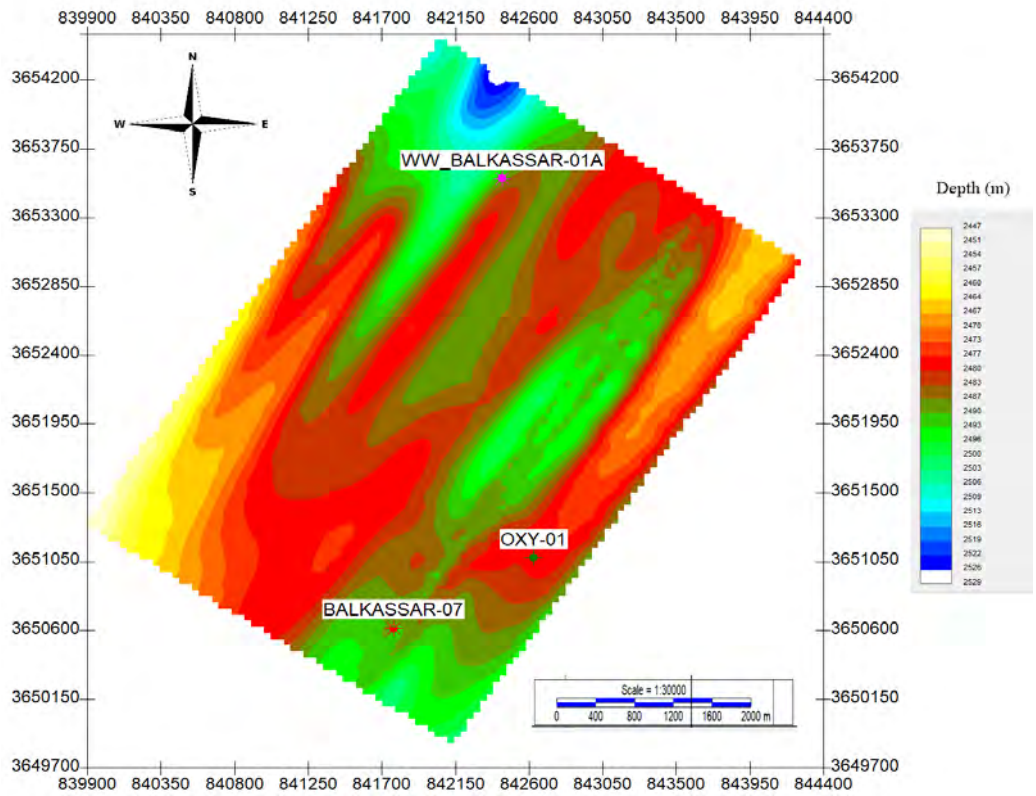

Figure 3.8 Depth grid map of Sakessar formation

3.2.5 Time contour maps

The final product in the seismic data interpretation is the construction of contours map. Contouring is most essential and important part of the seismic data interpretation. Generally, contours are lines which are joining the equal points of time, depth etc. (Coffeen, 1986). Simply contours joins the points of same properties. After gridding the variation in depth, time and the amplitudes are required to observe the specific intervals. Contours represent the 3D earth into 2D. These contours plots depict gradient of formation, structural break of the formation and any type of structural disturbance including faults fold etc. Four maps of the interpreted horizons were created and shown, with the inline and cross lines on the temporal contour map being indicated by red and black color lines, respectively. Time contour maps of Chorgali and Sakessar formation are constructed based on existing seismic reflection data. In all these time structure map points on equal time are contoured in which different time zones are illustrated in different color. Traces of seismic line and well are plotted on the time contour maps.

3.2.5.1 Time contour map of Chorgali Formation

Time contour map of Chorgali Formation was created with contour intervals of 0.0025 seconds and the TWT is ranging from 1.341 to 1.381 seconds. On the map Northern area at the north-west shows low topographic area with deepest TWT 1.382s while southern area at south-west shows high topographic area with shallowest TWT 1.355s. The lowest TWT noted on Balkassar anticline from this map on Chorgali formation time map from kingdom software is 1.351. The time contour map of Chorgali formation shows that the TWT is increasing towards north and decreasing towards south. The green color on the map shows the deepest part and the yellow color shows the shallowest part on the map (Figure 3.9).

3.2.5.2 Time Contour map of Sakessar Formation

Time contour map of Sakessar Formation is generated with contour intervals of 0.003 seconds and the TWT is ranging from 1.371 to 1.404 seconds. Northern area at the north-west shows low topographic area with deepest TWT 1.403s while southern area at south-west shows high topographic area with shallowest TWT 1.383s. The lowest TWT noted on Balkassar anticline in Sakessar formation time map from kingdom software is 1.366. The time contour map of Sakessar formation shows that the TWT is increasing towards north and decreasing towards south. The blue color depict the deepest part and the yellow color shows the shallowest part on the map.

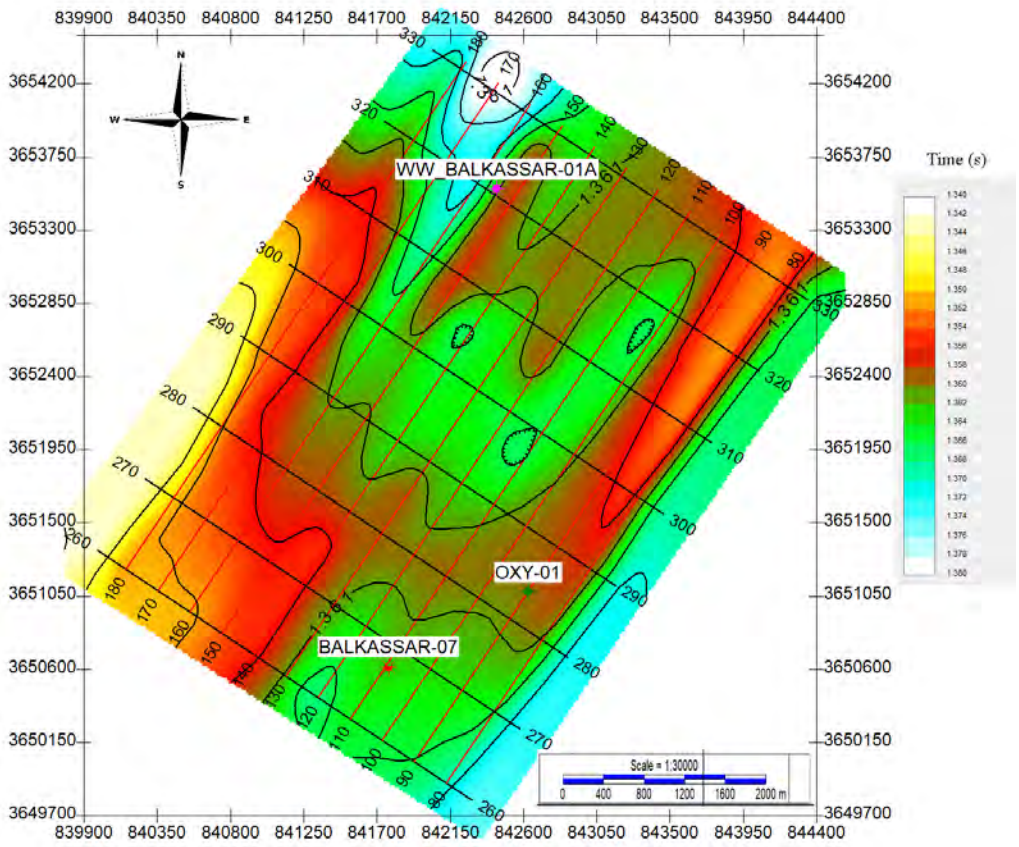

Figure 3.9 Time contour map of Chorgali Formation

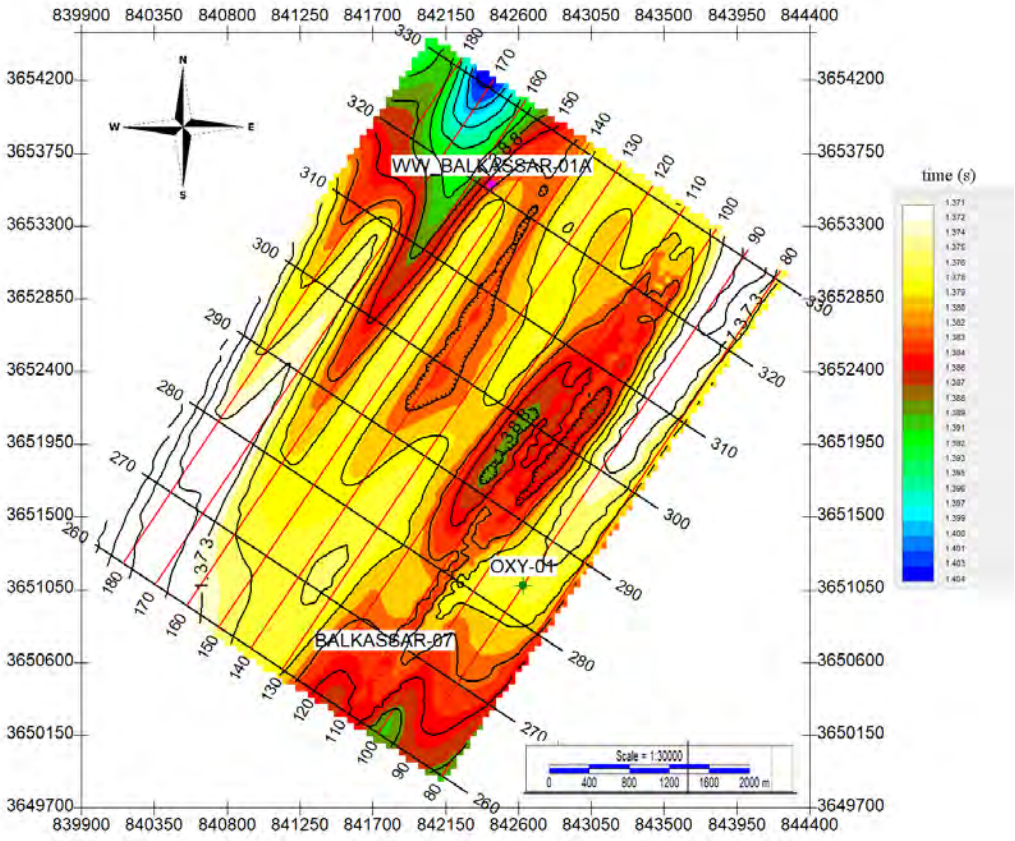

Figure 3.10 Time contour map of Sakessar Formation

3.2.6 Depth contour map

A line connecting points of equal depth below the seismic reference datum are the depth contours line. Time contour map is converted into depth contour map using the below equation in kingdom SMT software.

$$S = v * \frac{t}{2} \qquad (1)$$

S= depth v= velocity t= time

Depth contour map of Chorgali formation and Sakessar formation were generated using Kingdom SMT software. The depth contours map shows the depth of the horizons and hence depict the picture of the subsurface.

3.2.6.1 Depth contour map of Chorgali Formation

Depth contour map of Chorgali Formation was created with contour intervals of 4m and the depth is ranging from to 2394 to 2472 m. Northern area at the north-west shows low topographic area with highest depth of 2469m while southern area at south-west shows high topographic area with shallowest depth of 2431m. The shallowest depth noted on Balkassar anticline in Chorgali formation depth map from kingdom software is 2413m. The depth contour map of Choragli formation shows that the depth is increasing towards north and decreasing towards south. The yellow color on the map shows the deepest part and the blue color shows the shallowest part on the map (Figure 3.11).

3.2.6.2 Depth contour map of Sakessar Formation

Depth contour map of Sakessar Formation was created with contour intervals of 3m and the depth is ranging from 2451 to 2529 m. Northern area at the north-west shows low topographic area with depth of 2508m while southern area at south-west shows high topographic area with shallowest depth 2482. The lowest depth noted on Balkassar anticline in Sakessar formation depth map from kingdom software is 2466m. The depth contour map of Sakessar formation shows that the depth is increasing towards north and decreasing towards south. The blue color on the map shows the deepest part and the yellow color shows the shallowest part on the map. (Figure 3.12)

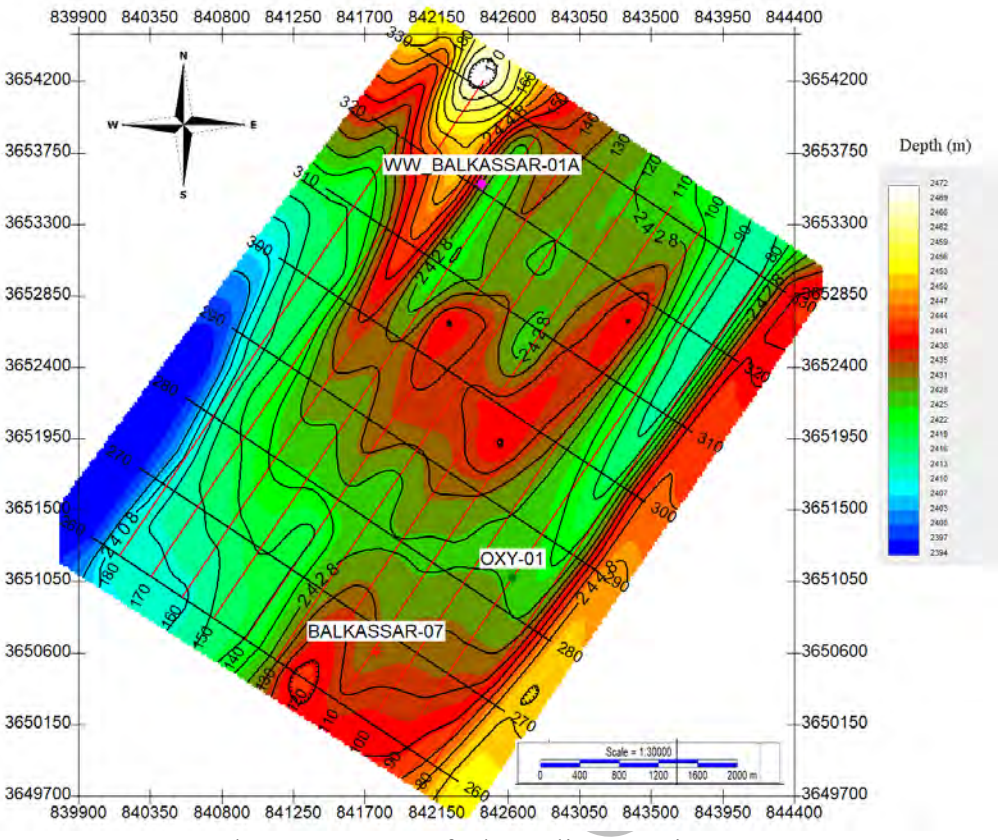

Figure 3.11 Depth contour map of Chorgali Formation

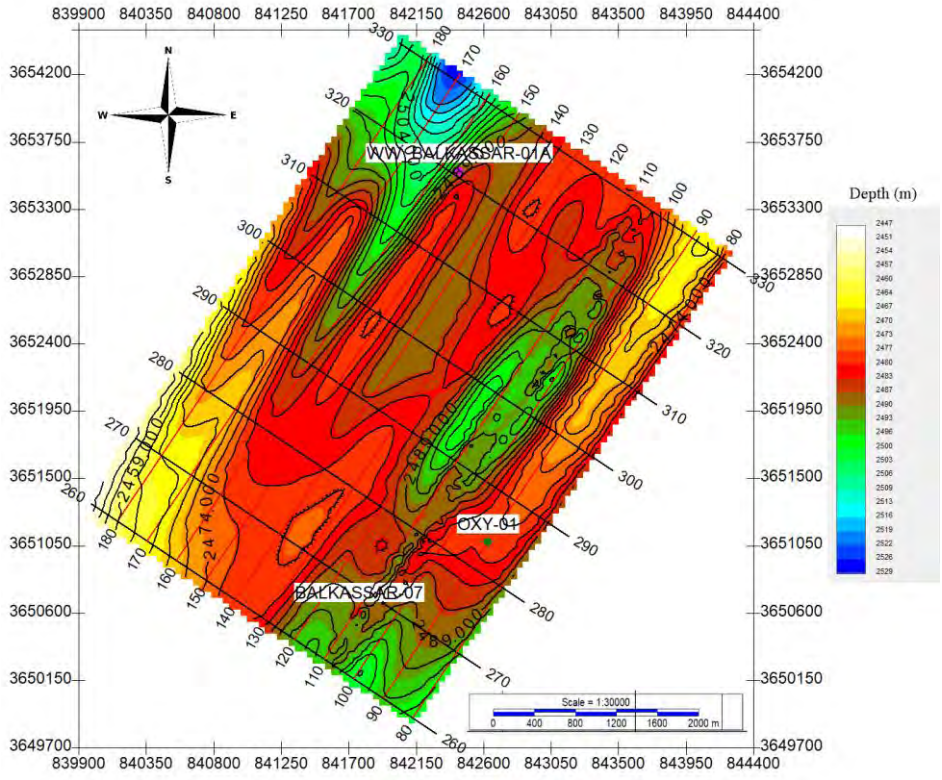

Figure 3.12 Depth contour map of Sakessar Formation

CHAPTER 4

PETROPHYSICS

4.1 Introduction

The study of the physical, chemical, and the hydrodynamics properties of rocks is known as petrophysics. Petrophysics play a very important role in reservoir characterization, and it is the main step in the exploration of hydrocarbon. Well logs contain a lot of information about the reservoir and hence they are most useful tool for reservoir characterization (Cosgrove, J. W. et al., 1998). Obtaining the properties of the reservoir from the well logs is called the Petrophysical interpretation. Petrophysics relates the matrix properties and the fluid properties of the reservoir (Asquith et al., 2004). With the help of the petrophysical analysis we can identify the hydrocarbon bearing zones in the reservoir (Daniel, 2003). Petrophysical analysis provides an approach to identify and quantify the fluids present in the reservoir (Ali et al., 2014). Geologist and Geophysicist perform the integrated study of Rock physics and petrophysics to understand the risk and opportunities. The job of Petrophysicist is to custom all accessible data information to characterize the effective chemical properties and physical properties of the rock in subsurface, and minerals components of rock with special preference on the distribution of three important fluids i.e., Gas, Water, and oil (Augilera et al., 2003). In petrophysical interpretation different types of logs are used including GR, Caliper, Density, Sonic, and Neutron in combination with core and production data to extract the effective properties of the reservoir (Zemke et al., 2010). Using the different geophysical logs in petrophysical interpretation Volume of Shale, Different types of porosities, Water saturation, hydro-Carbon saturation and Rock physical properties are extracted at well location.

4.2 Petrophysical well log analysis

To perform the petrophysical well log analysis abandoned OXY-01 well in the Balkassar oil field is used. From available well log data of OXY-1 we have used the Gamma ray log, SP log, Caliper log, Sonic log, Density log, neutron log, Laterolog deep, Laterolog shallow and Microspherically focused log to obtain the following petrophysical properties.

1. Volume of shale
2. Total porosity
3. Effective porosity

4. Water saturation
5. Hydrocarbon saturation

All these reservoir parameters are important to investigate capability and potential of reservoir to store the Hydrocarbon. Basic properties of all these well logs are discussed in below section.

4.2.1 Lithology Track

For the identification of lithology following three logs is used.

1. Gamma ray (GR) Log
2. Spontaneous potential (SP) Log
3. Caliper Log

1. Gamma ray Log

Gamma ray log is used to identify the natural radioactivity of the rock along the well bore. No active source is used in the Gamma ray logging hence it is passive logging. Different types of rocks emit different spectra of natural Gamma ray radiations. Shale usually emits the larger amount of Gamma ray radiations as compared to other sedimentary rocks e.g., sandstone, Limestone, Dolomite, Gypsum, salt, and coal etc. (Rider et al., 1990). This change in radioactivity of shale and sandstone/carbonates rocks allows Gamma ray log to differentiate between the shale and non-shale lithology (Myers et al., 1989) The Gamma ray log has unit API (American Petroleum Institute). There are different radioactive elements within the earth, but potassium, thorium and uranium are most important.

2. Spontaneous potential log

The SP log is also named as self-potential log. It is a passive logging technique like the Gamma ray log. SP log records the naturally occurring potential in the well bore. SP tool has an electrode that is moving in well bore while reference electrode is keep settled in the mud pit outside the bore at surface. Therefore, with the help of the SP log, Petrophysicist measures the potential difference between the surface electrode and the well bore electrode (Gibson, 2004).

3. Caliper log

With the help of caliper log size and shape of the well bore can be measured along with its depth. Caliper log having the extended arms which can be juxtaposed with the wall of well help us to identify the tight and loose zone during drilling. Hence caliper log can identify

cavities, washouts, and break outs. In front of all these cavities i.e., washout and breakout any log cannot gives the correct information.

4.2.2 Porosity track

The following logs is used to identify the porosity of the formation

1. Density Log
2. Neutron Log
3. Sonic Log

1. Density Log

Density log is an active logging tool. Density log records continues values of formation bulk density in well bore with constant depth interval. Bulk density is combination of Matrix density and fluid density of formation (Alger et al., 1963). A strong Gamma ray emitting tool usually caesium-137 or cobalt-60 are used to generate the gamma rays of higher to medium energy ranging from 0.2 - 2 MeV. Now these gamma rays are bombarded in the formation which collides with electrons present in the rock formation. Some of the emitting Gamma rays become absorbed in the formation while some scattered back Gamma ray (Compton scattering) received on the detecting tool. Increase in the bulk density of formation causing large number of Gamma ray absorption and less counter rate on detector. Hence indirectly counter rate gives us information about the bulk density (Tittman and Wahal, 1965). Bulk density can be processed further to obtain the porosity by mathematical calculation.

2. Sonic log (Delay time log)

Sonic log device comprises on a transmitter which emits sonic (Sound) waves continuously, while there is a recorder which record the compressional waves when they reach to the receiver. The sonic log basically measures the slowness time of waves that is taken by it to go across every foot of rock formation. Inverse of slowness time gives the velocity of that rock formation. This slowness transit time (DT) is dependent on lithology and porosity of the formation. The combination of sonic log with other logs can give the following.

1. Porosity with interval transit time.
2. Lithology identification with NPHI or Density log.
3. Mechanical properties in correlation with density log.
4. Abnormal formation pressure detection.

3. Neutron log

Neutron log is used to quantify the hydrogen concentration in the strata. Neutrons are continuously emitted from chemical source which is present in the neutron logging tool. When emitting Neutrons from source strike with nuclei in rock formation and results in loss of some energy. The mass of hydrogen is the same as the mass of the neutron, the collision of electron with the hydrogen results in huge loss of energy. The hydrogen is the basic atom in fluids so the presence of hydrogen in strata leads us towards the presence of fluid in the formation.
Hence the more we have loss of energy the more we have porosity distribution in the rocks, but the neutron derived porosity of the formation will be low if it contains gas, and it will be high if it contains oil or water because gas has less concentration of the hydrogen as compared to water and oil.

4.2.3 Resistivity log Track

Resistivity logs are used for measuring the electrical resistivity in well bore. Electrical resistivity is property that opposes the movement of electric current through it. In petrophysical interpretation mostly these logs are helpful to identify the different types of the fluids based upon the variation in resistivity values of oil, Water and Gas. The separation between the LLD and LLS gives the indication of Hydrocarbon bearing and non-Hydrocarbon bearing zone (Passey et al., 1999). Generally, the following three log is displayed in the resistivity track.

- Laterolog Deep (LLD).
- Laterolog shallow (LLS).
- Micro spherical focused log (MSFL),

1. LLD Logging

Laterolog deep (LLD) having the larger depth of penetration as compared to LLS. Laterolog deep is used for measuring the resistivity of uninvaded zone. Generally, it gives the resistivity of formation. This log can be used in both saline and the fresh mud.

2. LLS Logging

Laterolog shallow having less depth of penetration as compared to Laterolog deep. So, Laterolog shallow measure the resistivity of the transition zone/ invaded zone. Separation between the Laterolog deep and the Laterolog shallow gives the indication of hydrocarbon bearing zone.

3. Microspherically focused log (MSFL)

A pad mounted electrode system is employed by the Microspherical focused logging (MSFL) to quantify flushed zone resistivity (R_{xo}). Calculating the water saturation in the flushed zone (S_{xo}) is done by using the R_{xo} measurement. This resistivity measurement is a great indicator of moveable hydrocarbons and true formation resistivity (R_t) when paired with deeper reading resistivity measurement. The MSFL tool is great for defining thin beds because of its extremely fine vertical resolution.

4.3 Scale used in Petrophysical Interpretation

Scale is very important in petrophysics. The standard scale used in petrophysics for the derivation of different petrophysical parameters is in the table below.

Table 4.1 Scale used for different logs track in VGS software for petrophysical analysis.

S.No	Logs name	Abbreviation	scale	Unit
1	Gamma ray	GR	0------200	API
2	Spontaneous potential	SP	-100------100	Mvolt
3	Caliper	CALI	6------16	Inches
4	Sonic	DT	40------140	µsec/ft
5	Density	RHOB	1.95-----2.95	gm/cc
6	Neutron	NPHI	-0.15-----0.45	v/v
7	Laterolog Deep	LLD	0.2------2000	Ωm
8	Laterolog shallow	LLS	0.2------2000	Ωm
9	Microspherically focused log	MSFL	0.2-------2000	Ωm

4.4 Equation used for the derivation of rocks properties of the reservoir

Table 4.2 Equation used for the calculation of different petrophysical properties in the software.

S.No	Properties	Equations
1.	Volume of shale (vsh)	$Vsh = \frac{GRlog - GRclean}{GRshale - GRclean}$
2.	Porosity from Density (PHID)	$\phi_D = \frac{RHOmatrix - RHObulk}{RHOmatrix - RHOfluid}$
3.	Porosity from Sonic (PROS)	$\phi_s = \frac{\Delta log - \Delta matrix}{\Delta fluid - \Delta matrix}$
4.	Total porosity (PHI_Total)	$\phi_T = (\frac{\phi Density + \phi Neutron}{2})$
5.	Effective porosity (PHI_E)	$\phi_{effective} = (\frac{\phi Density + \phi Neutron}{2}) * (1\text{-}V_{sh})$
6.	Static spontaneous potential (SSP)	$Ssp = SP_{clean} - SP_{shale}$
7.	Resistivity of Mudfilterate (R_{mf2})	$R_{mf2} = \frac{(ST+6.77)*(Rmf1)}{FT + 6.77}$
8.	Formation temperature (F_t)	$F_T = (\frac{Bht - St}{Td})*F_d$
9.	Saturation of water (S_w) (Indonesian equation)	$S_w = \left\{ \frac{\sqrt{\frac{1}{R_t}}}{\frac{v_{sh}(1-0.5V_{Sh})}{\sqrt{R_{sh}}} + \frac{\sqrt{\phi e^m}}{a.R_w}} \right\}^{(2/n)}$
10.	Saturation of Hydrocarbon (S_{HC})	$HC_{saturation} = 1 - S_w$

4.5 Workflow used in petrophysical analysis

Petrophysical analysis is performed using the VGS (Visdom geosciences services) software. First of all, the raw log curves were given as input to the software by means of which different petrophysical properties are calculated. Different mathematical formulas and Charts are used for calculation of the different log properties.

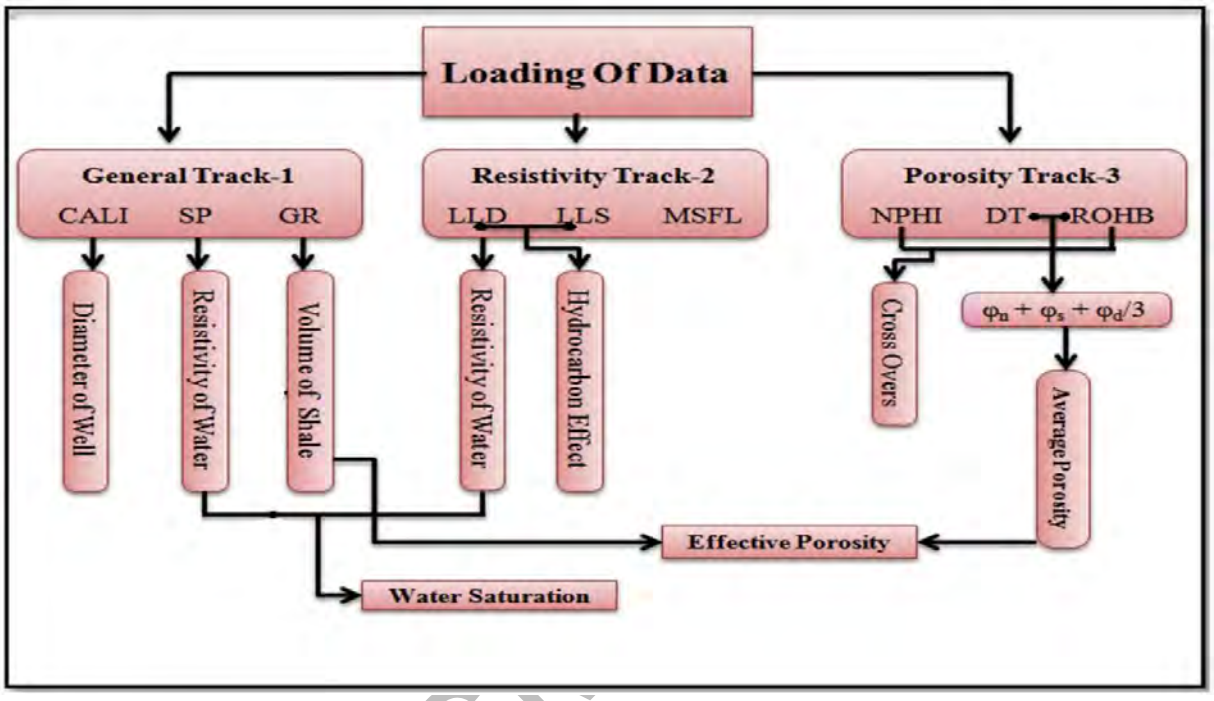

Figure 4.1 The Workflow used for petrophysical analysis divided into 3 tracks which has their own speciality. It Started from loading data and ends at water saturation (Ali et al., 2018)

4.6 Calculation of Rocks properties

Petrophysical analysis is used to calculate different types of rock properties. In this dissertation i have calculated the following properties using different equations which is listed in table 4.2 Main properties which are calculated in geophysical interpretation are.

1) Volume of shale (V_{sh})
2) Density derived porosity
3) Sonic derived porosity
4) Effective porosity
5) Water saturation
6) Hydrocarbon saturation

4.6.1 Volume of Shale (V_{sh})

In reservoir characterization V_{sh}/V_{cl} calculation is most significant step. V_{sh} is calculated by Gamma ray log information. Gamma ray log gives us information about the shale and non-Shale portion. Gamma ray having usually higher value in the Shale due to higher concentration of the radioactive materials while having low values in the reservoir portion i.e., carbonates and clastic rocks. So, volume of shale having higher value in front of shale and low in front of reservoir which is first clear-cut indication of producing zone in the reservoir. Volume of shale/clay of well Balkassar OXY-01 is calculated using the equation-1 given in table 4.2 by (Rider, 1996)

4.6.2 Calculation of Porosity

Porosity is one of the most important properties for the identification of petroleum system. The porosity is derived with the help of Neutron log, Density log, and the sonic (DT) log. DT log is acoustic measurement, and the Neutron log and Density log are nuclear measurement. By all these three logs one can calculate the most accurate and effective values of porosity. We have different types of the porosities which are given below.

1) **Porosity derivation from density log**

Density Logging is active logging in which the formation bulk density is measured. Gamma rays are emitted from highly active chemical source typically (Ce 137, Co 60). These gamma rays collide with electron in the formation. The density logging tool counts the number of returning radiations which is indirectly indication of electron density of formation. Average electron density gives us the bulk density of formation. Now putting this bulk density in Equation (2) given in Table 4.2 density porosity can be calculated. Returning rays having two different energy level causing the two different types of effect as below

1. Compton scattering
2. Photoelectric effect

High energy gamma rays causing the Compton scattering which is basic phenomena in density logging control the bulk density and hence porosity of the formation. Low energy Gamma rays causing the Photoelectric effect are most helpful in formation lithology identification. Such type of logging is called the PEF (Photo electric effect Logging). PEF log is one of the most reliable and highly used logs for lithology identification in petroleum industry.

2) Porosity derivation from Sonic log

Interval transit time of the wave passing through the formation can be calculated using the Sonic logging tool. Interval transit time is measure of the ability of formation to transmit the sonic waves which are basically sound waves. This interval transit time is called the slowness factor of formation which depends upon the rock matrix and the fluid present in it. Now putting this interval transit time in Equation (3) given in Table 4.2 Sonic porosity can be calculated.

3) Effective Porosity

Effective porosity is the volume of the connected pores in the rock through which fluid easily pass from one place to another place, and it can be calculated as the ratio between the pores volume of the rock and the total volume after subtracting the effect of shale volume gives the effective porosity. Effective porosity helps us to find the water saturation. The effective porosity is calculated by the equation of the (Schlumberger, 1989) listed in the table 4.2. Now to calculate the Water saturation we have required the Resistivity of the water in the formation. This is a Lengthy procedure which is explained as follow.

4) Average Porosity

The Porosity which is calculated from the sum of all porosities logs over the number of the logs.

4.6.3 Resistivity of formation water (R_w)

After the calculation of the volume of the shale, effective porosity, total porosity and sonic porosity the next step is the derivation of formation water resistivity. Computing the resistivity of the water is initial step in finding the saturation of the water. The below steps have been carried out to calculate the resistivity for water.

Step 1: first (S_{SP}) static spontaneous potential is calculated then the values of the surface temperature (S_T), maximum recorded temperature (B_{HT}), and the resistivity of the mud filtrate (R_{mf}) from the well headers. (Rider, 1996).

Step 3: In this step the resistivity of the mud filtrate is calculated using the relation given in equation 7 of the table 4.2.

Step 2: Formation temperature can be derived with the help of the relation which is given in the table 4.2 equation 8 by (Rider, 1996).

Step 4: In step 4 the resistivity of the mud equivalent (R_{mfeq}) is calculated via VGS software.

Step 5: R_{weq} (Water equivalent resistivity) is determined from the SSP (Static spontaneous potential).

After calculating all the above explained properties and the resistivity of the water equivalent the second step is to find the value for resistivity of the water (R_w) against (R_{mfeq}) at SSP value and BHT from the graph as shown in Figure 4.2

Step 6: In this step the value of water resistivity (Rw) is obtained against the value of the R_{weq} (resistivity of water equivalent) and formation temperature Figure 4.3. when Resistivity of water is determined the next step is to compute the saturation of the water by using the famous Indonesian equation as shown in the Table 4.2.

These all equation was applied via VGS software.

4.6.4 Hydrocarbon saturation

Final and most important product in Petrophysical interpretation is the calculation of hydrocarbon saturation. This step is quite easy because we have already calculated the water saturation hence, we will just subtract the saturation of water from total pore space to obtain the HC Saturation. For this purpose, Equation (10) given in Table 4.2 is used.

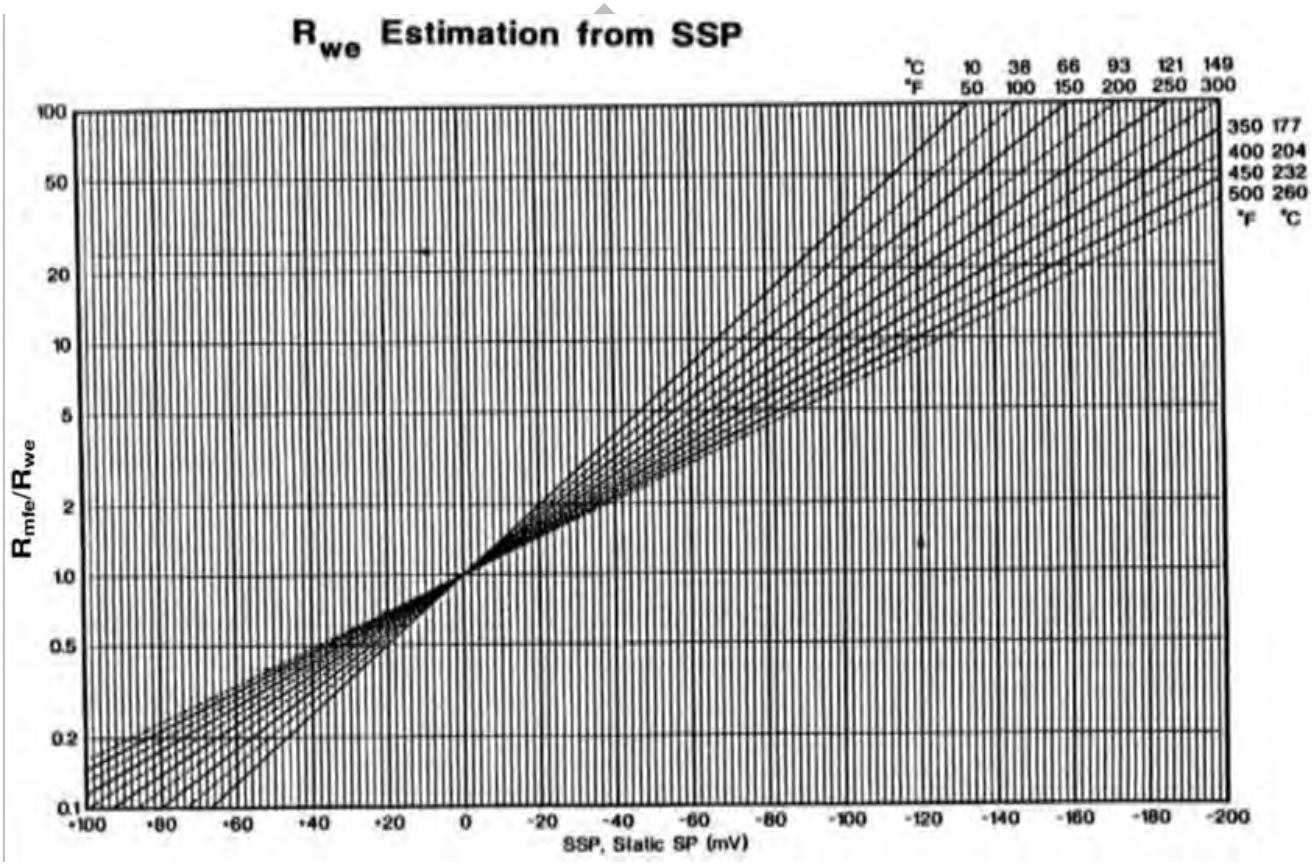

Figure 4.2 Typical Rmf/Rw versus static SP chart (Schlumberger, 1989).

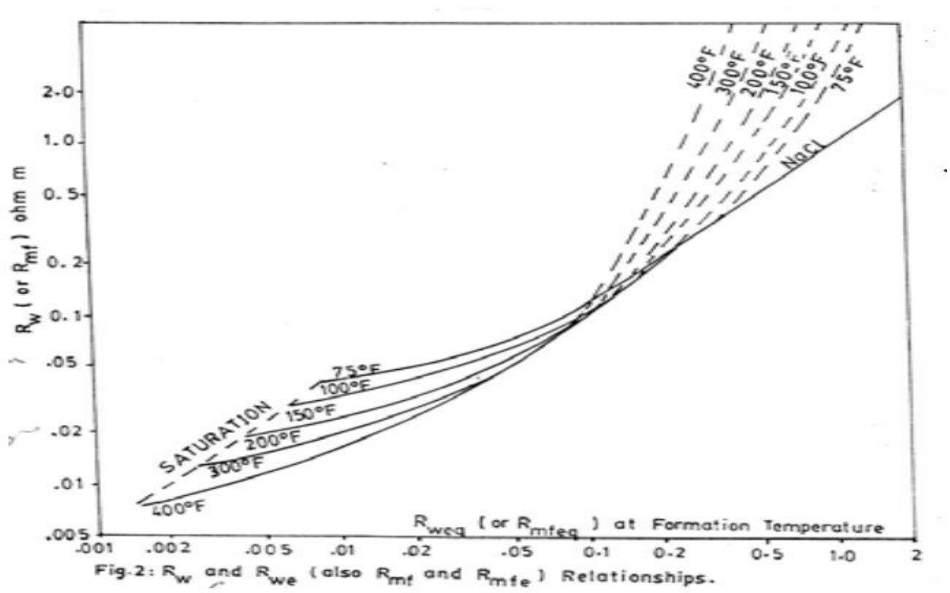

Figure 4.3 Determintion of resistivity of water from SP chart (Schlumberger, 1989)

4.7 Petrophysical interpretation of Balkassar OXY-1 at Chorgali and Sakessar level (2421 – 2602)

Petrophysical analysis is performed on Balkassar OXY-01 to find the effective properties of the reservoir Chorgali and Sakessar Formation. Caliper log is most important because it tells us about the borehole condition. If Caliper log disturb at any point, then in front of that location no log can gives the correct results. But in the Figure 4.4 the Caliper showing very nearly smooth values. Similarly, Gamma ray is most important indicator to differentiate between the reservoir and non-reservoir zone. Generally, the Gamma ray values are higher in shale as compared to limestone. Overall shale distribution in massive limestone beds is quite low, hence GR value and calculated volume of shale is small in carbonate reservoir as compared to the clastic reservoir. The separation between LLD and LLS is the main indication of presence of hydrocarbon or fresh water. Generally, LLD gives the higher value when gas or oil is present in reservoir and low when saline water exists. Another indication of Hydrocarbon bearing zone is crossover of density and NPHI (Neutron log). This crossover has very high values in gas bearing zone. While in case of oil-bearing reservoir this cross over is very minor, but in case of presence of water the cross over between LLD and LLS does not form. The well OXY-01 having maximum surface temperature 72º Fahrenheit and borehole temperature is 18º Fahrenheit with resistivity of mud filtrate 0.17 Ohmmeter as already noted on the hard copies of the OXY-01 provided by the DGPC. From the Figure 4.4. it is clear that there is no chance

of HC at Sakessar level but Chorgali has HC between the zone 2424m to 2427m. For successful well this is very small zone for enough Hydrocarbon accumulation although it has 27% porosity and has HC saturation of 44% with water saturation of 56% but this well is abandoned. For better visualization and understanding of the petrophysical properties the above figure is broken down into two parts. These two parts are shown in figure 4.5 and 4.6.

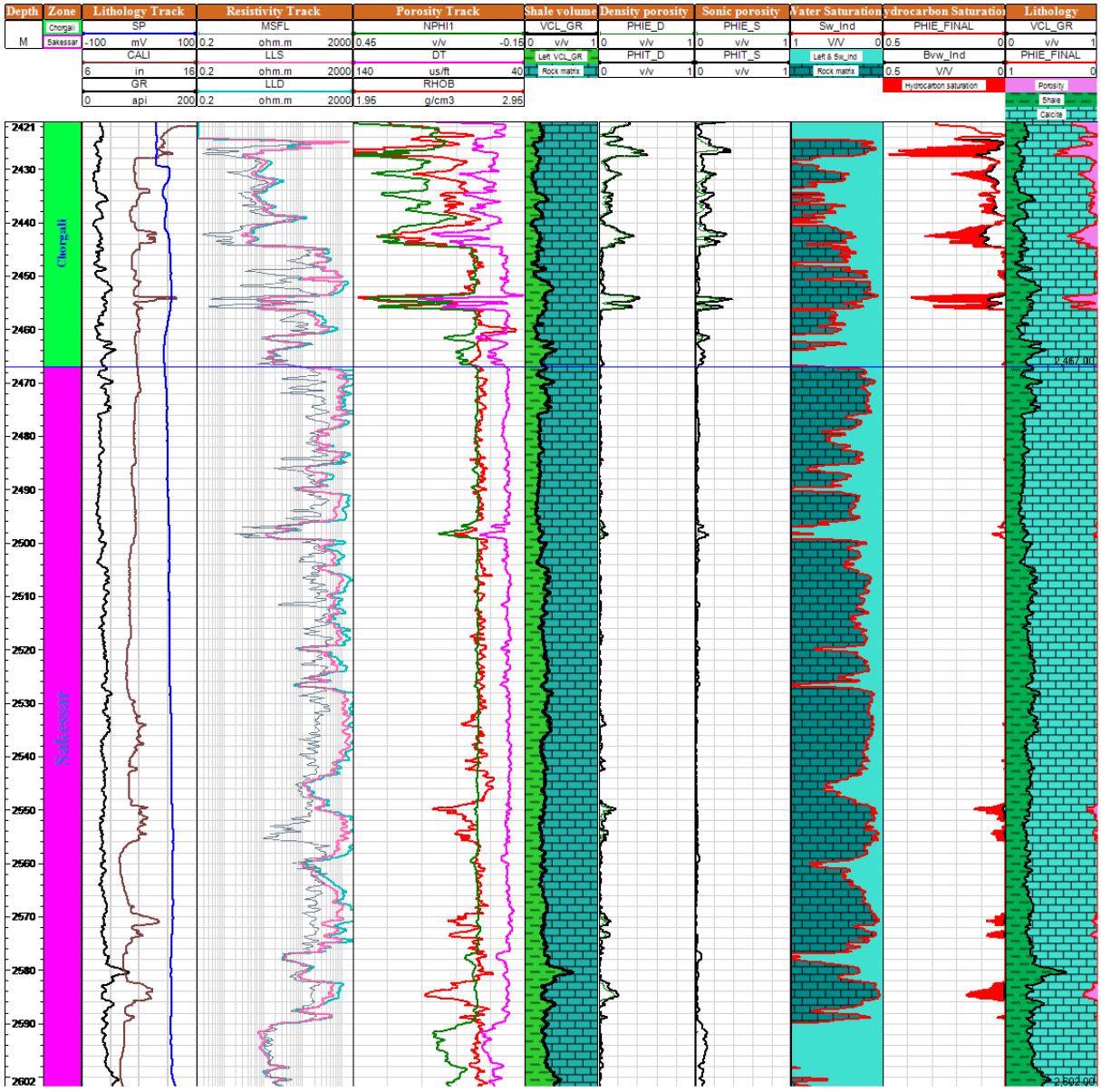

Figure 4.4 Petrophysical interpretation of the entire Chorgali and Sakessar Formation.

4.7.1 Petrophysical analysis of Chorgali Formation (2421-2467)

The derived petrophysical properties of Chorgali formation shows that over all there is very less chance of presence of hydrocarbon at well location of OXY-01. In this zone effective porosity is very low and is upto 9% and water saturation is 88% and 12% HC saturation with average total porosity derived from the desnsity log is 11%. The results are listed in Table 4.3.

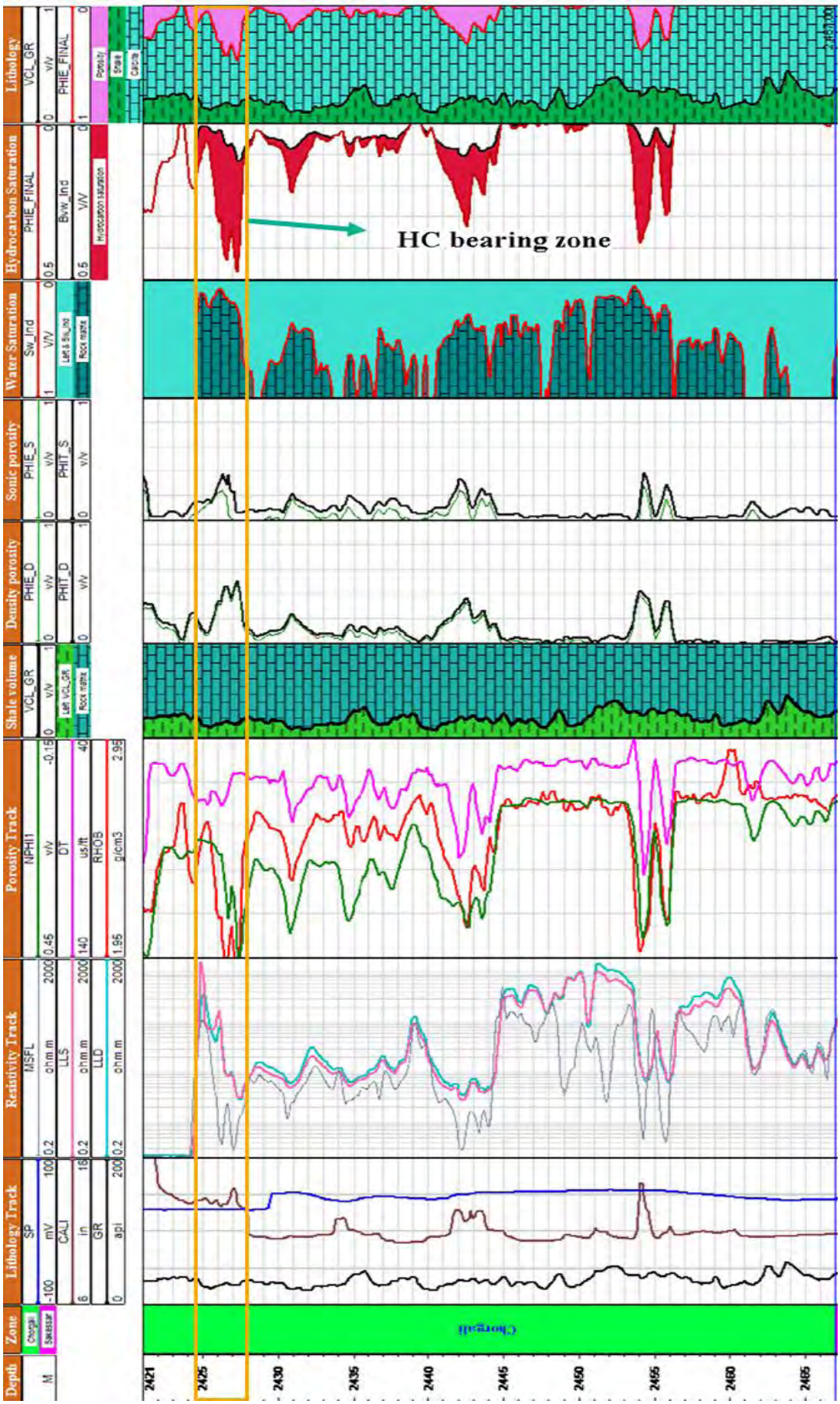

Figure 4.5 Petrophysical analysis of Chorgali formation showing porosity distribution along the borehole with saturation of water and Hydrocarbon in the blue and red color respectively. HC bearing zone is also indicated with yellow rectangle.

4.7.2 Petrophysical properties of Chorgali Formation and the Interpretation of the zone of interest (2424-2427m)

According to provided data information the OXY-01 is abandoned oil well as this is confirmed from the petrophysical analysis as shown in Figure 4.4 and Figure 4.5. Only a 3-meter zone between 2424 and 2427 meters in the entire Chorgali reservoir with hydrocarbon content up to 44%. However, this is a relatively small zone and the hydrocarbon content is too low to support sufficient production for a successful well. In the Chorgali reservoir the zone 2424 to 2427 there is a proper cross over between the NPHI and RHOB and the separation between the LLD and LLS which is the indication of the Hydrocarbon. Additionally, effective porosity is up to 25%, and the volume of shale is only 19%, indicating that the concentration of shale in limestone is typically quite low. There is no other hydrocarbon-producing zones in the entire well, this is the reason why the oil well OXY-01 is abandoned.

Table 4.3 Petrophysical properties of overall Chorgali formation and the zone of interest

S.No	Rocks properties	Entire Chorgali formation 2421-2467	Interest zone 2424-2427
1.	Average volume of shale	34%	19%
2.	Average sonic porosity (PHI_S)	10%	26%
3.	Average total porosity (PHI_D)	11%	27%
4.	Average effective porosity	9%	25%
5.	Average water saturation	88%	56%
6.	Average hydrocarbon saturation	12%	44%

4.7.3 Petrophysical interpretation of Sakessar limestone (2467-2602 m)

Petrophysical analysis has proven that Sakessar Formation lacks a zone that would be conducive to the accumulation of hydrocarbons. The effective porosity is 2 % and 86% water Saturation in this formation, which is very low for Hydrocarbon accumulation. There is no cross over between the NPHI and RHOB and no separation between the LLD, and LLS which shows that there is no favorable zone for hydrocarbon accumulation in this formation.

Since Sakessar is known to be a pure limestone and petrophysical investigation has demonstrated that Sakessar has a very low porosity and a very high water saturation, there is, in general, no chance that there will be any hydrocarbon in the reservoir.

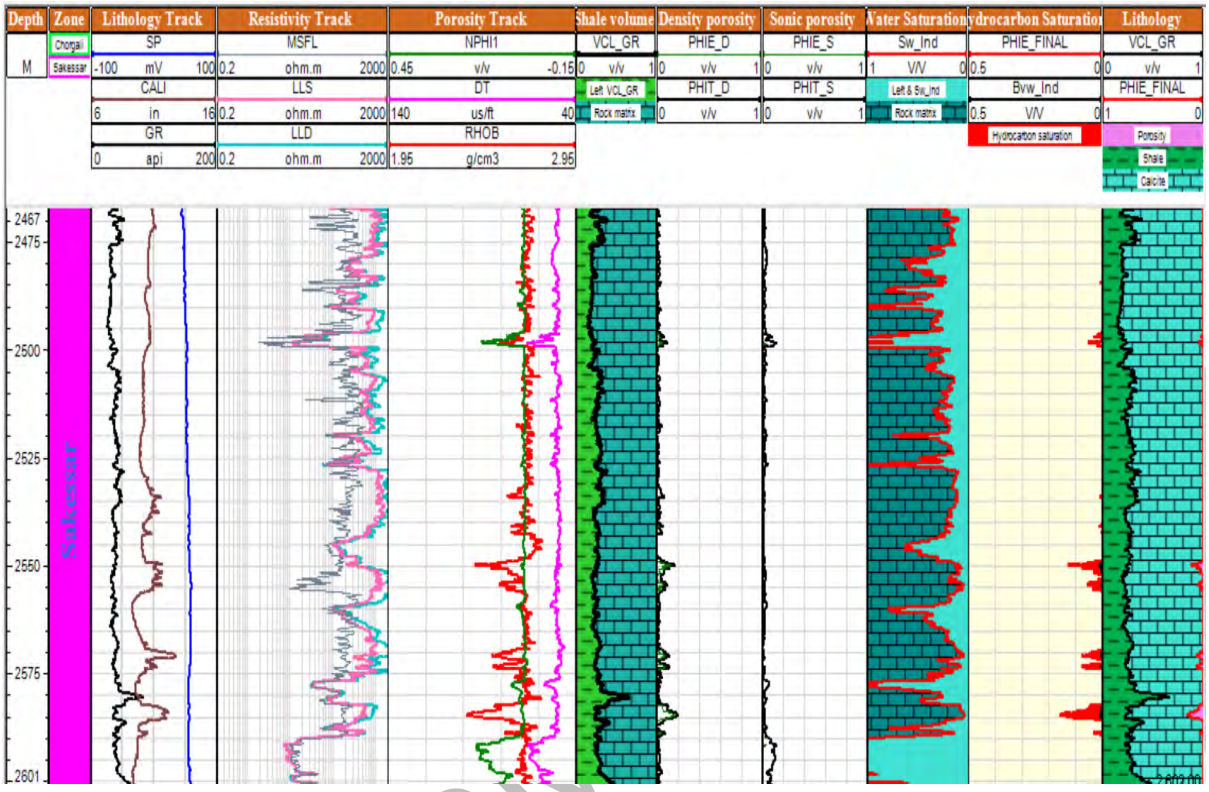

Figure 4.6. Petrophysical analysis of Sakessar Formation. Showing no possible zone for HC accumulation.

Table 4.4 Petrophysical properties of Sakessar limestone derived from the well log analysis.

S.No	Rocks properties	Sakessar formation 2467-2602
1.	Average Volume of Shale	46%
2.	Average Sonic Porosity (PHI_S)	4%
3.	Average Total Porosity (PHI_D)	4%
4.	Average Effective Porosity	2%
5.	Average Water Saturation	86%
6.	Average Hydrocarbon Saturation	14%

4.8 Cross plot of DT and Total porosity

In order to identify the outcome based on two or more types of data from the graphs or charts, cross plots provide a quick evaluation of the well log analysis.

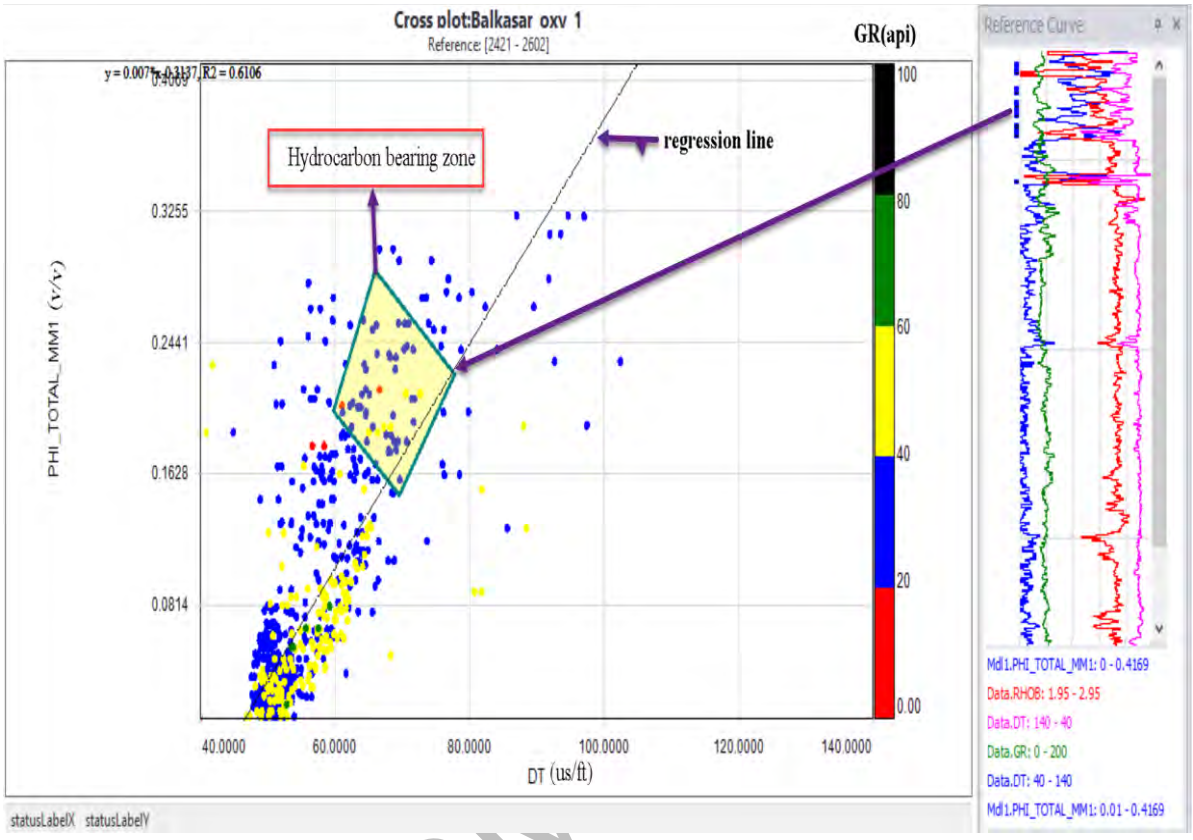

Figure 4.7 The cross-plot of DT and total porosity from OXY-1 for Chorgali and Sakessar Limestone.

The background trend is marked by black line, whereas the polygon highlights the hydrocarbon bearing zones at Chorgali level between 2424 to 2427).

CHAPTER 5

FRACTURE CORRIDORS MODELLING

5.1 Introduction

Fracture corridors are tabular areas with notably high fracture intensity or clusters of fractures that are closely spaced (usually joints, sheared joints, or veins) (Peacock et al., 2016), are common structural objects. Importance of fractures cannot be ignored because these fractures create drains for fluid in reservoir rocks. Fractures sometime developed due to the local structural and sedimentary heterogeneities, but there are other circumstances exist, when their mechanical origin is unknown. It is a challenging job to identify the vertical and horizontal dimension of the fractures as well as the distance between the fracture's corridors because complete section of the bearing mechanical unit are scarce.

More than 60% oil reserve of the world lie in the naturally fractured reservoir of carbonates rocks (Akbar et al., 2000). Fractured reservoir refers to the subsurface sedimentary formations that contain the Hydrocarbon in wide network of fracture. Efficient pore network development of such reservoir is extremely difficult (Casciano et al., 2004). In fractured reservoir fracture play a role of conductive pathway that can enhance the flow of fluid in better way to the well bore. The most famous fractured reservoir are limestone and dolomite which are founded all around the world and some of these reservoirs contain billion barrels of Hydrocarbon (Mace et al., 2004). Carbonates rocks are biochemically formed rocks of marine environment. According to their nature they are generally formed in shallow warm and clean marine environment. Sedimentary process including the diagenesis, lithification, cementation, compaction, Burial and uplift play a very important role to variate the reservoir quality in carbonates (Schmidt et al., 2000). Understanding and making full use of fractures network according to exploration scenario is very important factor to improve the reservoir performance. As of my research area and topic on which I am doing my research is fractured reservoir of Eocene carbonates of Balkassar area, so it needs to apply fractures attributes to see the orientation, shape and density of the fracture. This chapter is focused on the modeling and characterization of fracture network in the study area. Fractured corridors in carbonates reservoir generally exist in range from ten to hundreds metered in heights and width while having regional extent in km (Huang et al., 2017). Better understanding of fracture distribution can help us to evaluate the potential location of new well to improve drilling technique and direction among other things.

5.2 Attributes used for fractured corridors modeling

For characterization and exploration of reservoirs, seismic attributes are frequently used. In order to decipher the structural history of the subsurface, seismic attributes extract the hidden information from the seismic data, such as faults and fractures. Another way to directly identify hydrocarbons is to use seismic attributes. It is also used to identify the various tectonic regimes, such as extensional, strike-slip, and compressional environments. It is also useful for the identification of geological settings include carbonates, clastic, and salt-related basins. In recent decades, improvements in digital technology, recording systems, and visualization techniques have had a significant impact on seismic attributes.

The attributes used in this dissertation is to detect data disruption. Attributes used here in this chapter are, dip-magnitude, dip steered semblance, Enhanced-coherence, coherence, semblance, Enhanced-semblance.

5.2.1 Dip-magnitude of Chorgali and Sakessar Horizon

It is an angle between the steepest direction of a plane and a horizontal plane, with values ranging from 0 to 90^0. The maximum value is considered as a dip when computing the slope of fractures in various directions in the data using this attribute. As a result, events with various dips can be distinguished. These attributes show the deviation of a seismic reflector from a horizontal plane.

Chorgali is a major producing reservoir in Balkassar area. The available 3D seismic data having no major faults because the 3D seismic cube is below the crest of the anticline so with the help of the dip magnitude attribute fractured zone of Balkassar anticline is identified at Chorgali level as shown in Figure 5.1, this Figure clearly depicts that Balkassar anticline have a high fractured zone, the dark black color is a high dip magnitude while the light color is a low dip magnitude. The Figure 5.1 depicts a very low dip magnitude at the well OXY-1 and have high dip magnitude to the northwest of the OXY-1 so the results from the petrophysical analysis and dip magnitude attributes are in good agreement. The trend or orientation of the fracture is northwest and southeast because we have stresses from the north and south in the research area. Dip magnitude attributes is also obtained at Sakessar level to see the fractured zone at this level. Figure 5.2 clearly depicts that most fractures are oriented NW-SE direction. The location of OXY-1 well has a quite less value of dip magnitude at Sakessar level which indicates very low fractured zone or having very low secondary porosity.

The results of dip magnitude are in good agreement with petrophysical interpretation at OXY-1 well.

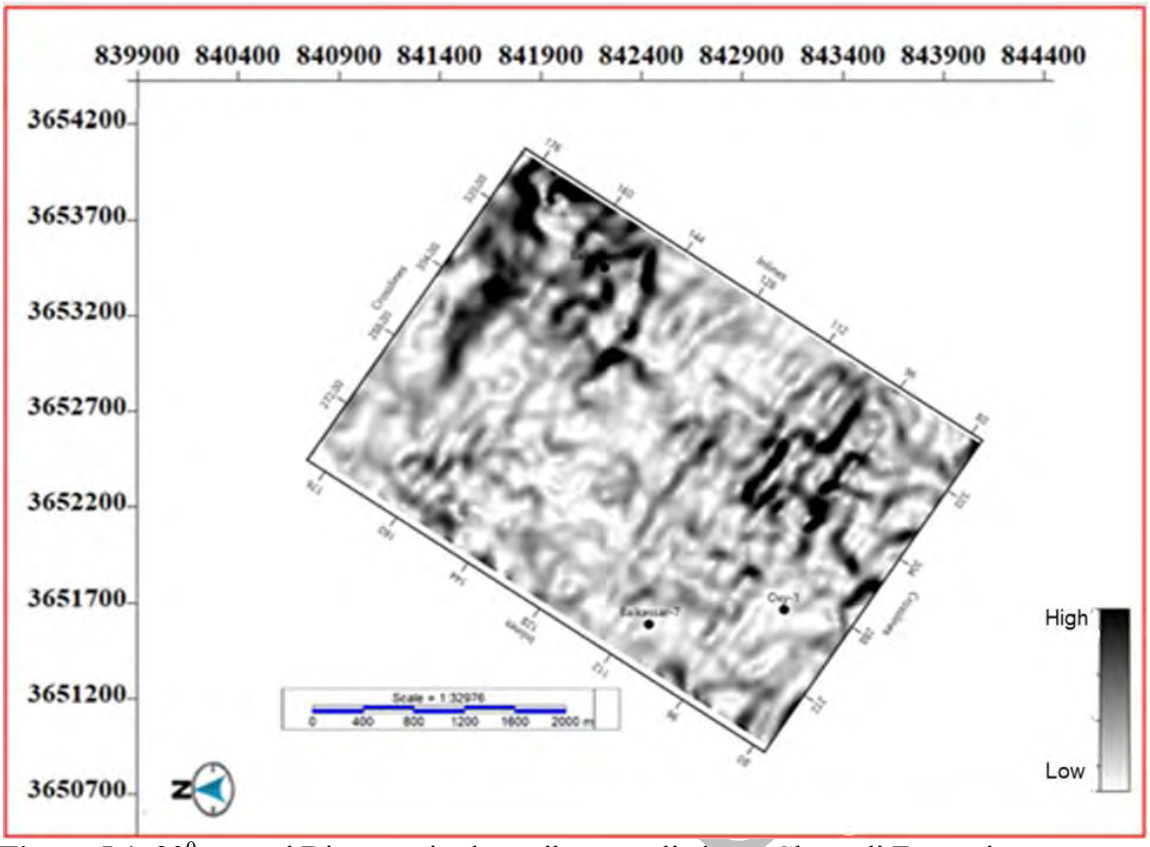

Figure 5.1 90^0 rotated Dip magnitude attribute applied to a Chorgali Formation.

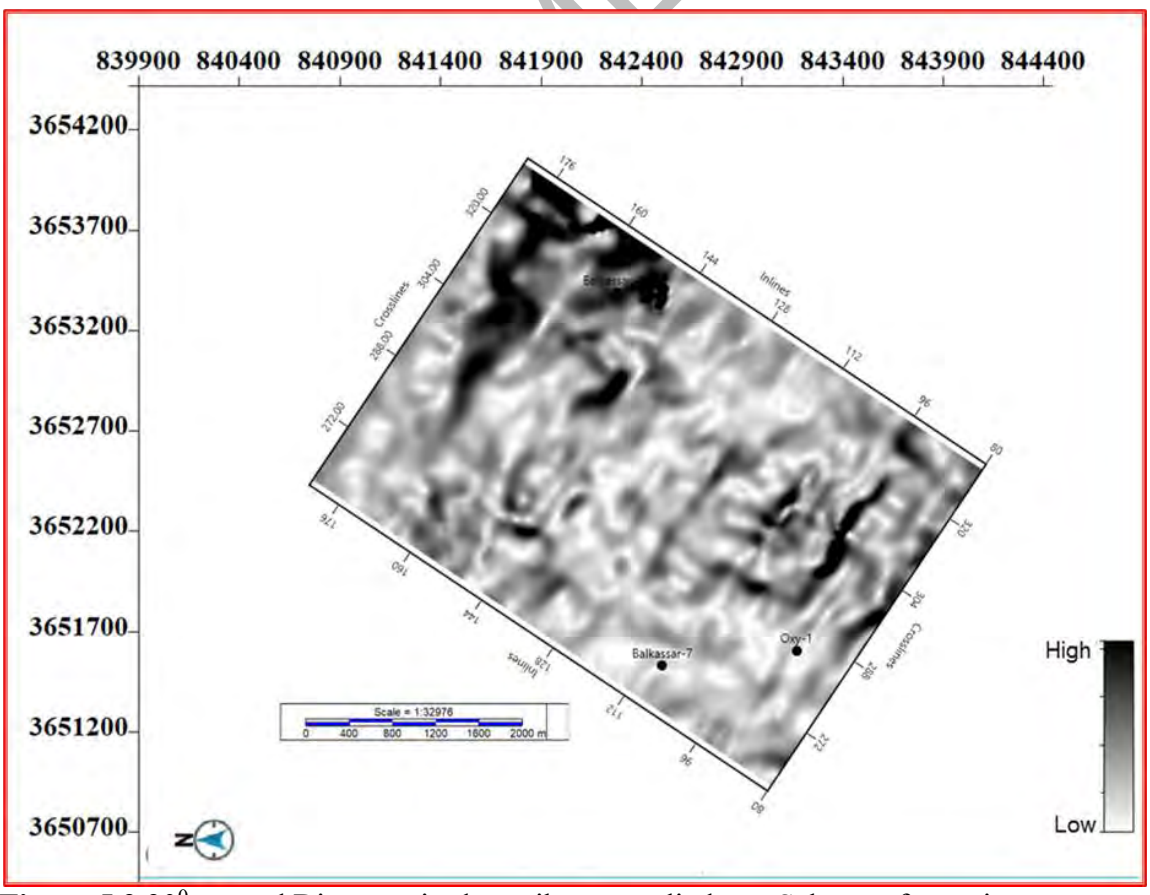

Figure 5.2 90^0 rotated Dip magnitude attributes applied to a Sakessar formation.

5.2.2 Dip steered semblance of Chorgali and Sakessar Horizon

The terms "semblance attribute" and "dip-steered semblance" are interchangeable. The dip is taken into account when calculating the waveform's trace-to-trace similarity. This required the calculation of a dip-steering volume, which was then utilized to conduct similarity analysis from the original seismic volume. It provides a more accurate depiction of cracks in horizon slices because it considers structural dip.

Dip steered semblance attributes is applied to the Chorgali horizon to see the fractured similarities at this level. From the Figure 5.3 we can say that there is a very high trace similarity at OXY-1 well and hence no fracture. This figure clearly depicts that OXY-1 well has a high dip steered semblance and shows that porosity will be very low at this level.

Dip steered semblance attributes is also applied to a Sakessar level to see the trace-to-trace similarity. From the Figure 5.4 it is clear that we have a very high similarity of traces at OXY-1 well and thus we have no fractured zone.

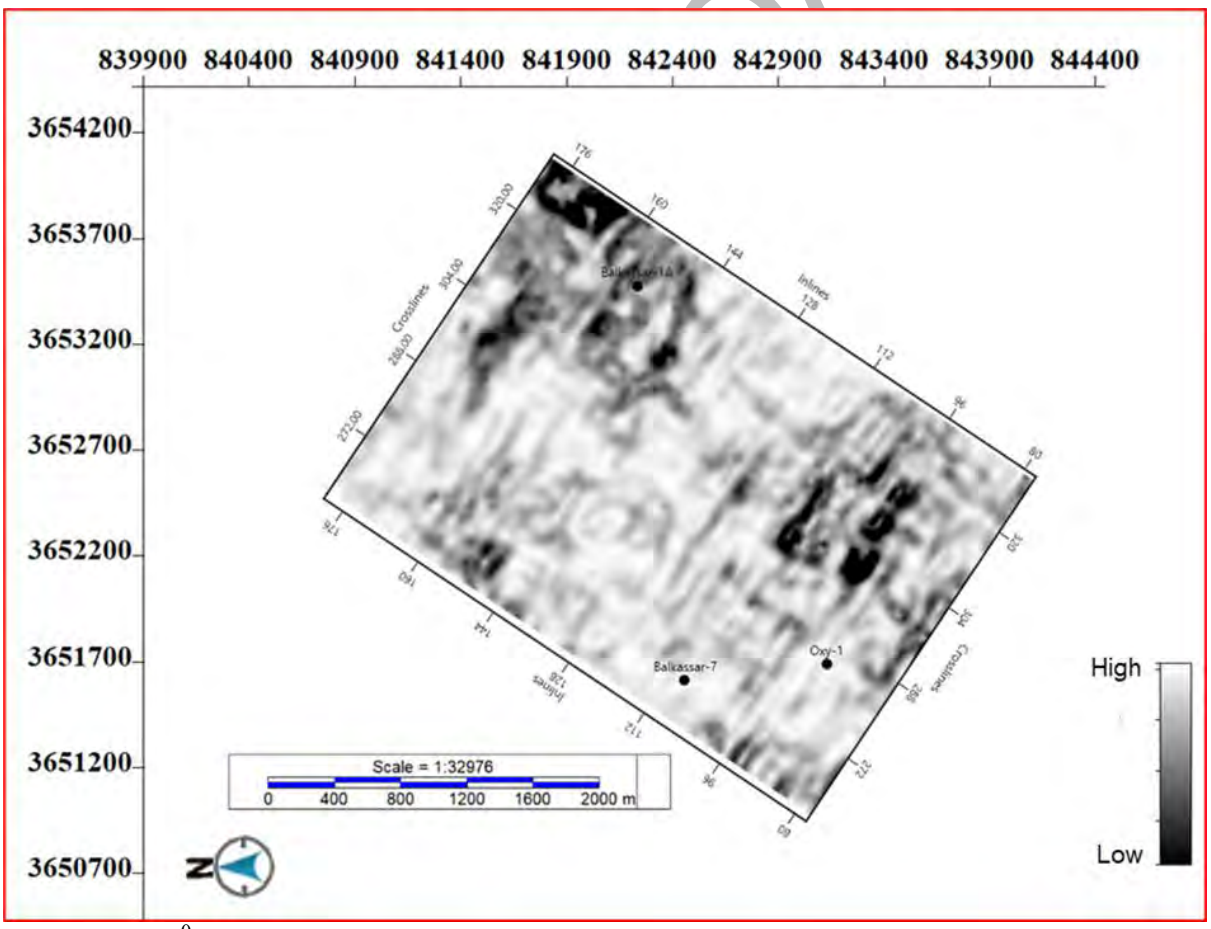

Figure 5.3 90^0 rotated dip steered semblance attributes applied to Chorgali Formatoin.

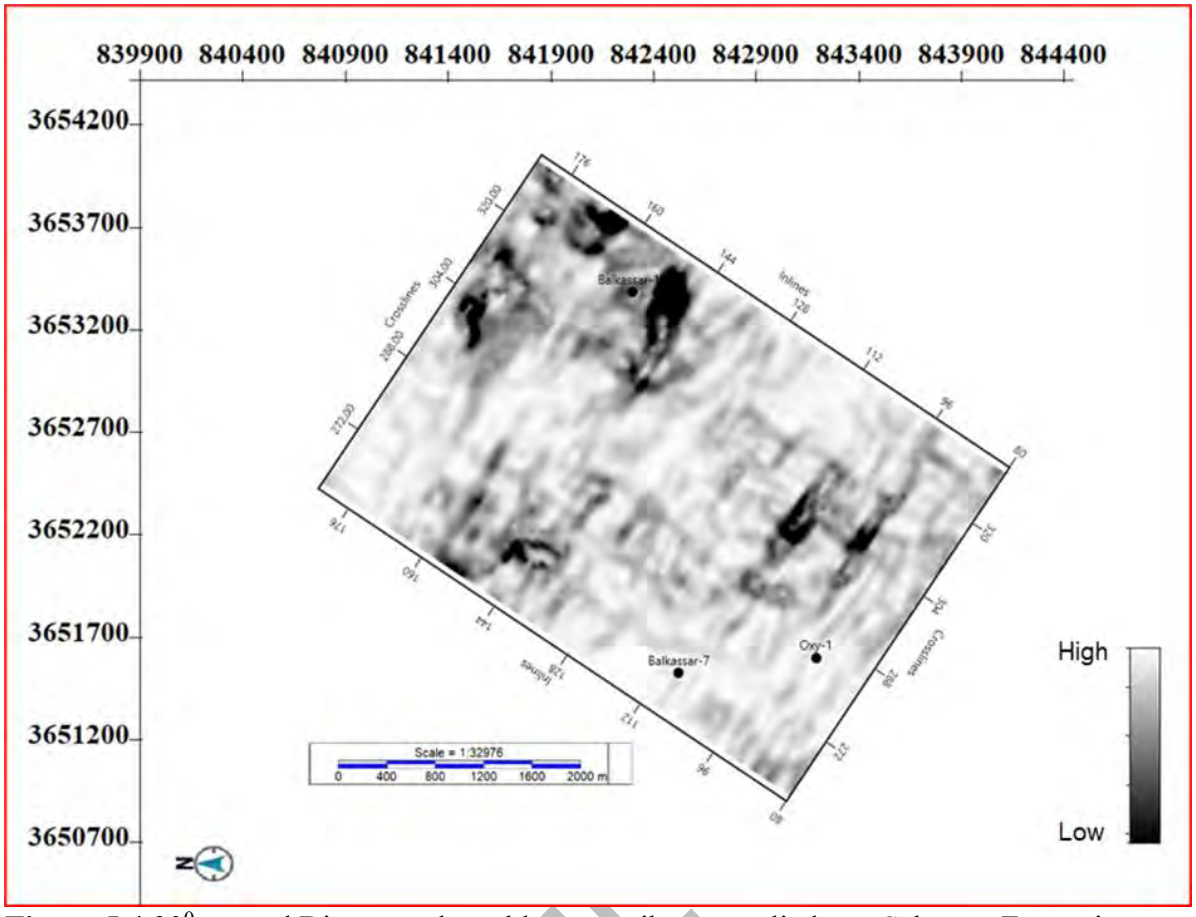

Figure 5.4 90^0 rotated Dip steered semblance attributes applied to a Sakessar Formation.

5.2.3 Enhanced-Coherence of Chorgali and Sakessar Horizon.

In reality, coherence is the reciprocal of discontinuity. It detects the continuity of seismic event. It is often a low similarity of reflection compared to a surrounding shows fracture. And the low coherency is the indication of the presence of fractures.

This attribute is applied to check the continuity of fracture at Chorgali level. The light colors shows very high continuity between the fractures and the dark color shows discontinuity at Chorgali horizon but the fractures at the well OXY-1 location is very low hence very low porosity at this level.

This attribute is also applied at Sakessar level to check the continuity of fractures. The fracture at this level is very low. The light color shows very high continuity of traces while the black color shows the very less continuity of fractures at this level. This attribute is nicely matches the results obtained from the petrophysical analysis.

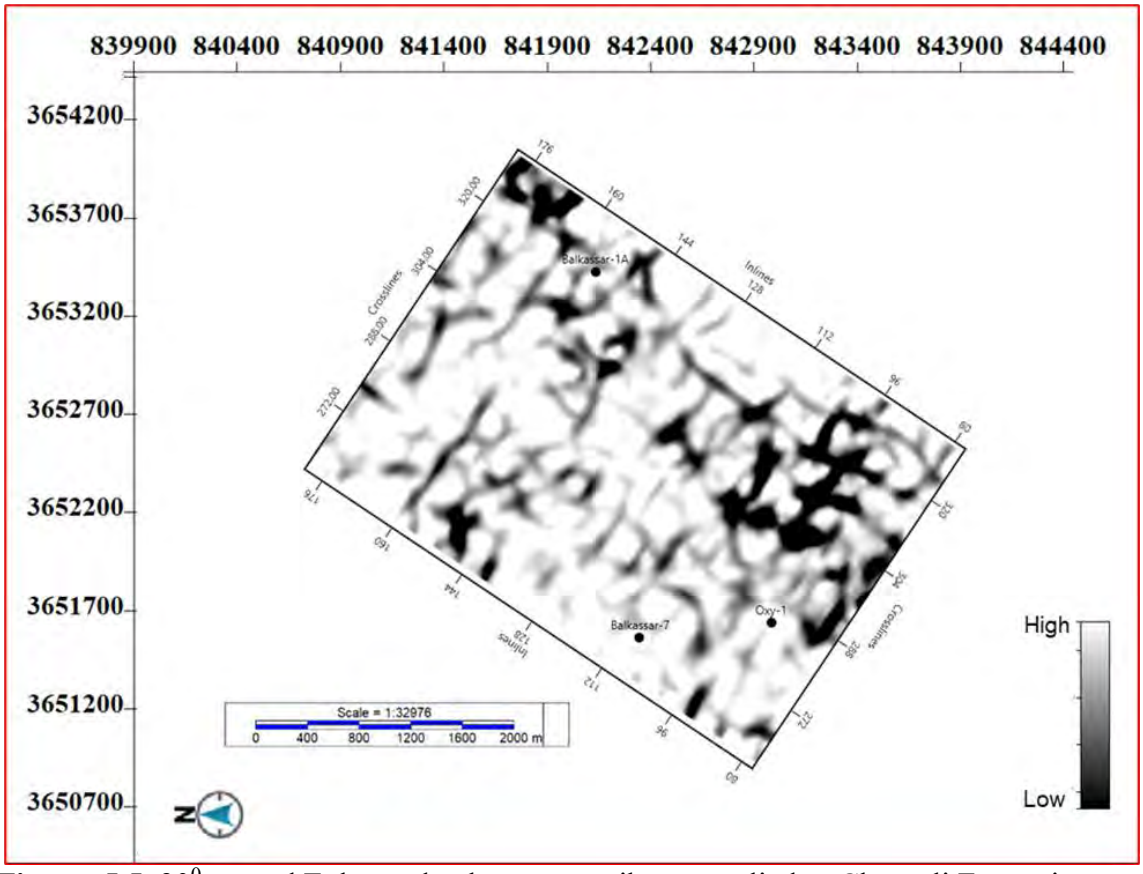

Figure. 5.5 90^0 rotated Enhanced coherence attributes applied to Chorgali Formation.

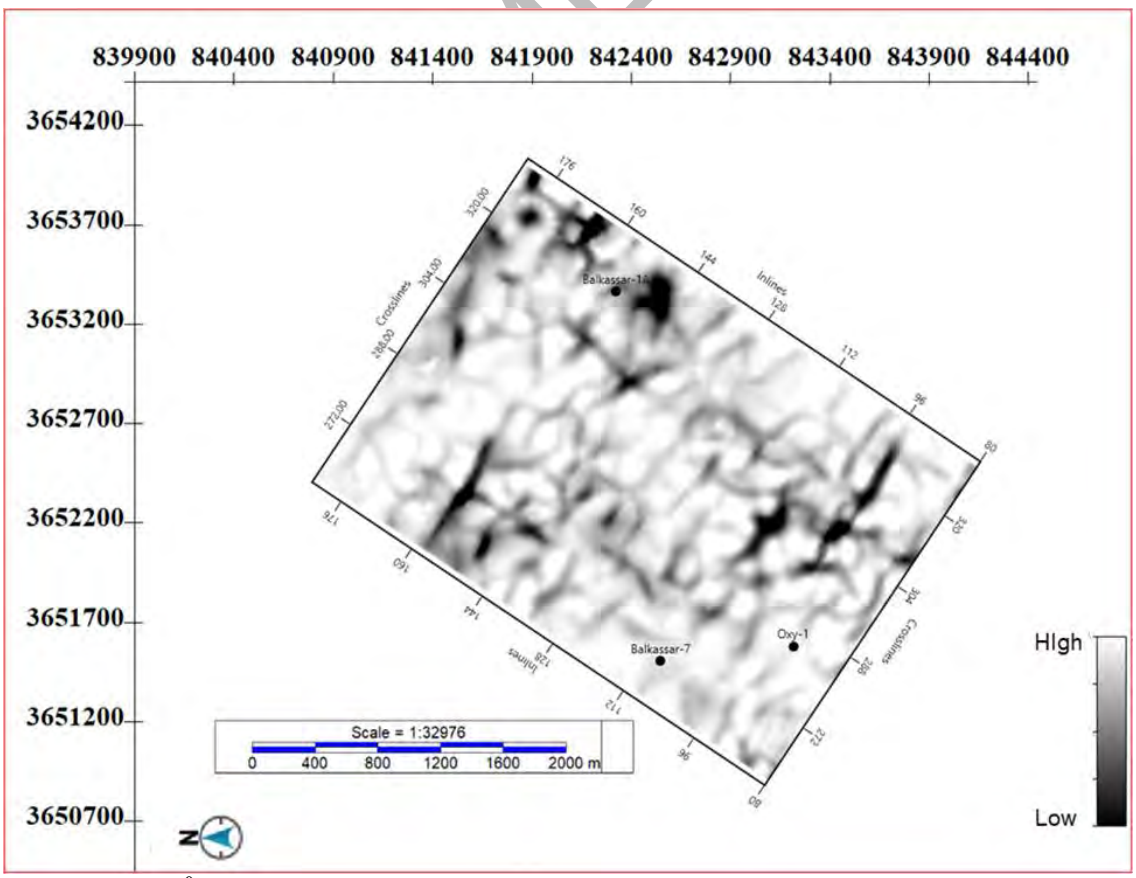

Figure 5.6 90^0 rotated Enhanced-coherence attributes applied to a Sakessar Formation.

5.2.4 Semblance of Chorgali and Sakessar Horizon.

Semblance is a waveform similarity measurement that is used to indicate discontinuity between traces. This attribute aids in the discovery of stratigraphic features like channels and sudden structural changes like faults.

This attribute is applied to a Chorgali formation to see the fracture zone at reservoir level. This picture depicts that it has a very low fracture zone at OXY-1 well and having higher fracture to the SE of this Figure 5.9. The light color shows a continuity of waveforms so from this Figure OXY-1 has a very good continuity at Chorgali level, but no fracture zone exists at the well location. The result of this attribute nicely matched with results calculated from the petrophysical analysis.

The attribute of semblance is also applied to Sakessar horizon which shows very high continuity of waveform but have very low fracture zone. The light color shows continuity of waveform and the black color shows discontinuity or fractured zone.

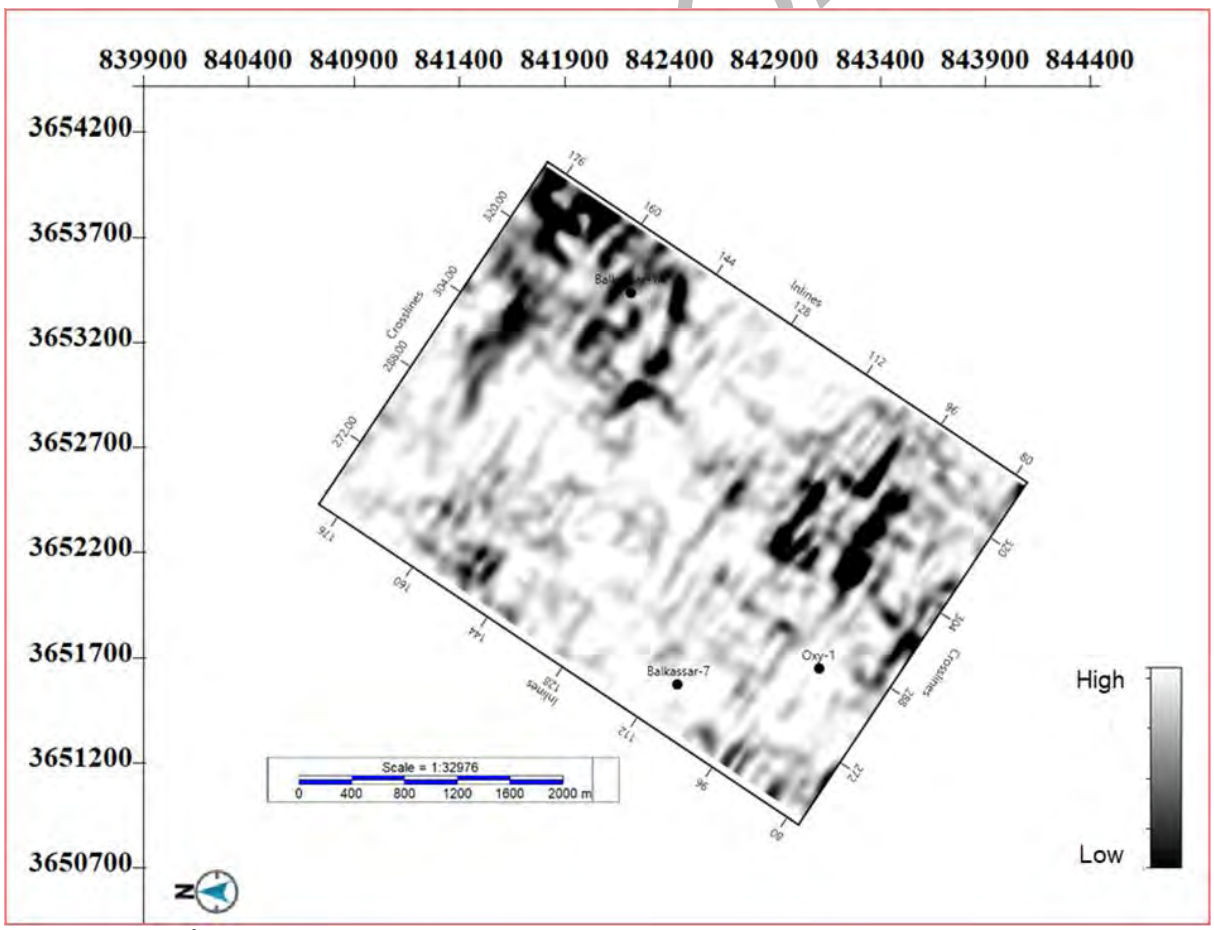

Figure 5.7 90^0 rotated Semblance attributes applied on Chorgali horizon.

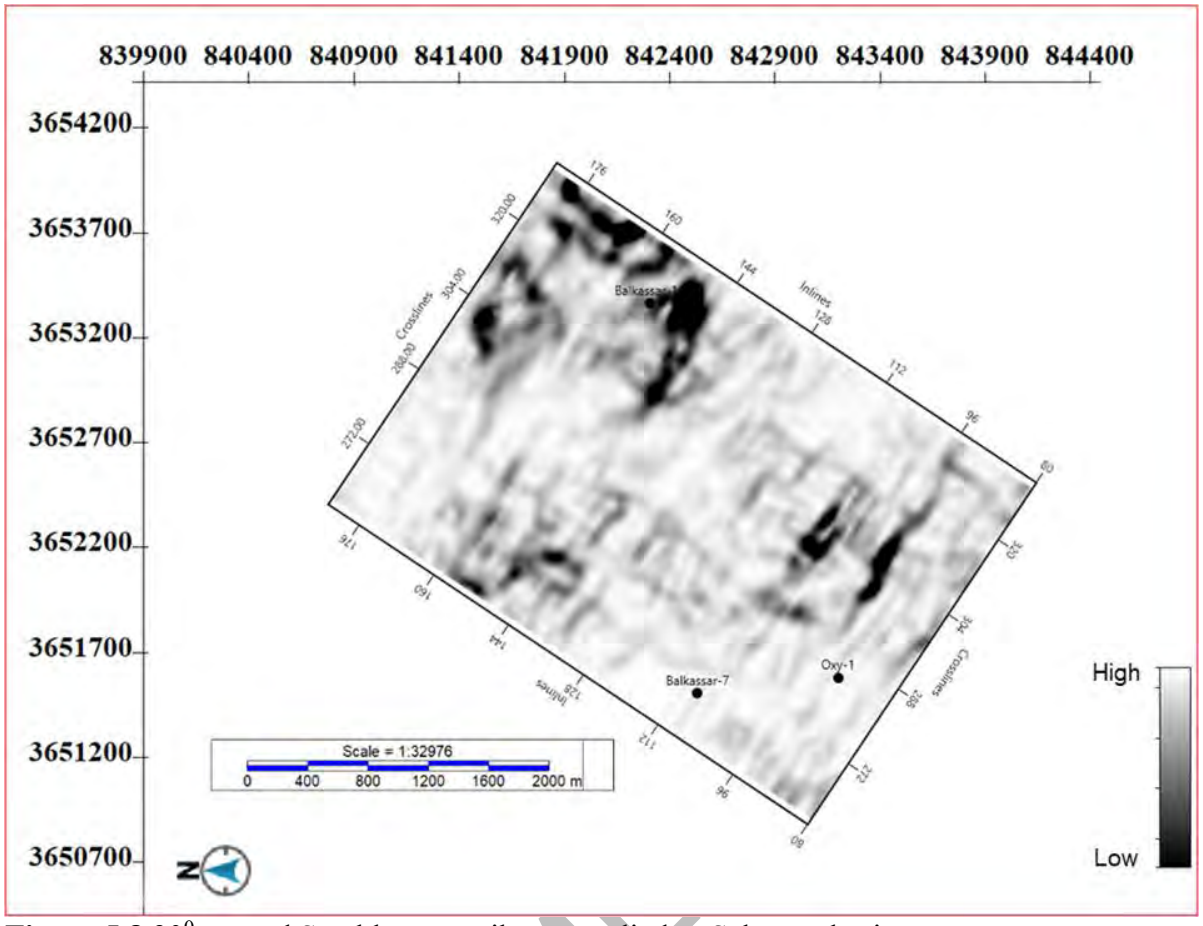

Figure 5.8 90^0 rotated Semblance attributes applied to Sakessar horizon.

5.2.5 Enhanced-semblance attribute of Chorgali and Sakessar horizon

Enhanced semblence is to further improve the quality of the waveform this attributes is applied to measure the similarity of the waveform. This attributes helps us to identfy the fracture, faults and sudden structural changes in the stratigraphic feature.

This attribute is applied at Chorgali level to see the trace-to-trace similarity or continuity between the waves form. The fractures orientation is NW-SE. The light color shows high values of continuity and dark color shows very low values of continuity at this level, although we have a very high values at OXY-1 well location but here we have very low fractures zone at OXY-1.

The enhanced semblance attributes is also applied to Sakessar to check the continuity of fractures. The porosity calculated from the petrophysical analysis at Sakessar level is very low and found no zone for hydrocarbon accumulation. The Figure 5.10 also shows very low fractures at OXY-1 well location hence the petrophysical analysis and attributes analysis are in good agreement with one another.

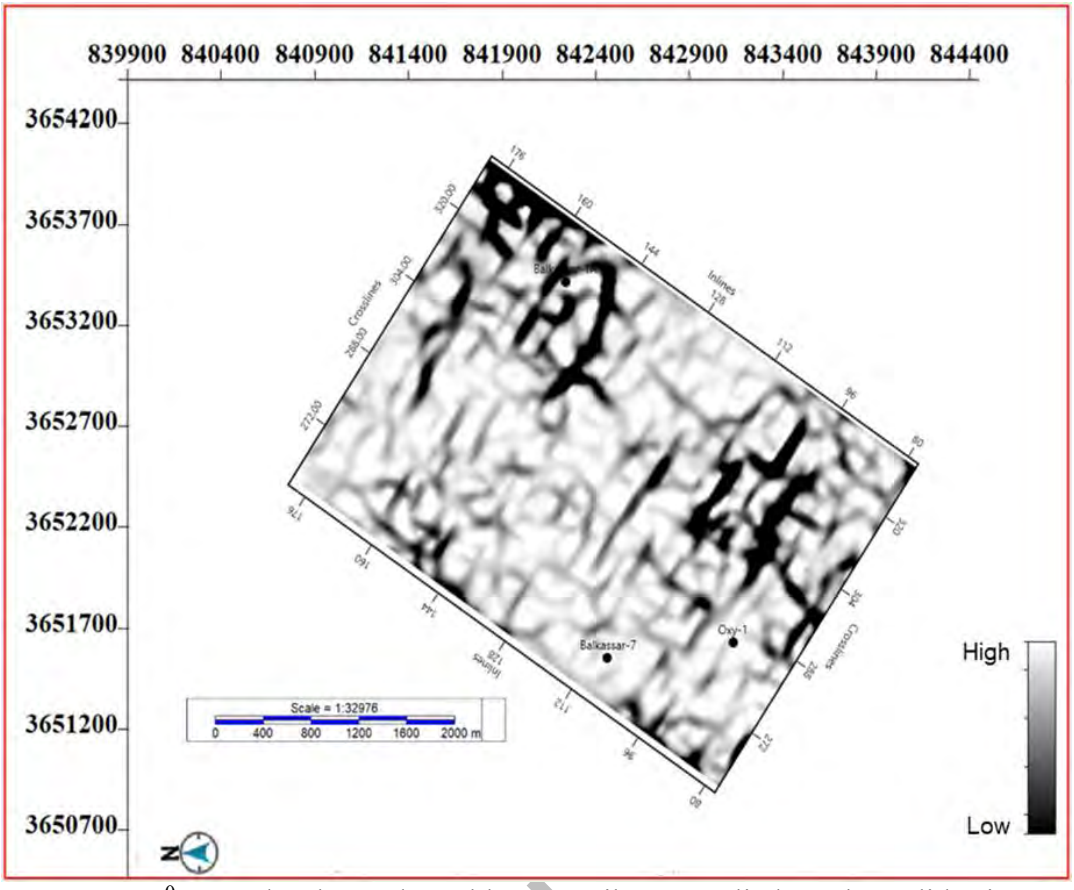

Figure 5.9 90^0 rotated Enhanced-semblance attributes applied to Chorgali horizon.

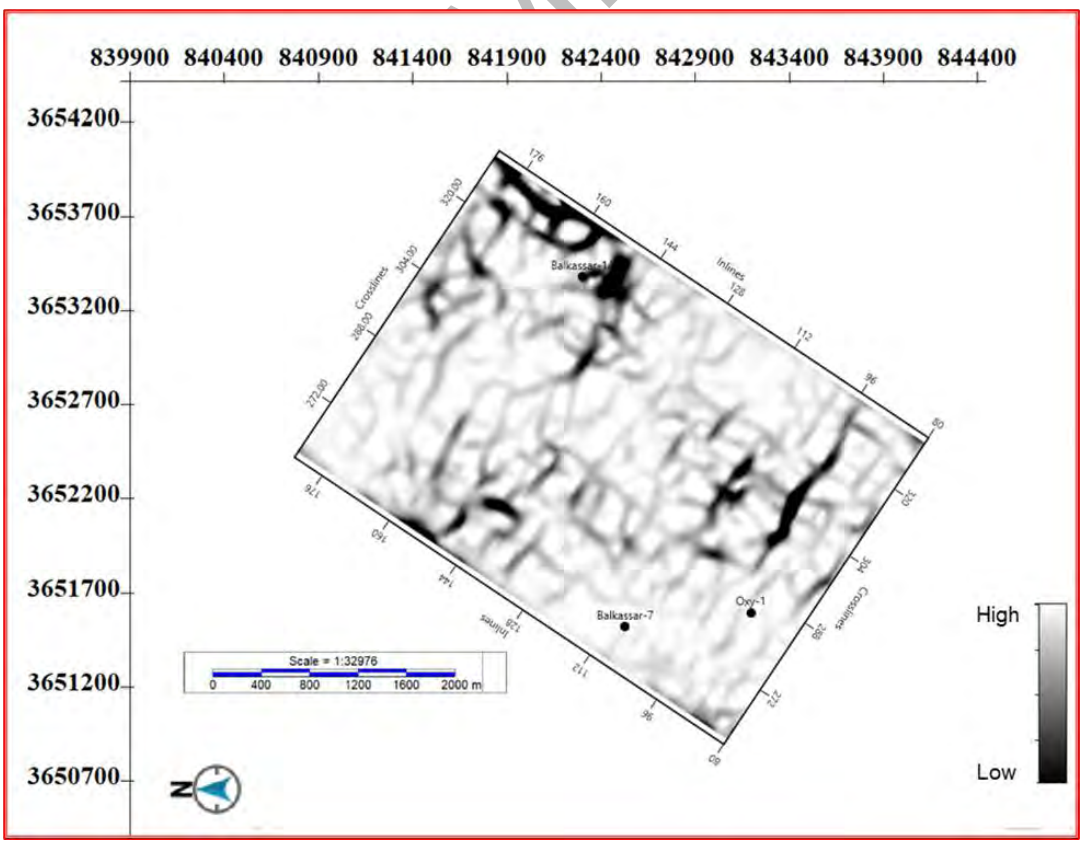

Figure 5.10 90^0 rotated Enhanced-semblance attributes applied to a Sakessar horizon.

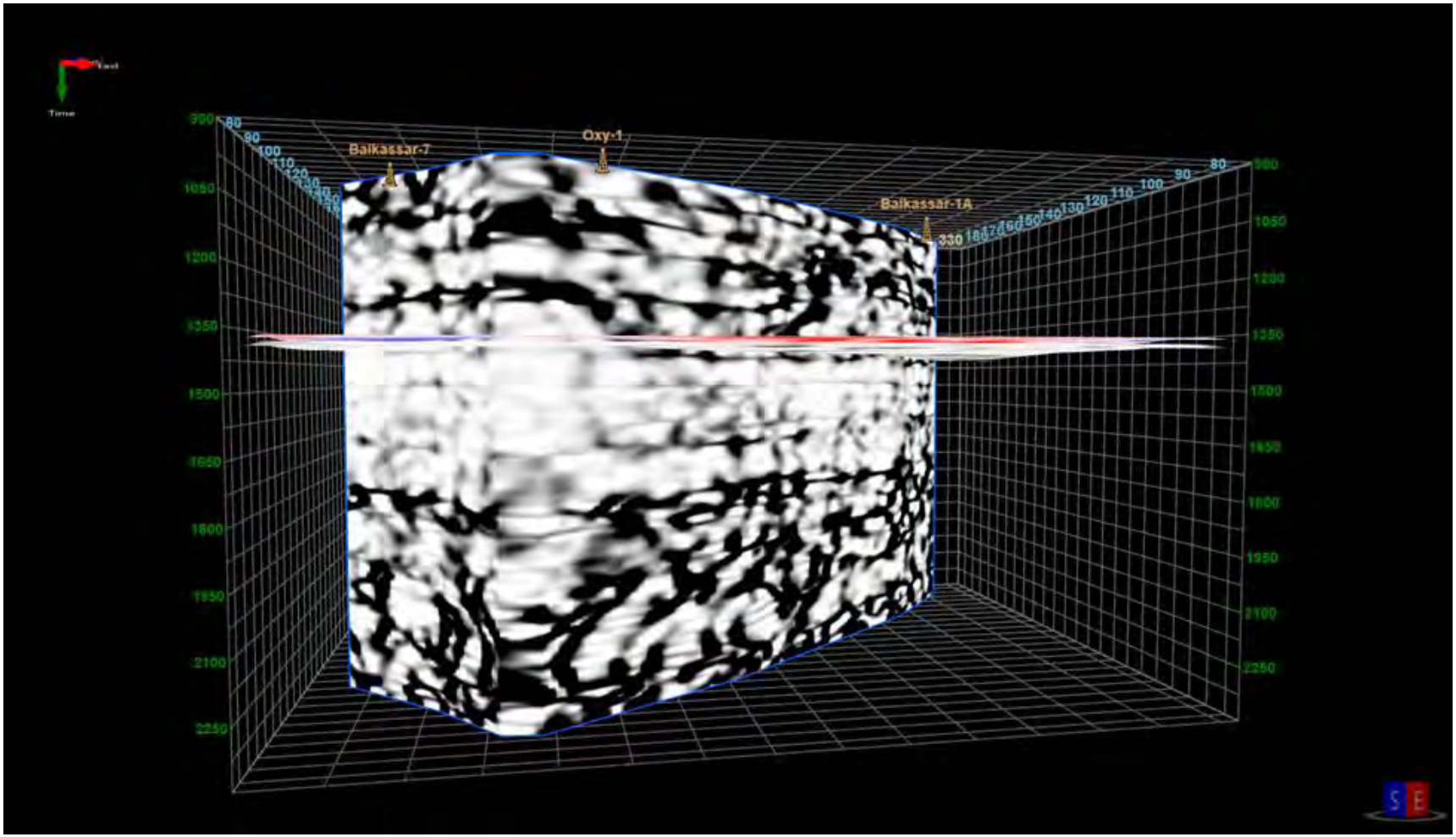

Figure 5.11 Enhanced-coherence- attributes applied to the horizon of Chorgali and Sakessar-3D view.

Sakessar showing very low fracture density hence there is no possibility of Hydrocarbon in at sekessar level.

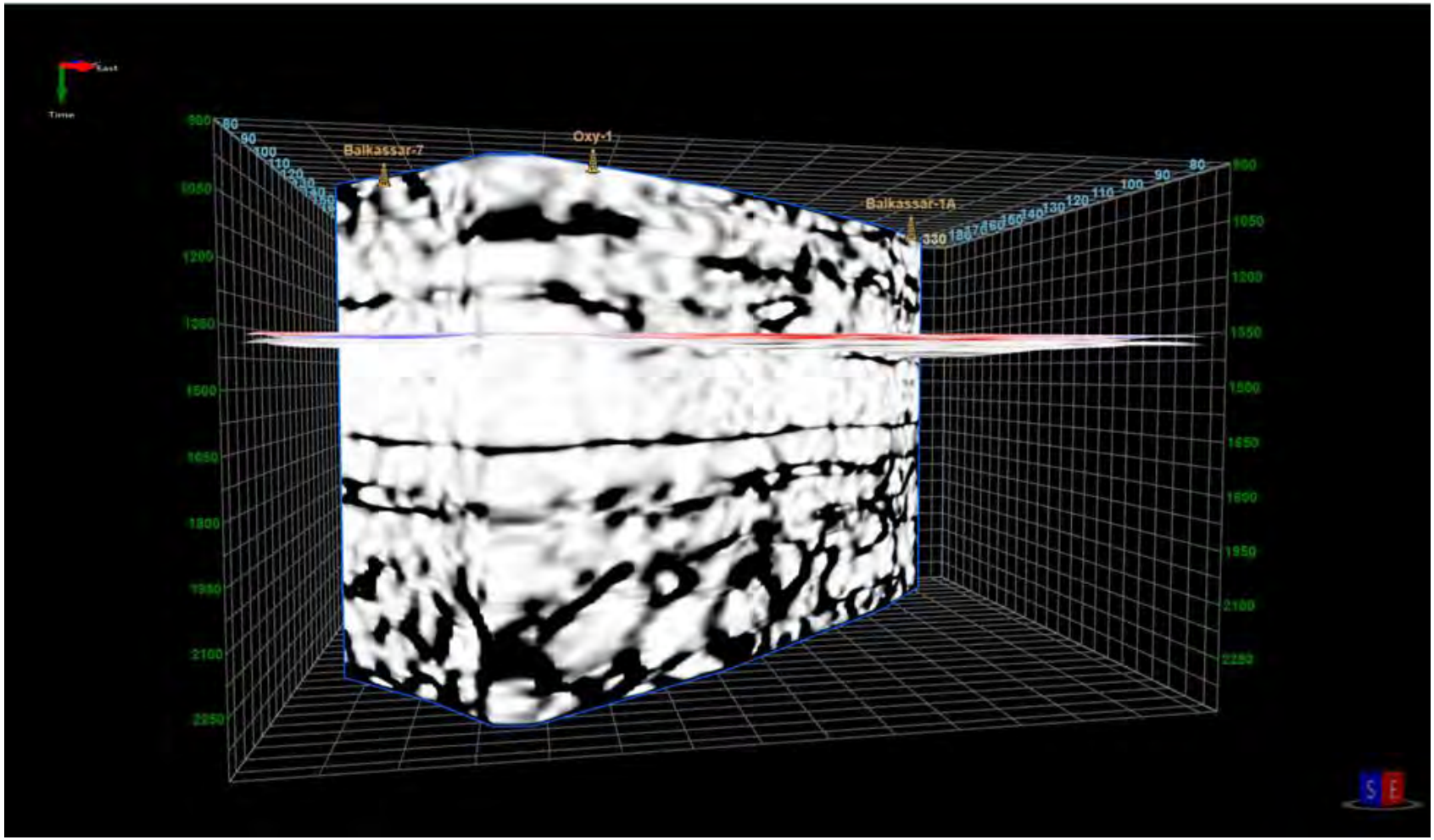

Figure 5.12 Enhanced-semblance with horizonof Chorgali and Sakesser-3D view.

Sakessar showing very low fracture density hence there is no possibility of Hydrocarbon at sakessar level. There is some minor fracture at Chorgali level but the place where OXY-1 well drilled has no significant fracture at this location hence it this the reason of abandonment of this well.

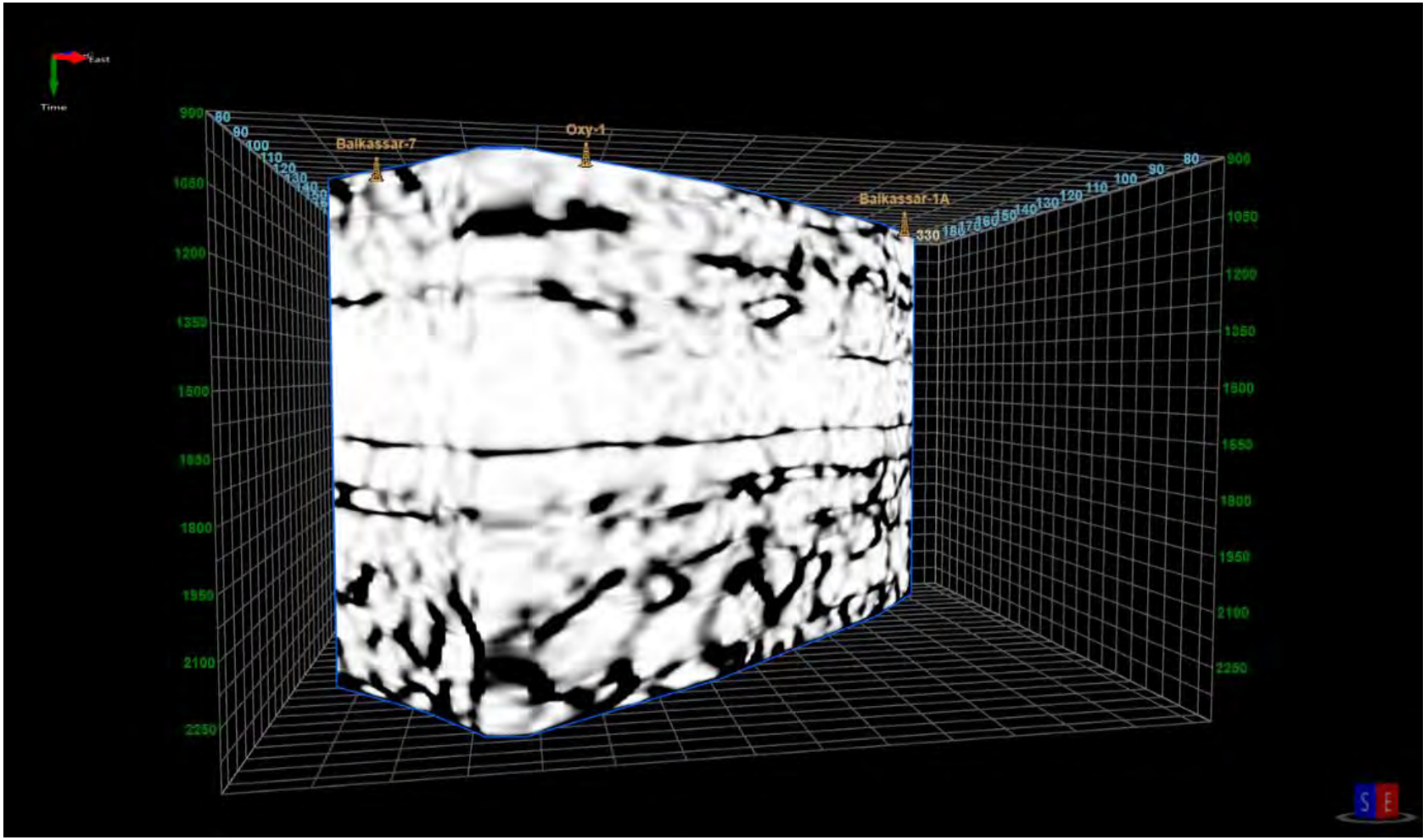

Figure 5.13 Enhanced coherence-3D-view of Chorgali and Sakessar Formation.

From this 3D view of Chorgali and Sakessar horizon it shows that Sakessar has very minor fractured zone and Chorgali formation has very high fracture zone but the location where Balkassar OXY-1 drilled shows very low fractured zone at both Sakessar and Chorgali level.

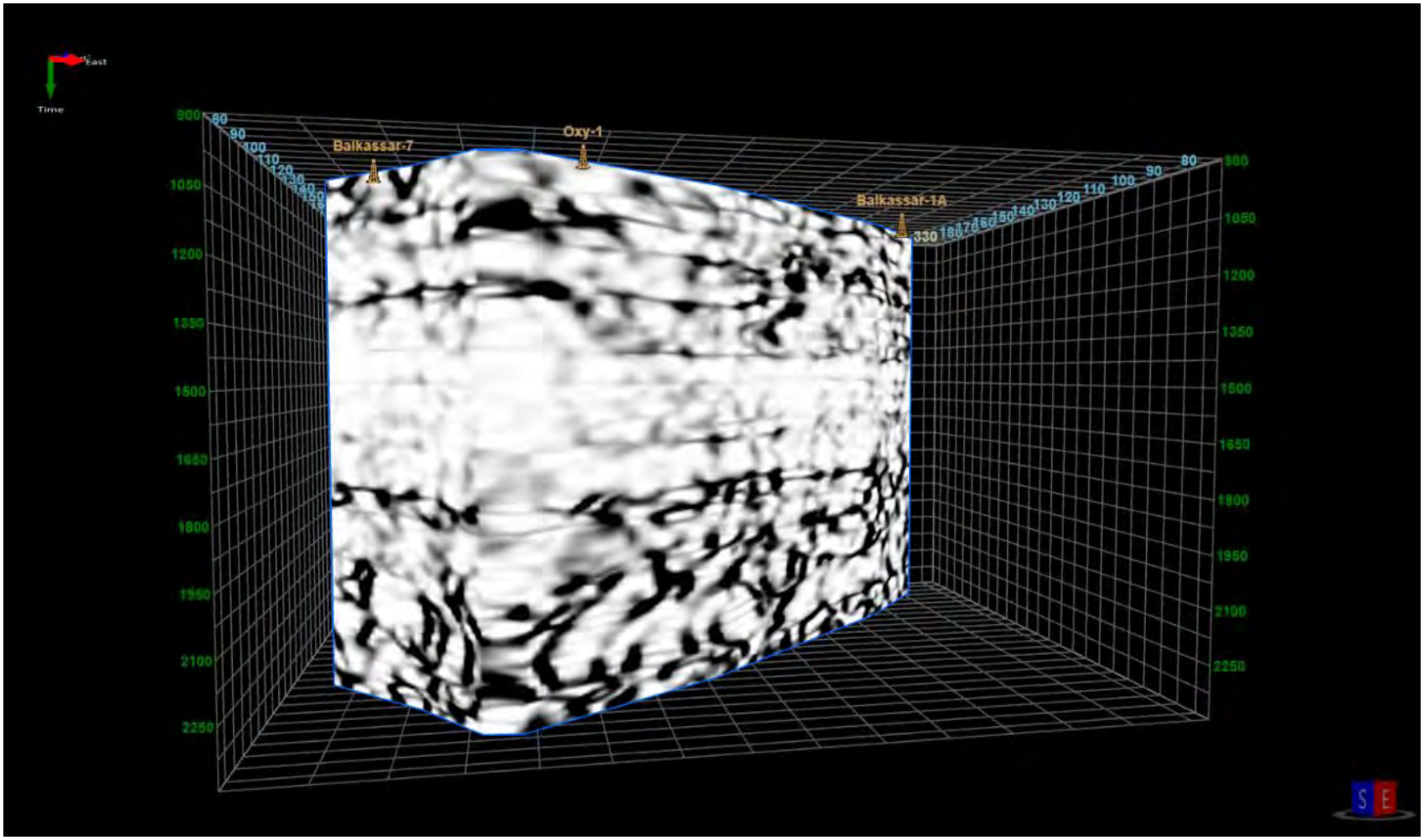

Figure 5.14 Enhanced semblance of Chorgali and Sakessar 3D-view.

From this 3D view of Chorgali and Sakessar horizons. It shows that Sakessar has no fracture and Chorgali formation has very high fracture but the location where Balkassar OXY-1 drilled shows very low fractured zone at both Sakessar and Chorgali level hence this is the reason of abandonment of the well OXY-1.

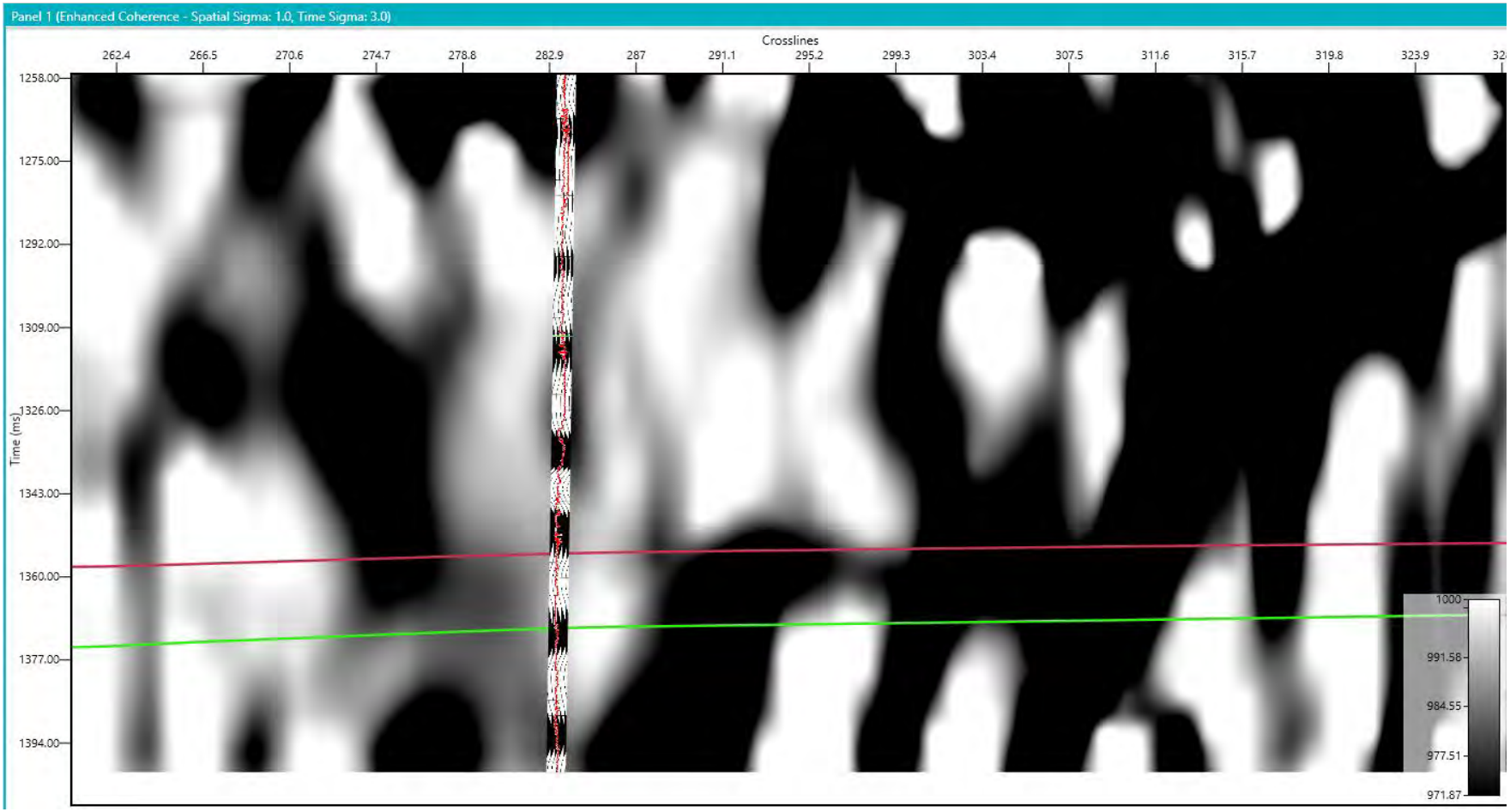

Figure 5.15 2D view of Enhanced coherence of Chorgali and Sakessar Formation.

Red line shows Chorgali horizon and green line shows Sakessar formation. This 2D view Clearly depicts that the well where Balkassar OXY-1 drilled is not at the place where we have a high fracture zone hence there is no chance of hydrocarbon in the well OXY-1 therefore this well has been abandoned.

CHAPTER 6

POST STACK SEISMIC INVERISON

6.1 Introduction to the post stack seismic inversion

A tool nowadays used for the extraction of rock's properties is the seismic inversion (Krebs et al., 2009). Acoustic Impedance is an important reservoir property for inversion specialist and from the inverted model of Acoustic impedance we can derive many physical properties of rocks like porosity, velocity, density, elastic properties i.e., lames parameters and brittleness etc. these all are extremely sensitive to a fluid property (Clochard et al., 2009).

Seismic inversion can be divided into two broad categories i.e., Pre stack and Post stack inversion.

Pre-Stack inversion is used to predict fluid and reservoir properties on seismic data with preserved angular information, such as AVO analysis (amplitude variation with offset) (Margrave et al., 1998).

Post-stack inversion at zero offset is helpful in finding the reservoir property by utilizing the well logs data, geological, seismic data, and this post stack seismic inversion converts seismic data which is in amplitude to acoustic impedance (Downton, 2005). At the end this final AI model can be used to extract the reservoir property from the reservoir at reservoir scale (Veeken and Da Silva, 2004).

Post-stack inversion turns the reflected seismic waves in amplitude into acoustic impedance, this property is unique for imaging the rocks unit, and makes it easier to understand key stratigraphic units in the subsurface (Torres verdín, 2008).

Acoustic impedance increases the resolution of the subsurface layers with the indication of the reservoir potential if the problem of side lobes, tuning, and wavelet effects is minimized (Ziolkowski et al., 1998).

Seismic reservoir characterization is most important and critical tool to predict the reservoir properties for economic potential development of the field, to identify and reduction of risk for the new drilling sites very detailed and accurate study of the reservoir behavior is required by applying different geophysical technique (Karbalaali et al., 2013). In order to achieve this goal integrated study of available seismic and well log data is most significant (Torres et al., 2004). 3D seismic data having quite higher resolution in order to identify the formation interfaces deeply where there is higher contrast between upper and low-lying lithology. This is possible

because seismic waves reflected from the interface of lithology where there is contrast in acoustic impedance (Barclay et al., 2008). The acoustic impedance is the product of density of formation and the velocity of seismic waves passing through it. Hence with the help of 3D seismic amplitude data, formation interface properties can be studied in detail rather than full reservoir characterization (Latimer et al., 2000).

With the help of 3D seismic data, we cannot characterize the full reservoir rock properties because 3D seismic amplitude is property of interface not full rock properties (Pendrel et al., 2007). Now to overcome this limitation of 3D seismic data for obtaining rock properties seismic inversion is used extensively in Geophysical field.

The part of Upper Indus basin that is the Potwar plateau has been extensively studied by the researchers to assess the petroleum system and the associated HC potential.

This research mainly focuses on the evaluation of reservoir characterization from the seismic 3D data and borehole data by applying the post-stack inversion technique.

A seismic 3D data and borehole data from one well (Balkassar OXY-1) is assimilated in our inversion technique. The well logs data consisted of SP log, Gamma ray log, Resistivity log, Caliper log, Density log, and Sonic log and the seismic data consists of 118 inline and 72 cross lines. In this research work, following types of inversion analysis is performed to identify the hydrocarbon bearing zone in the reservoir and other reservoir properties i.e porosity.

1. Model-based seismic inversion
2. Sparse-spike inversion

Results of these inversion are nearly analogous; both the inversion is applied to convert the data from amplitude to acoustic impedance for better visualization but the results of Model-based inversion were far better than Sparse-spike inversion.

6.2 Model-based inversion

Model-based inversion is most suitable technique for inverting the reservoir properties through seismic amplitude data because it reduces the risk of recursive inversion by continuously changing the low frequency model in order to provide the best least square fit (Russel, 1991). Acoustic impedance of earth is recovered using the seismic inversion by which then porosity and other lithological properties can be evaluated (kneller et al., 2013). In Model-based post stack inversion Density and DT logs are combined with seismic data to enhance the resolution of seismic data.

6.2.1 Algorithm for Model-based seismic inversion

In Model-based Inversion we firstly extract wavelet from the original seismic data after this we generate the initial impedance model then this initial model in congestion of the wavelet, we will generate a synthetic trace if this synthetic trace best fit the original seismic section then this would be assumed as the final model if not then repeat the model and generate again the initial model until we get a nice match. This process will go on iteratively.

Background algorithm used in MB inversion is quite simple. In this algorithm software assumes that wavelet and seismic trace are already known. During applying this algorithm initial low frequency guess model is modified frequently until the matching between the synthetic trace and actual trace reaches to a proper acceptable level (Gavottiet al., 2014). In simple words initial guess low frequency geological model is altered until the error between original and synthetic trace become minimized. This error can be minimized upto larger level if we have strong background of geological knowledge of that field (kneller et al., 2013).

Approach used in MB inversion algorithm have basic purpose to minimize the function which is shown in Equation 6.1, Because basic assumption in MB Inversion is to reduce and measure error (Misfit) between the synthetic and real seismic data.

$$J = \text{Weight1} \times (S - W*R) + \text{Weight2} \times (M - H*R) \qquad (6.1)$$

J is the Error between the real and Seismic trace which we must reduce up to acceptable level, S is the Original seismic trace, R is the Reflection coefficient series, W is the Extracted seismic trace at well location, M is the Initial guess low frequency geological model or Interpreted reservoir Horizon, H is the Final integration operator which gives the resultant Impedance by convolution with reflectivity series R.

At the end Integration operator will be convolved with reflectivity (R) to extract final impedance (Gavotti et al., 2014). First part of Equation 6.1 models the original seismic trace and second part of the Equation 6.1 models the low frequency initial Guess geological model. Some constraints are used in MB Inversion to reduce the noise and error.

First constrained (hard constrained) is a well data which is generally controls the random noise and modeling error. Second constrained is initial low frequency geological model which can be incorporated using variogram model. Advantage of all these constrained is to reduce the noise and error between the synthetic and real model (Gavotti et al., 2014).

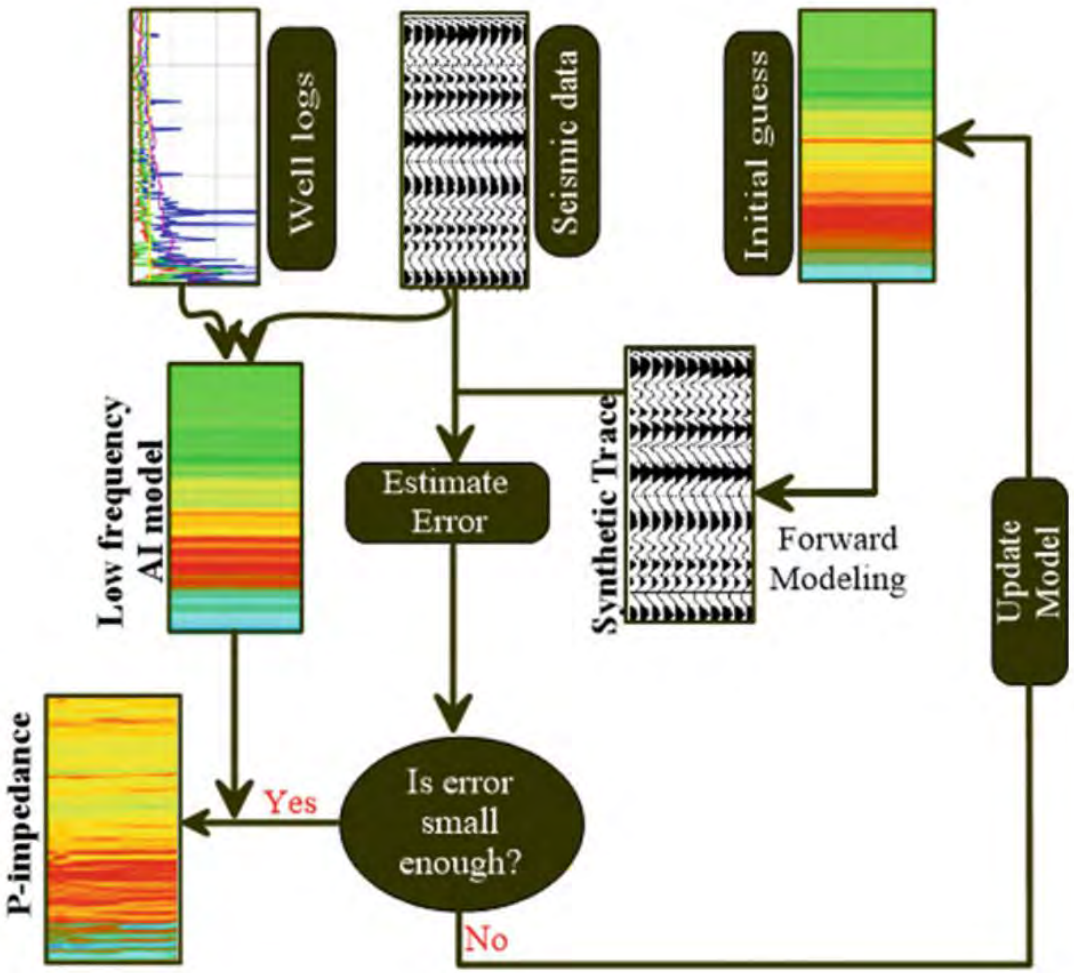

Figure 6.1 Schematic work flow of Model-based seismic inversion (Maurya et al., 2020)

6.2.2 Wavelet extraction process

Wavelet is basically approximation of wave pulse for a seismic source which may contains many frequencies, and it is time limited. In inversion process wavelet is very necessary because it is used in correlation with seismic trace (Cooke and Cant, 2010).

To perform the seismic inversion a Zero phase wavelet is extracted through HRS software as shown in Figure 6.2. This wavelet is then used in correlation of inverted and original extracted reflectivity series at well location of OXY-01. Estimated correlation between the synthetic and real trace was 0.8845l with the wavelength of 100ms.

To obtain most accurate and desirable results in 3D seismic data interpretation and Post stack inversion analysis extracted wavelet should be Zero or minimum phase (Jain, 2013). Phase shift amount of input extracted wavelet play very important role in full inversion analysis. If the phase shift will be larger than there will be quite higher error in final impedance results (Kallweit et al., 1982).

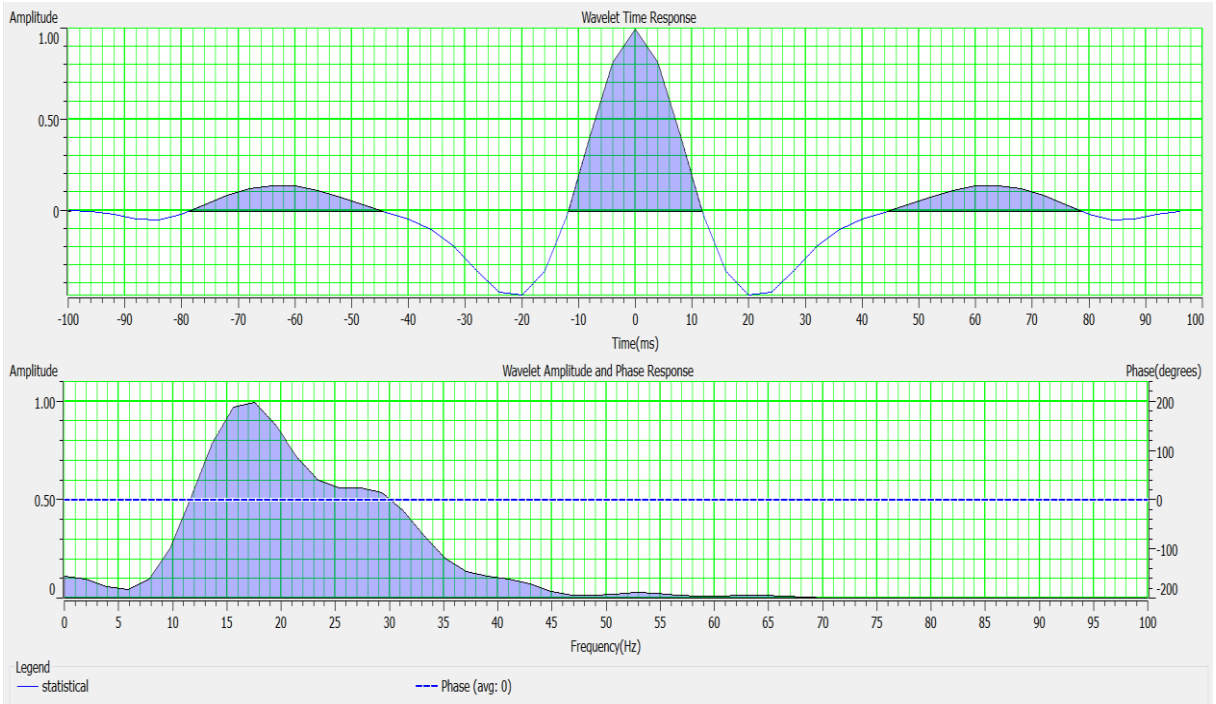

Figure 6.2. Full wavelet in time and frequency domain. Total length of extracted wavelet is 100 ms and phase of extracted wavelet is set to be constant. (a) full wavelet in frequency domain (b). The straight line which intersects the frequency domain wavelet illustrate the phase of wavelet.

6.2.3 Background Low Frequency Geological Model

Low frequency model plays a key role in MB Inversion. During the seismic data processing for reducing noise and due to band limited nature of 3D Seismic data low and high cut filters are applied. Due to these filters highest and lowest frequencies are missed in final PSDM seismic data.

These low frequencies having a lot of information about fluid properties, Porosity, permeability, and other reservoir properties which are very essential in reservoir characterization (Sukmono, 2002).

To enhance the accuracy and for a unique solution we must have to incorporate the Low frequency model in Inversion algorithm (Sorneo et al., 2007). Initial model used in inversion algorithm is obtained by interpolating the Acoustic impedance from well which is present in data as OXY-01 in this research. Two logs sonic and density are used to generate the Al from well and then this Acoustic Impedance is displayed in the form of single log in calculation window. After generating the AI log, this is filtered using 10-15 HZ high cut filter to obtain the Initial low frequency geological model for inversion algorithm. This process is performed

only to retrace the low frequencies component those are removed during processing in PSDM seismic data (Lindsith, 1979).

There is different algorithm suggested by authors in literature to generate the low frequency model for MB inversion such as linear programming, Autoregressive algorithm and generalized linear inversion (Schneider, 1983). Background low frequency model used in MB Inversion is shown in Figure 6.3.

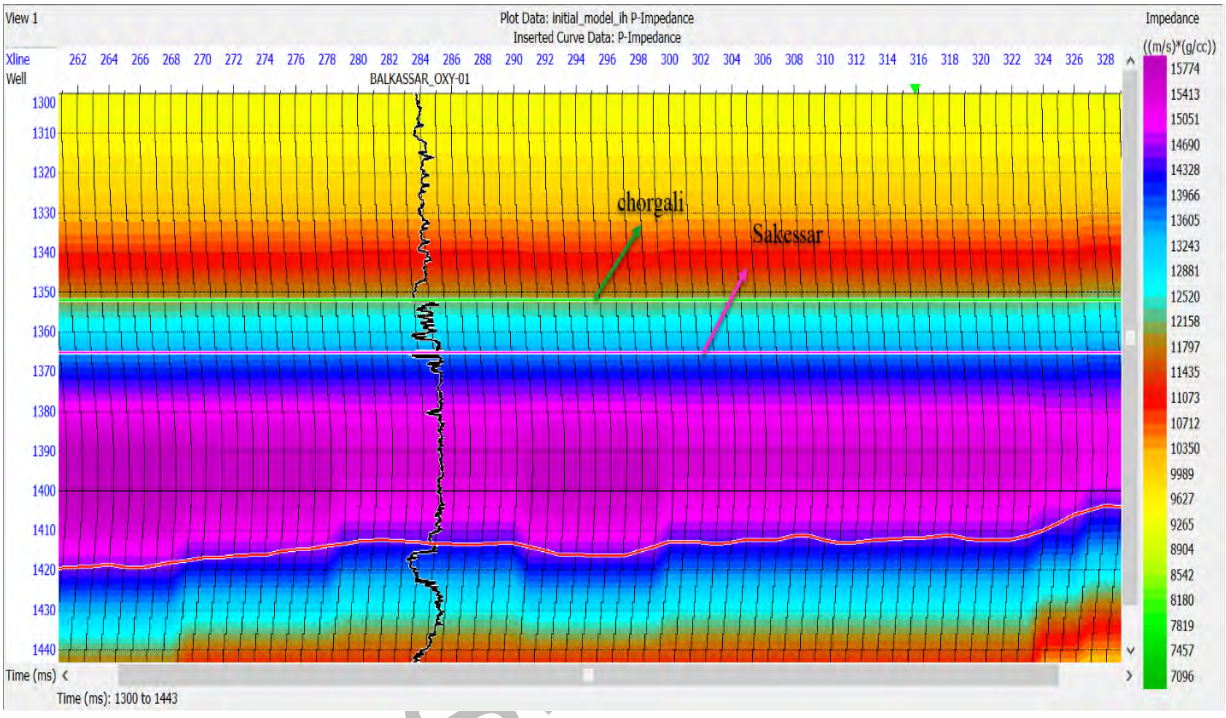

Figure 6.3. Background low frequency impedance model on inline 90

6.2.4 Inversion Analysis

Inversion analysis is performed at well location of OXY-01 for Model-based inversion on provided 3D Seismic cube of Balkassar as shown in Figure 6.4. First of all, a statistical wavelet was extracted in time window of 1330-1430 ms to cover the full reservoir range. The Impedance extracted from well log data is compared with the inverted impedance in time window of 1330-1430 ms. From Figure 6.4 (a) it is clear that inverted Impedance (Red curve) nearly follow the same trend as original impedance from well (Blue curve) with an error of (1360.01) while the black curve is representing the background low frequency Impedance curve. Next window (b) 1s representing the extracted constant phase statistical wavelet while the window (c) and (d) shows the synthetic and seismic trace respectively. It is clear from the Figure 6.4 that there is best correlation between the synthetic and seismic trace with higher

value of correlation coefficient 0.999 which shows that results of inversion analysis are correct and consistent. RMS Error between both these traces is quite low with value of only 3% (0.0388) as shown in Figure 6.4.

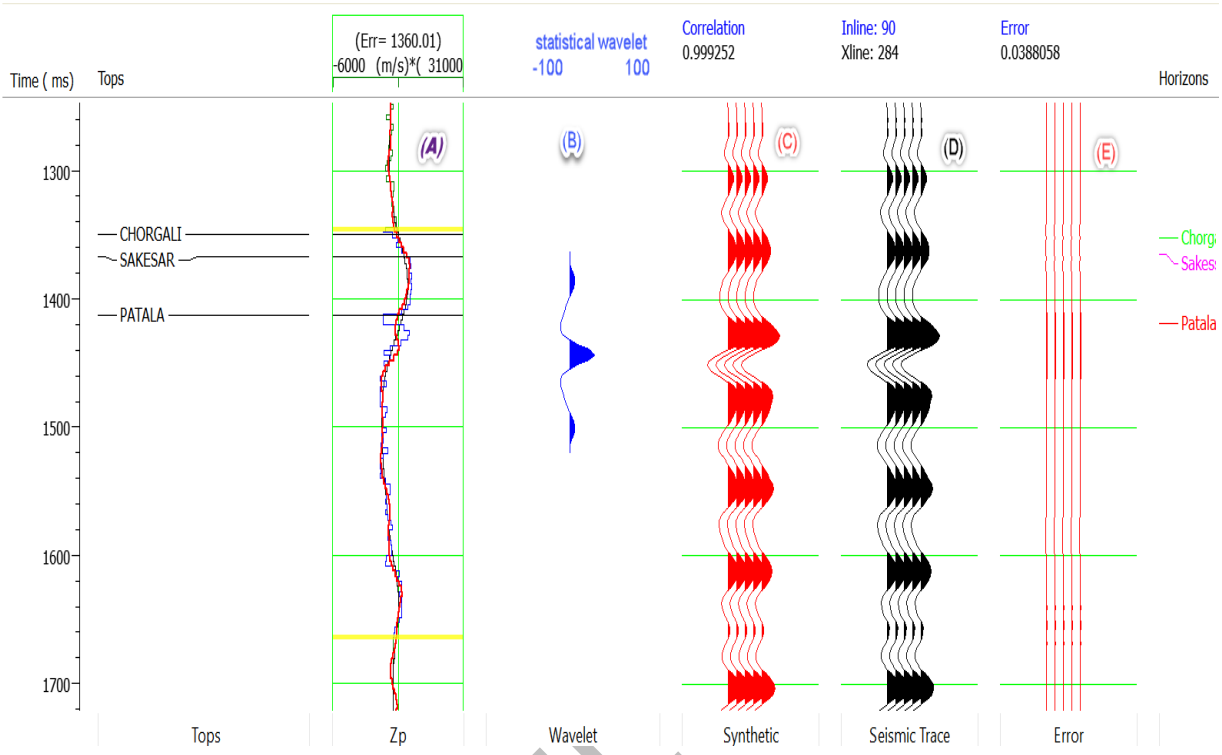

Figure 6.4 Analysis of Model-based inversion at well Balkassar OXI-1: block (A) the blue color shows filtered impedance log, black color is the initial model, red color line shows inverted acoustic impedance log ; (B) shows statistical wavelet in blue color; C) red color shows synthetic trace derived from inversion ; D) black color shows Extracted trace from the seismic . (E) shows RMS error between the synthetic and seismic traces.

6.2.5 Results and Discussion for Model-based Inverted Acoustic Impedance

Model-based inversion is performed on the time window 1200-1500 ms generally to cover the reservoir zone. As it was discussed in Petrophysics that Chorgali is producing reservoir in Balkassar with major hydrocarbon component as oil. From petrophysics in Chapter- 04 1t was predicted that there is a good productive reservoir zone at 2424-2427m in Chorgali formation where there is quite higher porosity, Suitable separation between the LLD and LLS and Positive cross over between the NPHI and RHOB at 2424 to 2427 which have the 44% of HC. This oil-bearing zone is also predicted on inversion results as shown in Figure 6.5 with low acoustic Impedance. The upper layer from it with yellow color having quite higher AI is shale layer of Chorgali formation and Shale and clay Stone of Murree formation which are acting as seal in this There is quite higher AI value in Sakessar formation because it is not so good productive

reservoir in Balkassar as compared to Chorgali which is also confirmed from the petrophysical results. At the time of 1350 ms on inline 90 there is very low acoustic impedance layer which is not predicted as reservoir because it cannot be confirmed as producing reservoir through petrophysics.

Inversion results also showing the good lateral variation in Al and also the inverted section as shown in Figure 6.5, provide better subsurface image as compared to original seismic section. Hence we can say that MB Inversion can be used as a helpful tool in delineating the reservoir and there hydrocarbon potential.

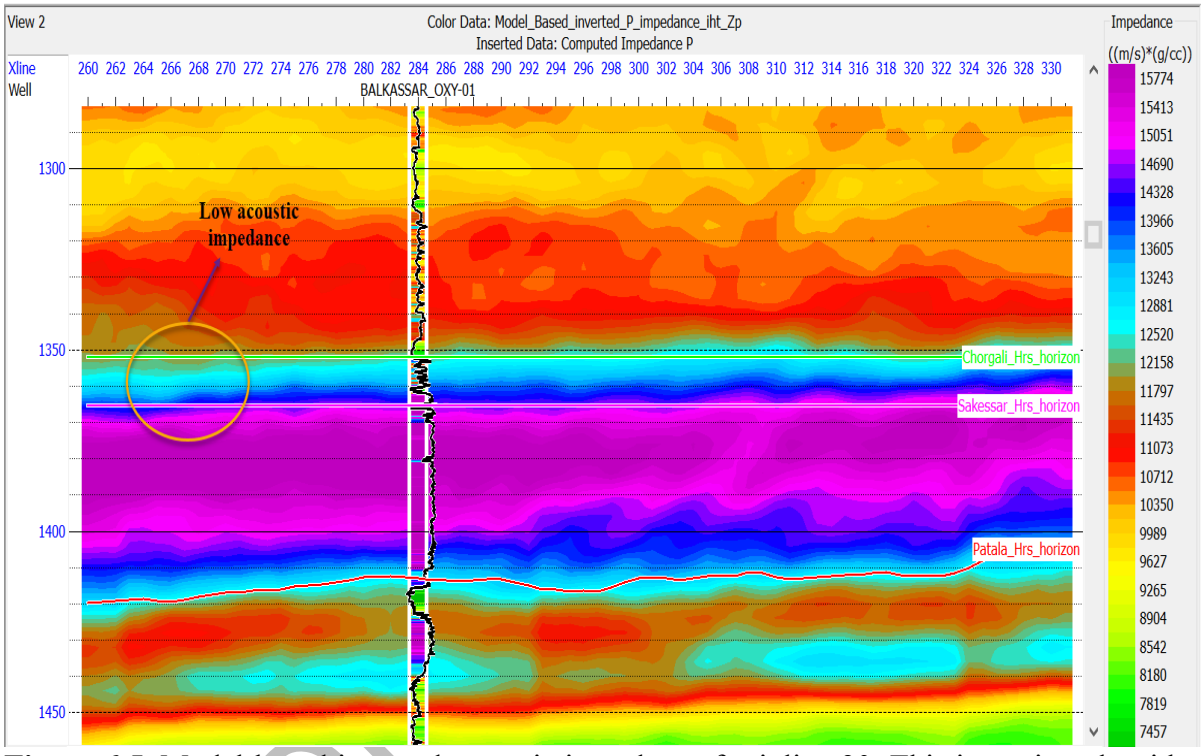

Figure 6.5. Model-based inverted acoustic impedance for inline 90. This inversion algorithm can capture detailed lateral variations of lithology. best location for well is also shown in ellipse at inline 90 but a cross line of 266 to the southwest direction of the map. The horizon Chorgali and Sakessar are also shown in green and pink line respectively.

6.3 Sparse-spike post stack seismic inversion

Sparse-spike inversion based on the assumption that major lithological boundaries represent larger event, and these larger events are the spike on seismic section.

Theoretical procedure of SSI is,

- Calculate reflectivity
- Improve the wavelet
- Again, calculate reflectivity
- Again, improve the wavelet

This procedure can be repeated again and again until we find the best solution of the inversion.

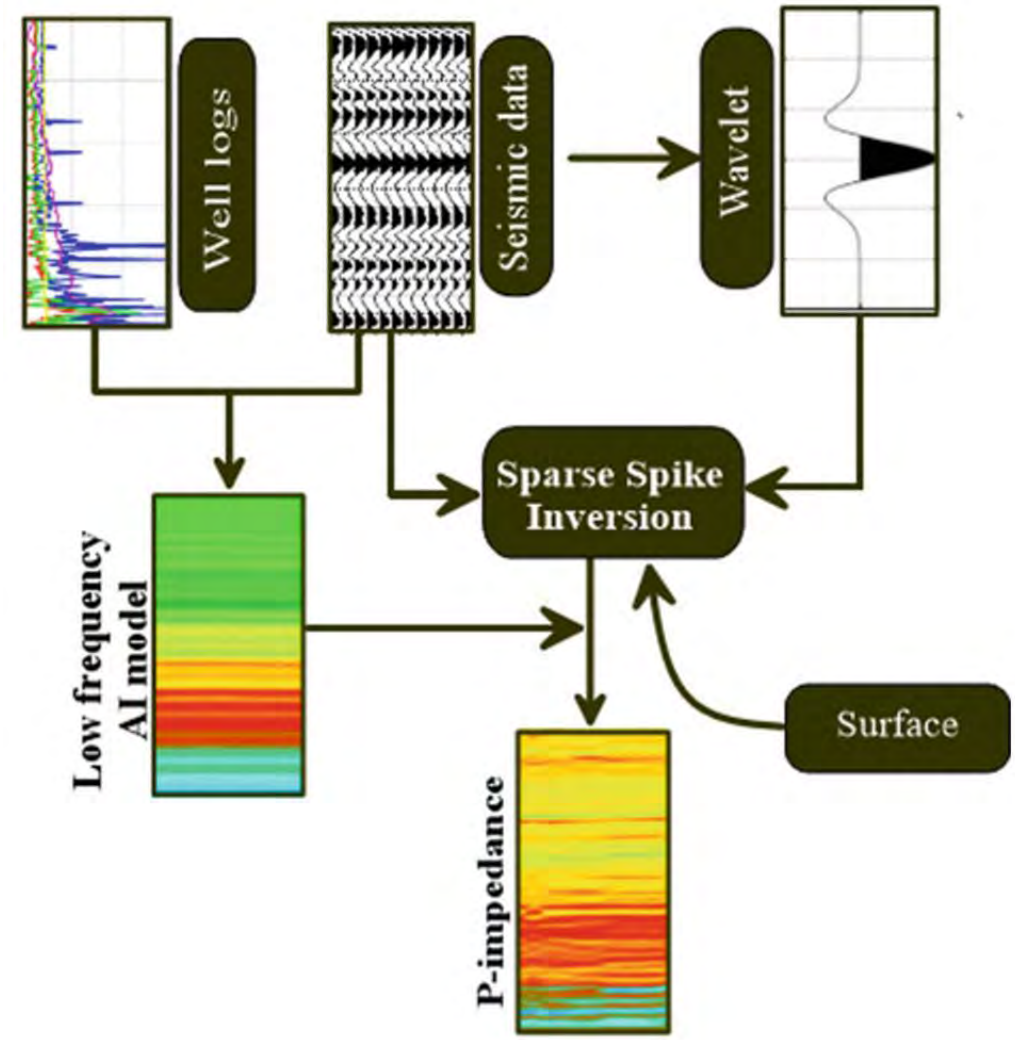

Figure 6.6. Flow chart for Sparse-spike inversion (Maurya et al. 2020)

6.3.1 Wavelet extraction process

To perform the seismic Sparse-spike inversion a Zero phase wavelet is extracted through HRS software as shown in Figure 6.7. This wavelet is then used in correlation of inverted and original extracted reflectivity series at well location of OXY-01. Estimated correlation between the synthetic and real trace was 0.8445l with the wavelength of 100ms.

To obtain most accurate and desirable results in 3D seismic data interpretation and Post stack inversion analysis extracted wavelet should be Zero or minimum phase (Jain, 2013). Phase shift amount of input extracted wavelet play very important role in full inversion analysis. If the phase shift will be larger than there will be quite higher error in final impedance results (Kallweit et al., 1982)

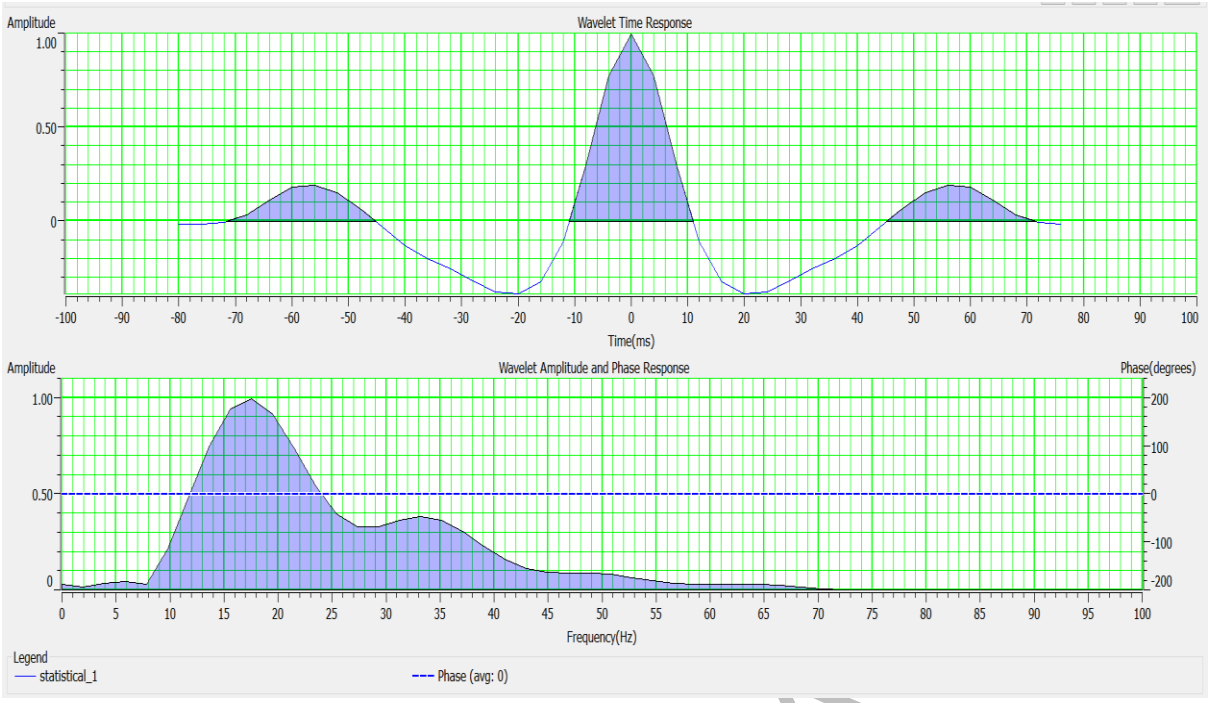

Figure 6.7 Full wavelet in time and frequency domain. Total length of extracted wavelet is 100 ms and phase of extracted wavelet is set to be constant. (a) full wavelet in frequency domain (b). The straight line which intersects the frequency domain wavelet illustrate the phase of wavelet.

6.3.2 Addition of Low Frequency model in SSI.

We add low frequency model into a seismic because it is missing from the data due the below reason. We have not recorded it due to a ground roll problem and it has been eliminated in the processing due to the noise and this might be missing due to the limitation of the Geophone during survey. We add it because in the Absence of the LFM create the false impedance layer on final seismic data.

6.3.2.1 Generation of Low Frequency Model.

- It can be calculated or generated from filtered sonic.
- It can also be generated from the velocity analysis.
- And it is also extracted from the geological model as well.
- Every method has its limitation but normally you can use the combination of both sonic and seismic velocity data.
- Low frequency can be added either at reflectivity or acoustic impedance stage but adding it at the reflectivity stage is better.

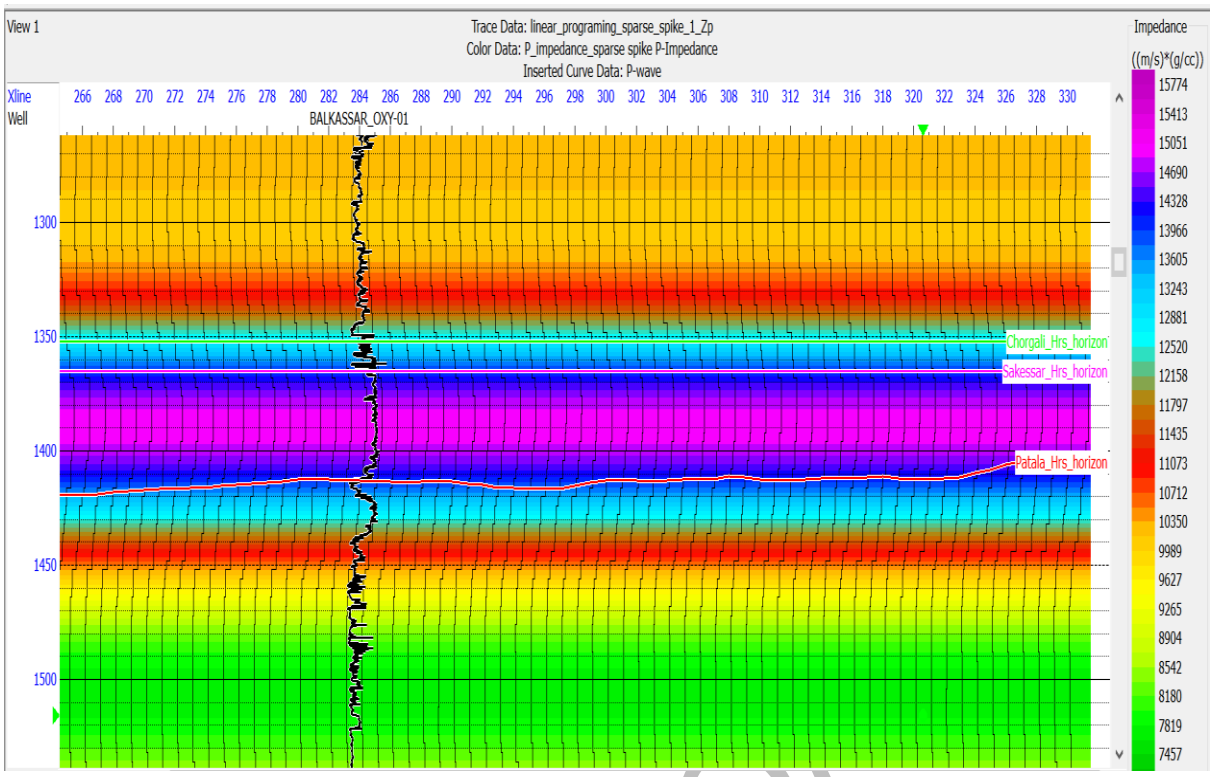

Figure 6.8 Background low frequency impedance model used in Sparse-spike seismic inversion.

6.3.3 Inversion analysis of Sparse-spike inversion

Inversion analysis is performed at well location of OXY-01 for Sparse-spike inversion on provided 3D Seismic cube of Balkassar as shown in Figure 6.9. First of all, a statistical wavelet was extracted in time window of 1330-1430 ms to cover the full reservoir range. The Impedance extracted from well log data is compared with the inverted impedance in time window of 1330-1430 ms. From Figure 6.9 it is clear that inverted Impedance (Red curve) nearly follow the same trend as original impedance from well (Blue curve) with an error of (1417.61) while the black curve is representing the background low frequency Impedance curve. Next window (B) 1s representing the extracted constant phase statistical wavelet while the window (C) and (D) shows the synthetic and seismic trace respectively. It is clear from the Figure 6.9 that there is best correlation between the synthetic and seismic trace with higher value of correlation coefficient 0.995 which shows that results of inversion analysis are correct and consistent. RMS Error between both these traces is quite low with value of only 3% (0.0388) as shown in Figure 6.9

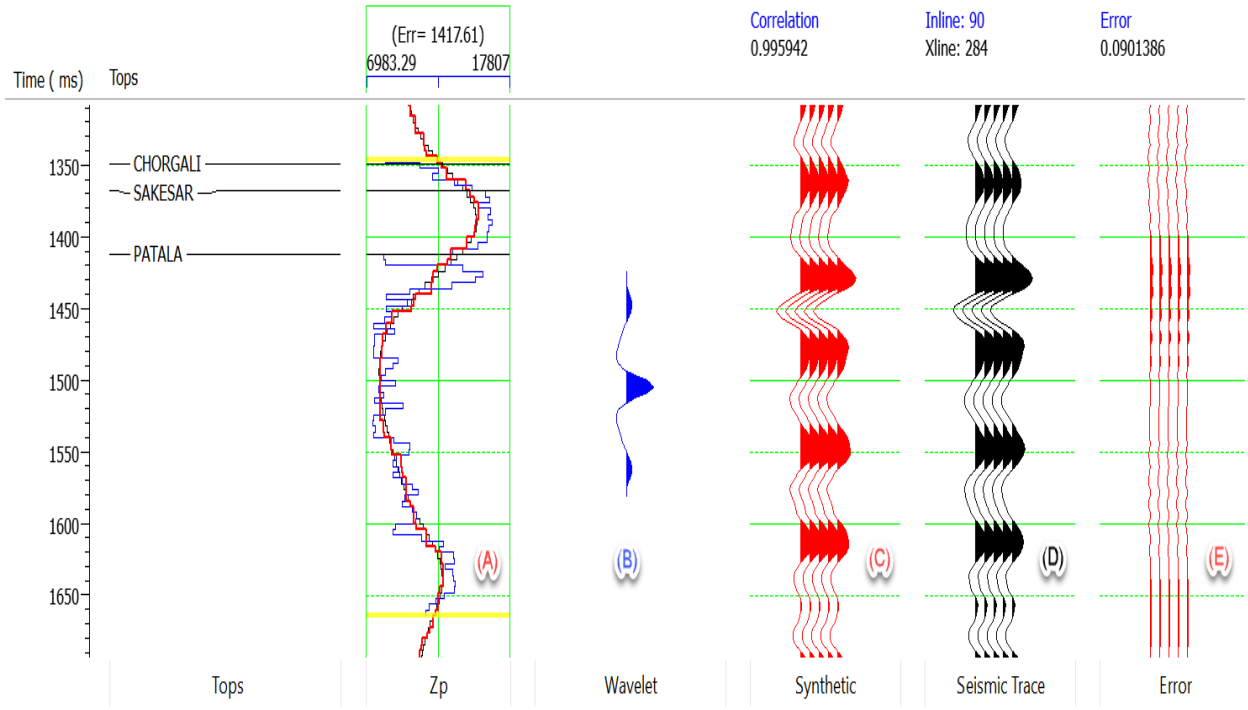

Figure 6.9. Analysis of Sparse-spike inversion at well Balkassar OXI-1: block (A) the blue color shows filtered impedance log, black color is the initial model, red color line shows inverted acoustic impedance log; (B) shows statistical wavelet in blue color; C) red color shows synthetic trace derived from inversion; D) black color shows Extracted trace from the seismic. (E) shows RMS error between the synthetic and seismic traces.

6.3.4 Results of the inverted Acoustic Impedance from Sparse-spike Inversion

Sparse-spike inversion is performed on the time window 1200-1500 ms generally to cover the reservoir zone. As it was discussed in Petrophysics that Chorgali is producing reservoir in Balkassar with major hydro-carbon component as oil. From petrophysics in Chapter- 04 1t was predicted that there is a good productive reservoir zone at 2424-2427m in Chorgali formation but having an average porosity of 19% and the hydrocarbon saturation is upto 44% which is not suitable for the success of the well and that is why it is the reason of abandonment of the well OXY-1. This oil-bearing zone is also predicted on inversion results as shown in Figure 6.10 with low acoustic Impedance.

There is quite higher AI value in Sakessar formation because it is not so good productive reservoir in Balkassar as compared to Chorgali which is also confirmed from the petrophysical results. At the time of 1350 ms on inline 90 there is very low acoustic impedance layer which is not predicted as reservoir because it cannot be confirmed as producing reservoir through petrophysics.

Inversion results also showing good lateral variation in Al and the inverted section provide better subsurface image as compared to original seismic section. Hence we can say that Sparse-spike Inversion can be used as a helpful tool in delineating the reservoir and it's hydrocarbon potential.

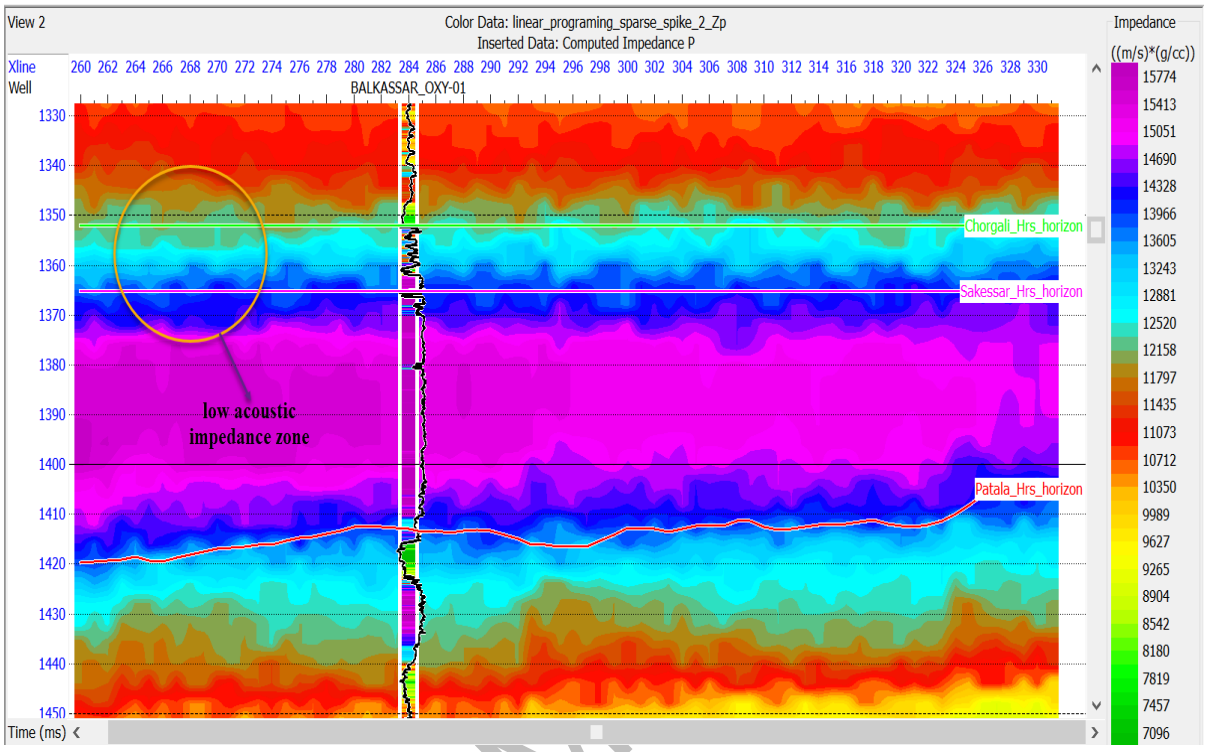

Figure 6.10. Sparse-spike inverted acoustic impedance for inline 90. This inversion algorithm can capture detailed lateral variations of lithology. best location for well is also shown in ellipse at inline 90 but a cross line of 266 to the south west direction of the map.

6.4 Results comparison of Model-based and Sparse-spike inversion

As it is clear from the Figure 6.5 and 6.10 that result of Model-based inversion is far better than Sparse-spike inversion in terms of the resolution of the data and we can easily identify the low impedance on Model-based inversion as compared to the Sparse-spike inversion. This result also give strength to the paper (Ali et al., 208). The algorithm of Model-based inversion is better than the algorithm of the Sparse-spike inversion. Hence, we can say that Model-based inversion is not only suitable for the clastic reservoir but this method is also suitable for non-clastic reservoir as well.

CHAPTER 7

SPATIAL DISTRIBUTION OF POROSITY

7.1 Introduction

One of the most crucial factors in determining reservoirs for oil and gas exploration to characterize the storage capacity of the reservoir is porosity. Thus, in the realm of geoscience and specially in the field of oil and gas, porosity extraction from seismic data is a difficult task (Kaiyuan et al., 2021).

In seismic the Spatial distribution is to display or the distribution of very low scale information like a well to a large-scale information like seismic cube. Spatial distribution of physical properties is crucial in oil and gas industries.

Now porosity is derived from the well log data. This derived porosity is integrated with seismic to see the spatial distribution of porosity at the whole seismic cube.

The cross plots of porosities in this chapter further enhanced the relation between reservoir actual porosities and the seismic predicted porosities by developing geostatistical relationship. The data used to accomplish this objective is 3D seismic cube and the wireline log data of Balkassar OXY-1 well. The focus of this chapter is merely to extract porosity from the Chorgali and Sakessar limestone from the seismic data and to show their spatial distribution of porosity at the whole seismic cube. Different cross plots and porosity slices of Chorgali and Sakessar were generated to see the spatial distribution of porosity at the whole seismic cube. To do this we need to establish a geostatistical relationship between well data and seismic data.

7.2 Geostatistical analysis

The geostatistical approach is used to derives a surface by applying the values which are calculated from the specific location to assess the data points for each location between the data points (Ali et al., 2019).

Geostatistical approach consists of three types of attributes these are the single attributes analysis, multi-attribute regression and neural networking. Neural networking is further divided into the Multilayer feed forward and Probabilistic Neural network

Below are the steps followed in geostatistical approach.

1. Variograms are used to visualize the spatial continuity of the quantified well log data.

2. Cross validation plots are used to check the statistical relationship between the logs and seismic data at the well location. Among the three types of geostatistical analysis neural networking uses the non-linear relationship while the rest shows the linear relation.
3. These linear and nonlinear relationship is used to assess the well log property away from the borehole.
4. The reliability of the predicted well log property is assessed.

In **single attribute analysis**, several attributes are initially derived from the seismic data either directly or indirectly, and then the best attribute is selected after analysis. The best attribute chosen based on correlation to the desired log values. Additionally, the target value from the well log data is cross plotted with the best attribute, and the best fit straight line is selected, providing the desired relationship. Now the basic purpose of this required relationship is to predict the petrophysical properties in the inter well region.

The second type of geostatistical analysis for the prediction of petrophysical properties is the **multi-attribute regression**. The difference between the multi attribute regression and single attribute is that multi attributes used more than one attribute at a time while single attributes utilized one at the same time. In this approach the best attribute combination (more than one attributes) is chosen, and it is cross plotted with a desired value to produce a linear relationship that is used for further analysis. This analysis is linear which has some limitation now to extend the analysis to a nonlinear relationship, it is necessary to consider the neural network for the nonlinear relationship. The neural network is further divided into multi-layer feed-forward neural network and Probabilistic Neural network. But to accomplish this dissertation I focused only on Probabilistic Neural network.

7.2.1 Probabilistic Neural network (PNN)

The (PNN) is in fact, a mathematical interpolation system that uses neural network design to execute it. PNN used mathematical formulas and that the only reason that it is better than MLFN. The background scene behind the PNN is that it uses one or more measured values and these values are called the independent variables and the predicted values are called the dependent variable.

Suppose that the independent variable is shown by vector $x = x_1, x_2\ldots.., x_p$, (eq.1) the p in this shows number of independent variables. Apart from this, the dependent variable L shown in the equation 1 is a scalar. The PNN takes variables $x_1, x_2..., x_p$ as input and create y as output. Using known independent variables as a starting point, this seeks to estimate the unknown

dependent variable, L. This estimate is based on the Probabilistic Neural network's fundamental equation for general regression, which is shown below.

$$\hat{L}(\mathrm{x}) = \frac{\sum_{i=1}^{n} L_i \exp\left(-D(x,x_i)\right)}{\sum_{i=1}^{n} \exp\left(-D(x,x_i)\right)} \qquad 7.1$$

n in this equation denotes the number of examples and D (x, x_i) is the distance between the input point and each of the training points x_i. The quantity D(x, x_i) can be calculated as follows.

$$D(x,x_i) = \sum_{j=1}^{3} \left(\frac{x_{j-x_{ij}}}{\sigma_j}\right)^2 \qquad 7.2$$

The D (x, xi) is measured in the multidirectional space covered by the attributes and is scaled by the quantity σj, which may differ for each of the attributes. the equations (1) and (2) depict the application of the PNN whereas the training of the network consists of determining the optimal set of smoothing parameters called σj. The minimal validation error in the resultant network is the benchmark for choosing these settings. The total validation error for the nth the target sample is defined as follows.

$$E_y(\sigma_{1,}\sigma_{2,}\sigma_3) = \sum_{i=1}^{N}\left(L_i - \widehat{L_\iota}\right)^2 \qquad 7.3$$

Additionally, it should be highlighted that the selection of the parameter σj has a significant impact on the prediction error. A nonlinear conjugate gradient approach is used to minimize the validation error with regards to the smoothing parameters.

To predict porosity from PNN using 3D data set of Balkassar oil field Upper Indus Basin Pakistan. The PNN generates a non-linear relationship which is set up between attributes and well log porosity. Following the selection of the desired attributes, a nonlinear relationship is set up at each sample point to forecast the porosity in the inter-well region. In the analysis of PNN, the impedance derived from Model-based inversion was used as one attribute.

From the Figure 7.1 for total porosity and Figure 7.2 for effective porosity, it is noticed that the modeled error is very small. Additionally, a cross-plot between predicted and actual porosity is created and is displayed in Figure. 7.3 and 7.4 The dispersed point distribution indicates that the inverted porosity is extremely similar to the actual porosity, which is also supported by the correlation coefficient. The RMS error is 0.043 and the estimated correlation coefficient for the PNN is 0.88, suggesting a strong correlation and RMS.

7.2.1.1 Workflow used in Probablistic Neural networks (PNN)

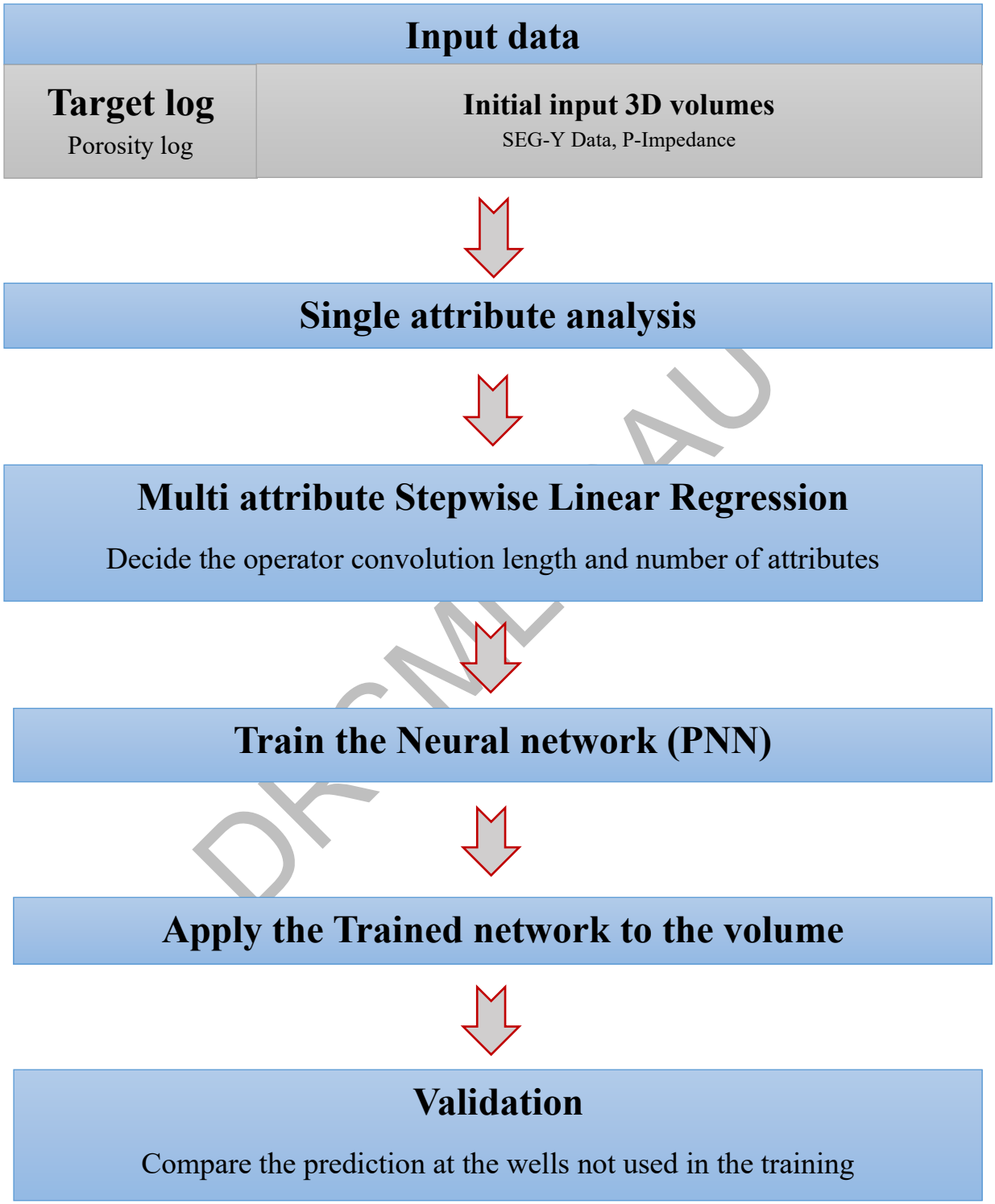

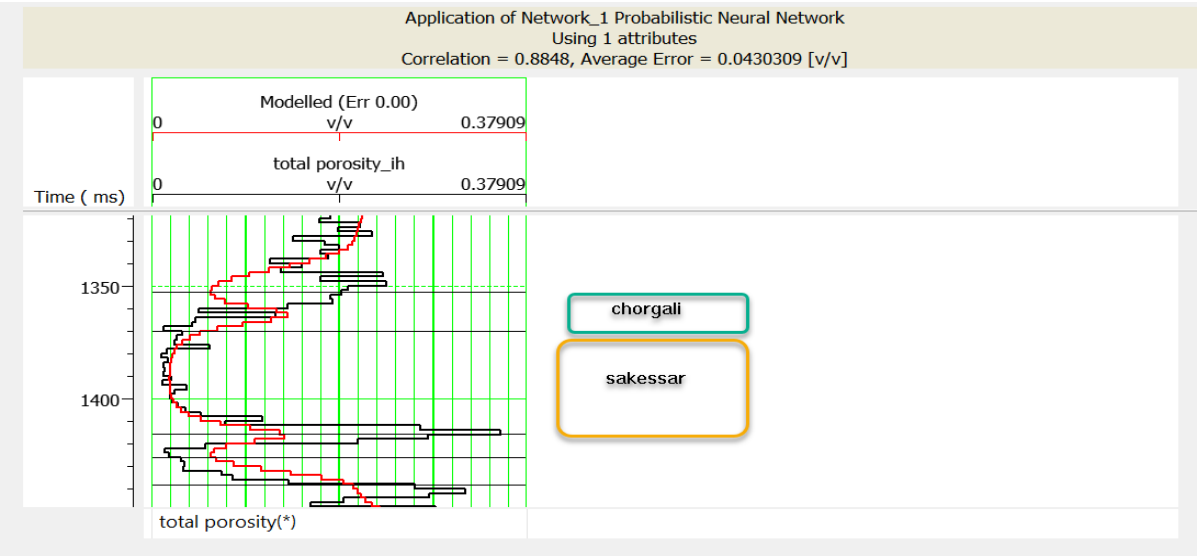

Figure 7.1 Model error vs total porosity. Red curve showing the model error while black curve showing the porosity curve at corgali and Sakessar level.

The Figure 7.1 clearly depicts that the error is very small hence the model is correct. The red curve follows very nicely the porosity curve which shows very small error in model hence we can say that the model is correct.

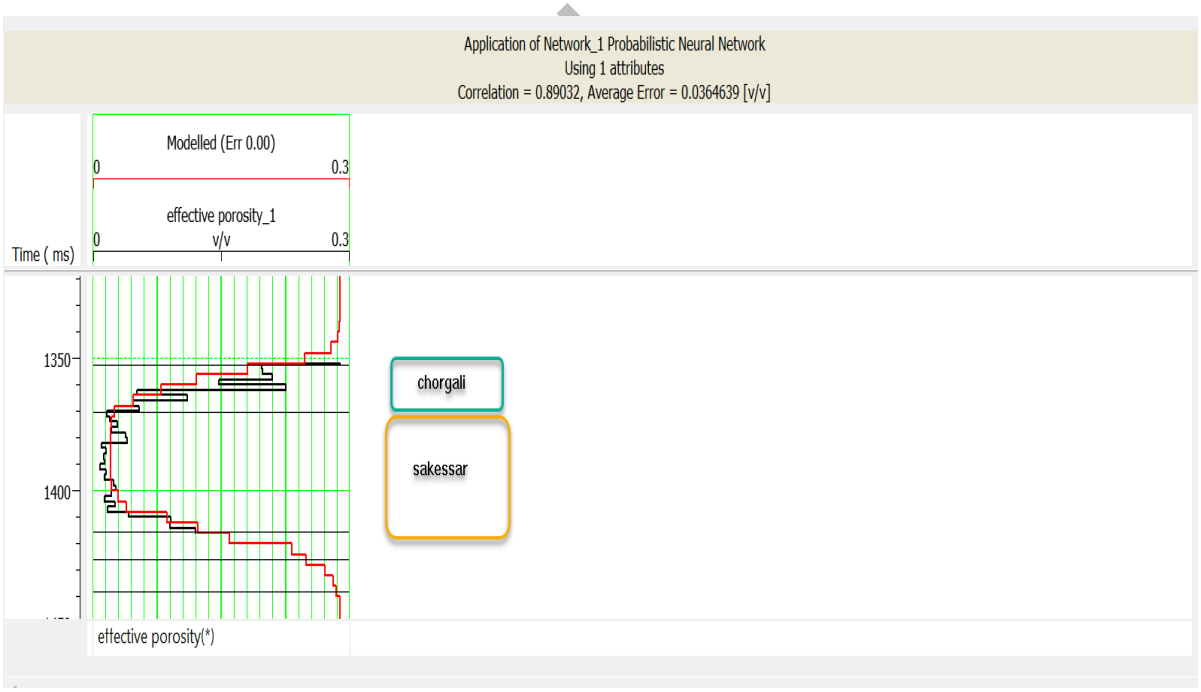

Figure 7.2 Model error vs effective porosity at Chorgali and Sakessar level

The Figure 7.2 clearly depicts that the error is very small hence the model is correct. The red curve follows very nicely the effective porosity curve which shows very small error in model hence we can say that the model is correct.

7.2.1.1 Cross plots of Actual total porosity vs predicted porosity

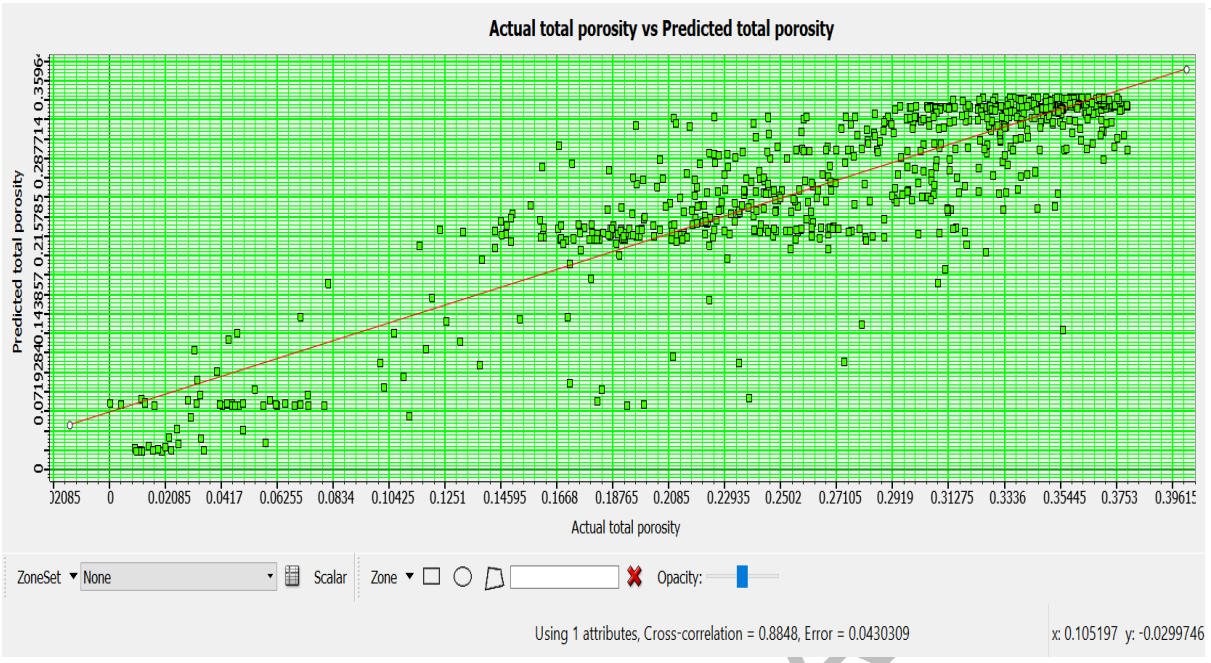

Figure 7.3 Actual total porosity vs predicted total porosity at Chorgali level.

As it is clear that the predicted porosity is following the same trend as actual porosity. The cross correlation in this cross plot is 0.88 while the error is very small that is 0.043.

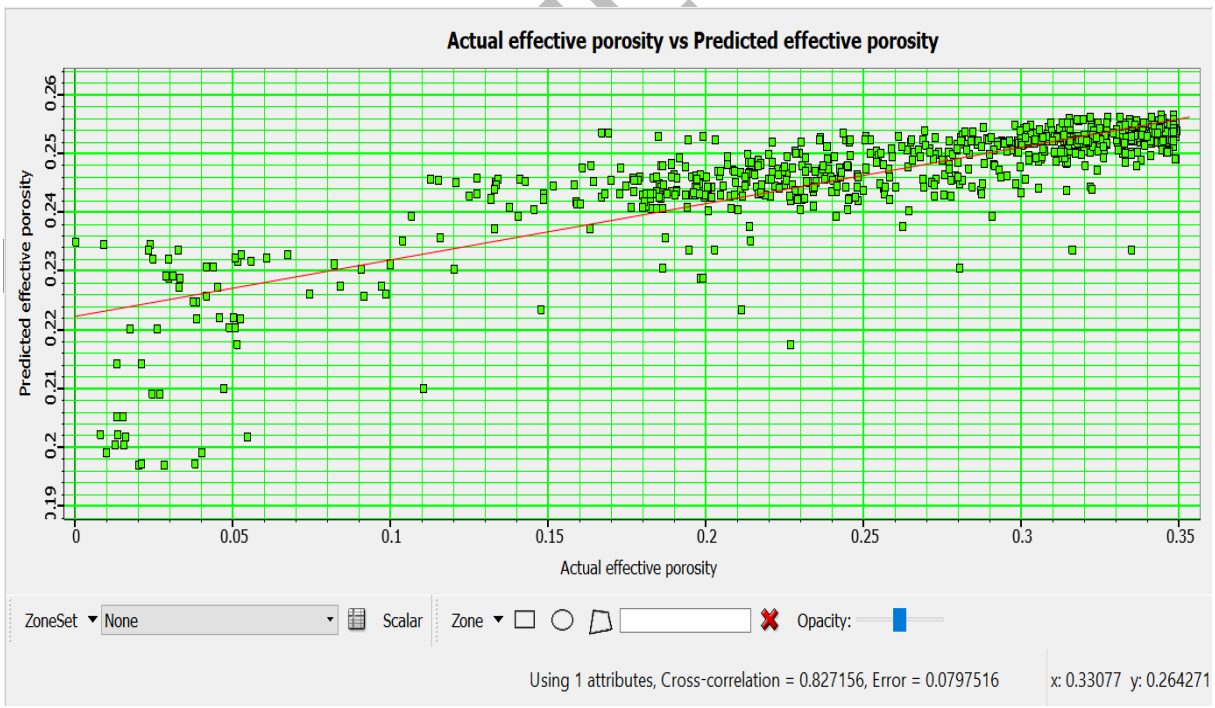

Figure 7.4 Actual effective porosity vs predicted effective porosity at Chorgali level.

The trend followed by the predicted effective porosity in this cross plot is same as the actual effective porosity. The cross corelation in this cross plot is 0.82 while the error is very small that is 0.07.

7.2.1.2 Cross plots of P-impedance vs predicted porosity

Additionally, the cross plotting is crucial method to link the inverted impedance with the predicted porosities and to estimate the relationship between them we would fit the linear line or higher order polynomial. The cross plotting is a useful technique for connecting the impedance with porosities that were measured from the borehole or calculated from density and neutron logs. (Kumar, 2016). This relationship will be more applicable and more useful, compared to the relationship established from the well log curves at the same location. The relationship formed from the cross-section is valid anywhere in the region and provides a better estimate than the well log derived equation, which is only valid at the specific spot.

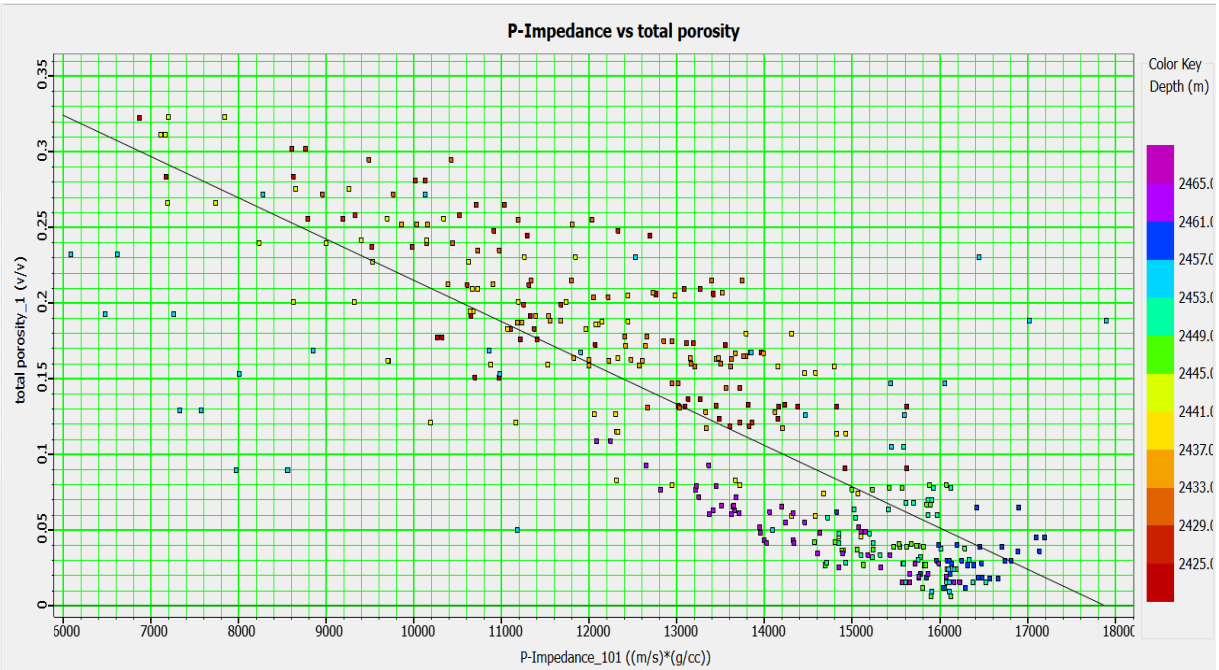

Figure 7.5 P-impedance ((gm/cc)*(m/s)) x-axis versus total porosity (v/v) y-axis at Chorgali level.

The regression error 0.021 while the correlation is very high that is 0.95 which shows that the model is true upto an acceptable level. As we know that porosity is inversely related with the impedance so with the increase of impedance the porosity will be decrease.

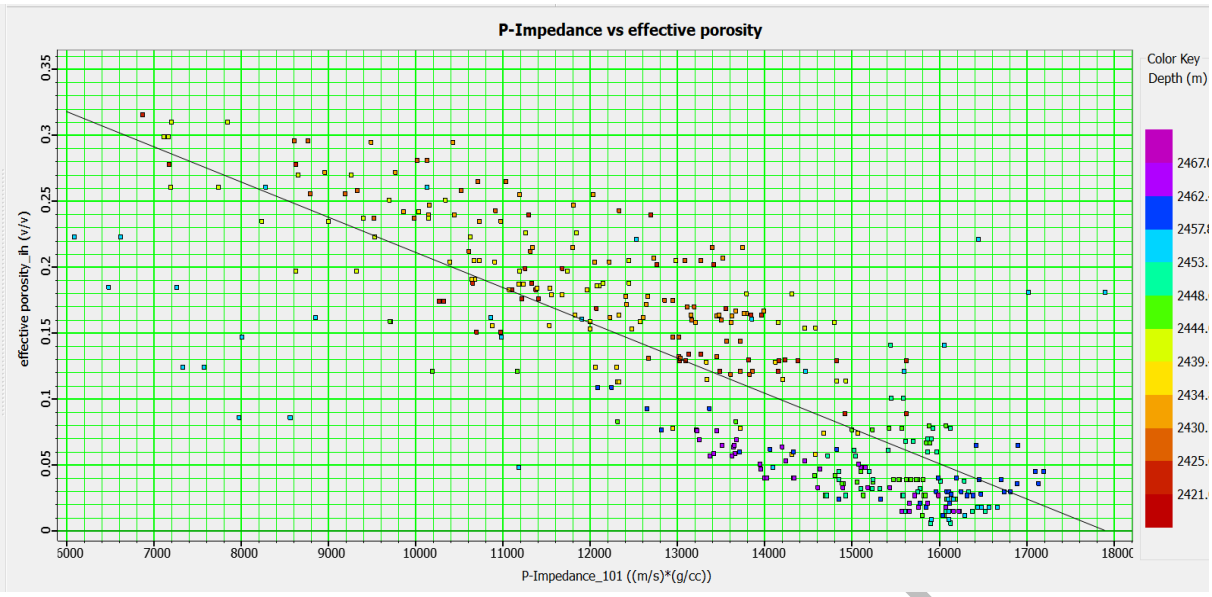

Figure 7.6 P-impedance ((gm/cc)*(m/s)) y-axis versus effective porosity (v/v) x-axis at Chorgali level.

The regression error 0.019 while the correlation is very high that is 0.95 which shows that the model is true upto an acceptable level. As we know that porosity is inversely related with the impedance so with the increase of impedance the porosity will be decrease.

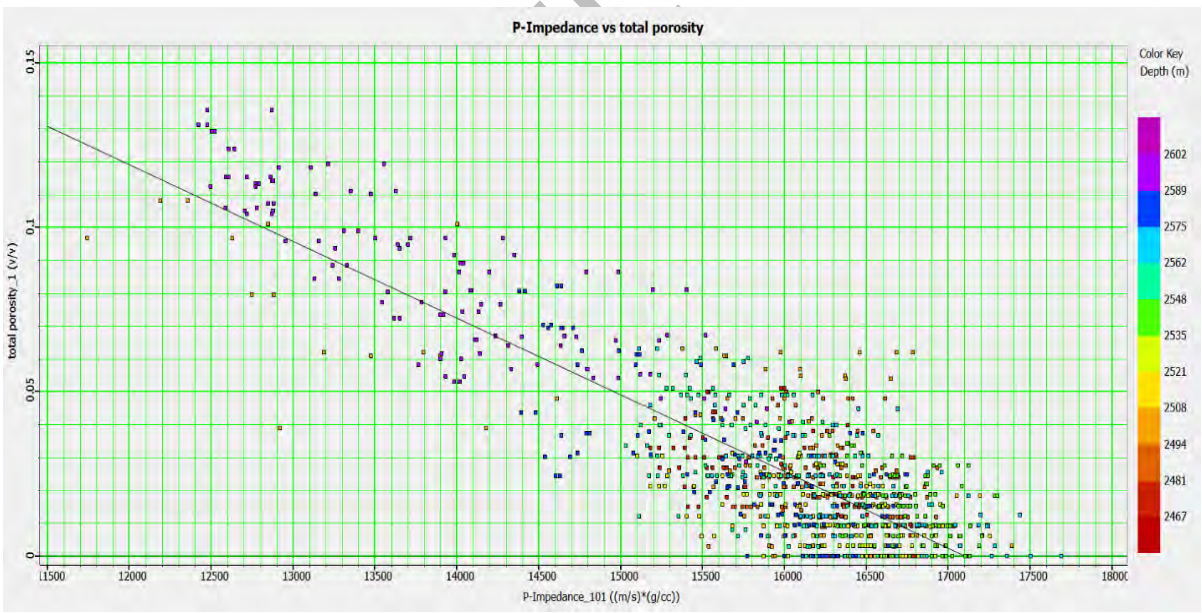

Figure 7.7 P-impedance ((gm/cc)*(m/s)) y-axis versus total porosity (v/v) x-axis at Sakessar level.

The regression error 0.021 while the correlation is very high that is 0.94 which shows that the model is true upto an acceptable level. As we know that porosity is inversely related with the impedance so with the increase of impedance the porosity will be decrease.

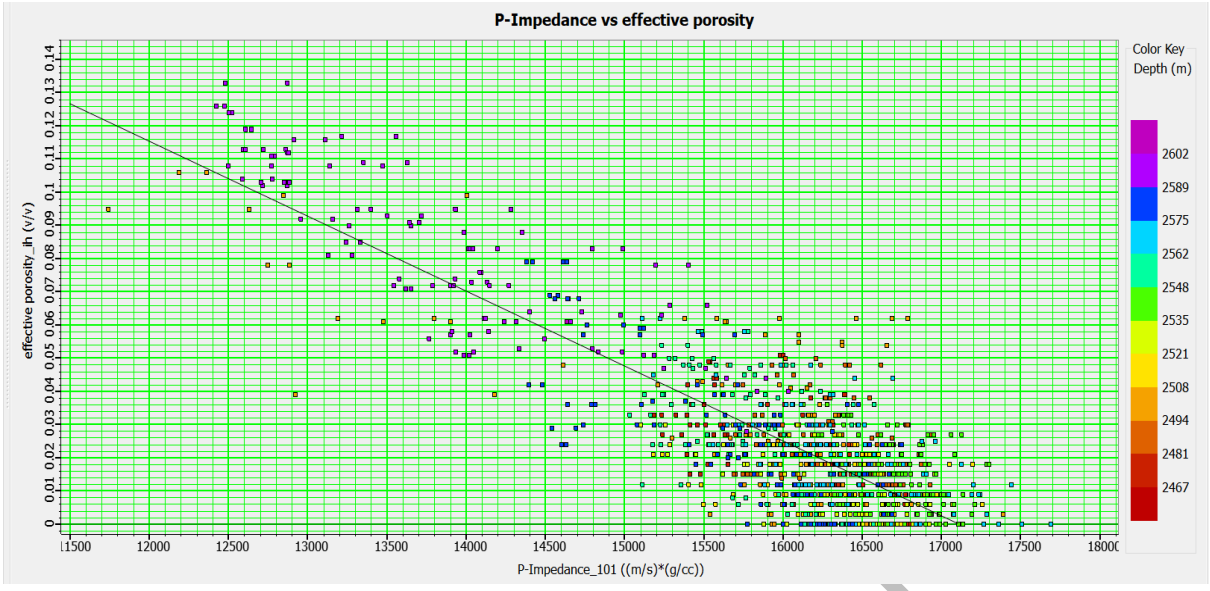

Figure 7.8 P-impedance ((gm/cc)*(m/s)) y-axis versus effective porosity (v/v) x-axis at Sakessar level.

The regression error 0.020 while the correlation is very high that is 0.93 which shows that the model is true upto an acceptable level. As we know that porosity is inversely related with the impedance so with the increase of impedance the porosity will be decrease.

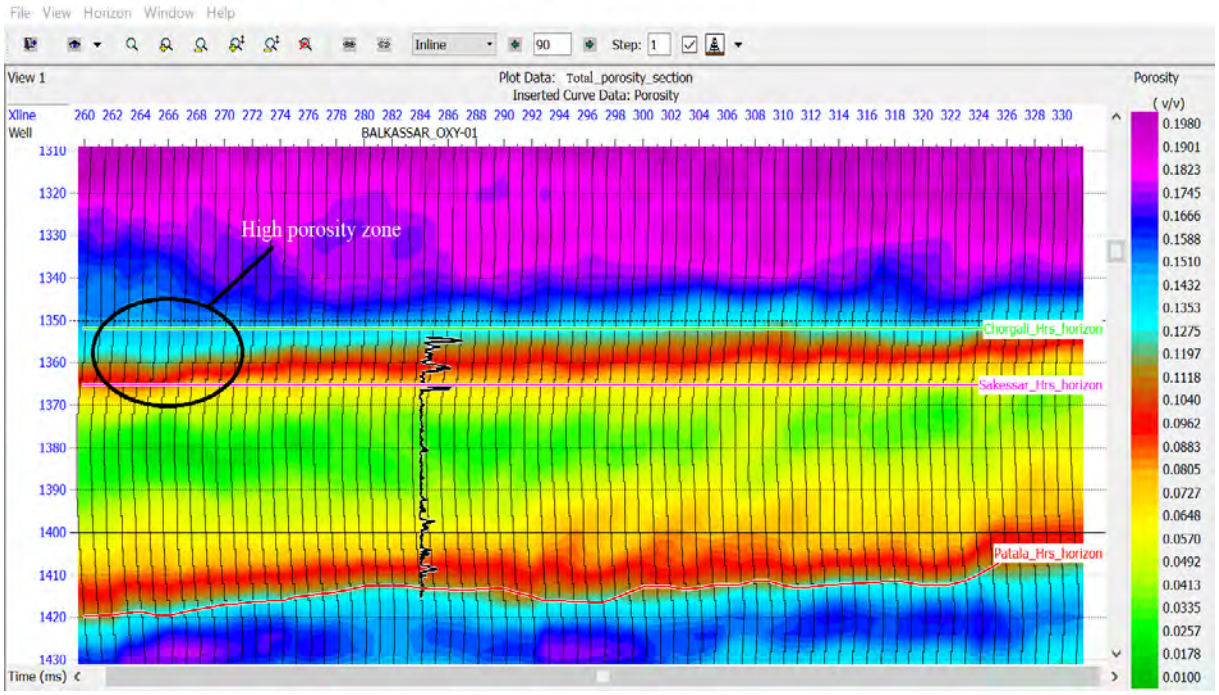

Figure 7.9 Predicted Total porosity from the Model-based seismic inversion via Probabilistic Neural network.

The Figure 7.9 depict the total porosity at both Chorgali and Sakessar level. Green line represents the Chorgali horizon while the magneta line represents the Sakessar horizon. The porosity log is also shown at the inline 90 and cross line 284 at the well location that is

Balkassar OXY-1. The porosity in the Chorgali formation at the well location is upto 11% which matched nicely to the total porosity derived from the petrophysical analysis which is also 11%. The overall porosity anticipated for the Sakessar formation from this section is 4%, whereas the derived porosity in this formation is similarly nicely matched at 4% from petrophysics.

As the Balkassar OXY-1 is not so producing, and we already proved it in the petrophysical analysis so here it also shows that the porosity at the well location is very low which is not suitable for the success of the well.

At the same inline 90 but cross line 266 highlighted with a black circle is suggested to be a good place for drilling the well which have the high total porosity i.e., 15% in average.

Let's apply other technique of post stack inversion to predict the porosity from the seismic section and to give strength to the above discussion.

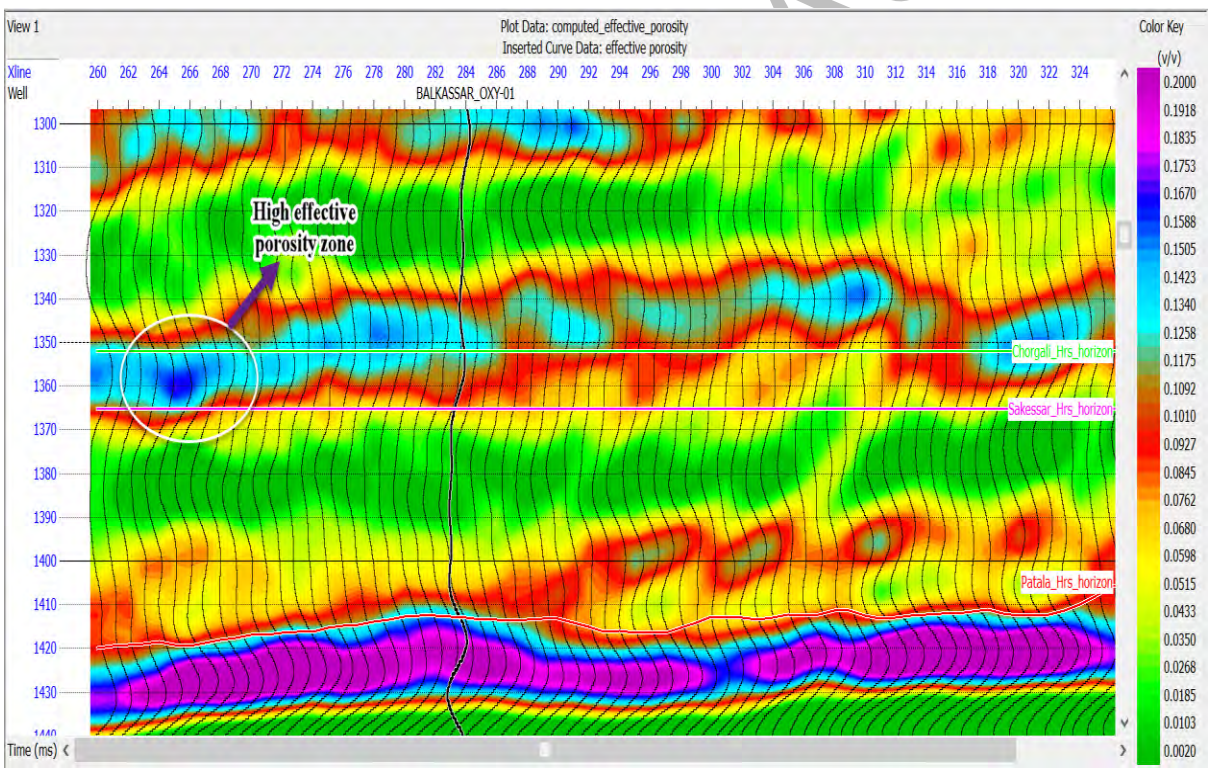

Figure 7.10 Predicted effective porosity from the Model-based seismic inversion via Probabilistic Neural network with a high effective porosity zone shown in white circle.

The computed effective porosity is shown in Figure 7.10, and it shows a very good calibration with the effective porosity obtained from the petrophysical analysis. Here in this section the effective porosity at a well location is 9% in Chorgali formation, and the effective porosity calculated from the petrophysics in Chorgali formation is also 9%. The spatially distributed predicted porosity from this section for Sakessar formation also nicely matched with the actual

derived porosity from the petrophysics. The effective porosity at Sakessar level in petrophysics is 2% and the effective porosity from this section is also 2% in average.

Since Balkassar OXY-1 is a abandoned oil well, it may also be inferred from this section that its location was unsuitable. The suggested location for drilling a well is the same inline 90 but cross line 266 which shows a very high effective porosity zone i.e., 14% in average shown with white circle in the figure 7.10.

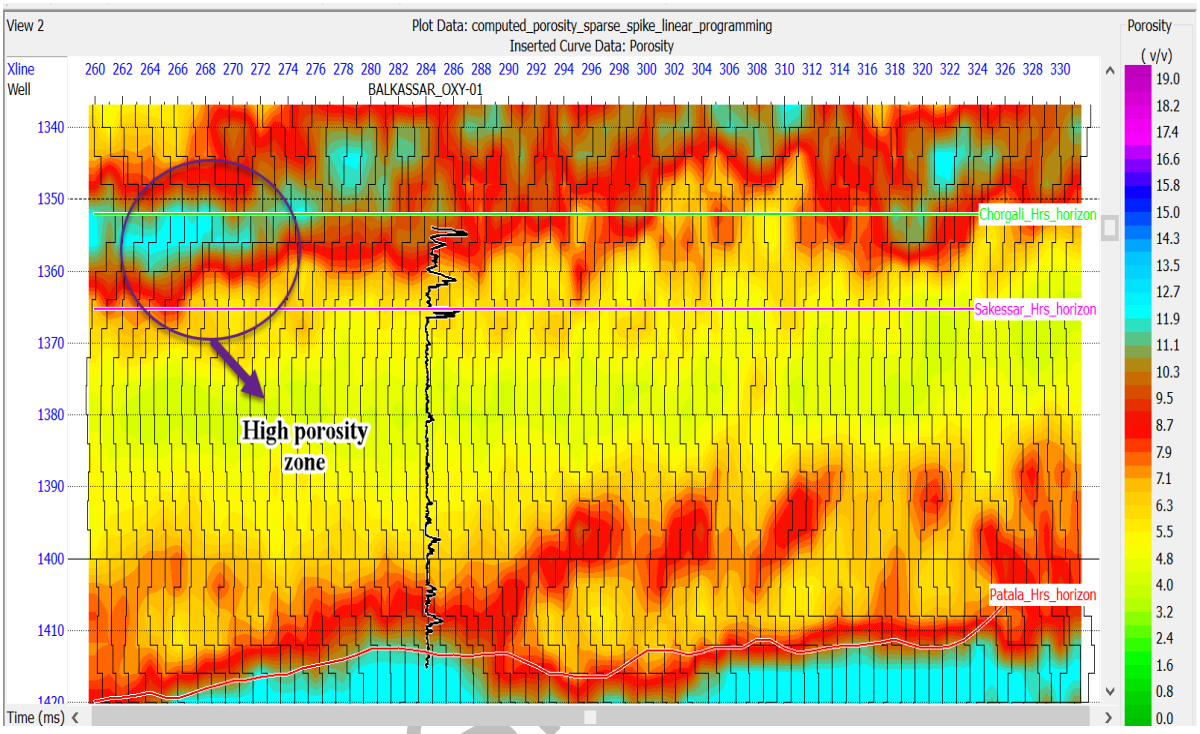

Figure 7.11 Predicted Total porosity from the Sparse-spike inversion via Probabilistic Neural network with high porosity zone shown in circle to the south west of OXY-1 .

The black curve at the well location is the total porosity log. The formation Sakessar has a very low porosity, up to 4%, according to the seismic section, which is also determined from the petrophysical result i.e., 4%. But there is a little difference between the petrophysical derived porosity and computed porosity from this section. The petrophysical porosity is 11% in average while here in this section it is 10% in average therefore we can say that Model-based inversion is good in predicting the porosity from seismic data via Probabilistic Neural network. It is also evident from this section that Sakessar has a very low porosity while the Chorgali has a significant porosity. It has also been demonstrated through the use of this post stack seismic inversion technique that the 266 cross line and inline 90 was the suitable locations for the drilling of the Balkassar OXY-1 well here the porosity at this location is 13% shown with purple circle in the figure 7.11.

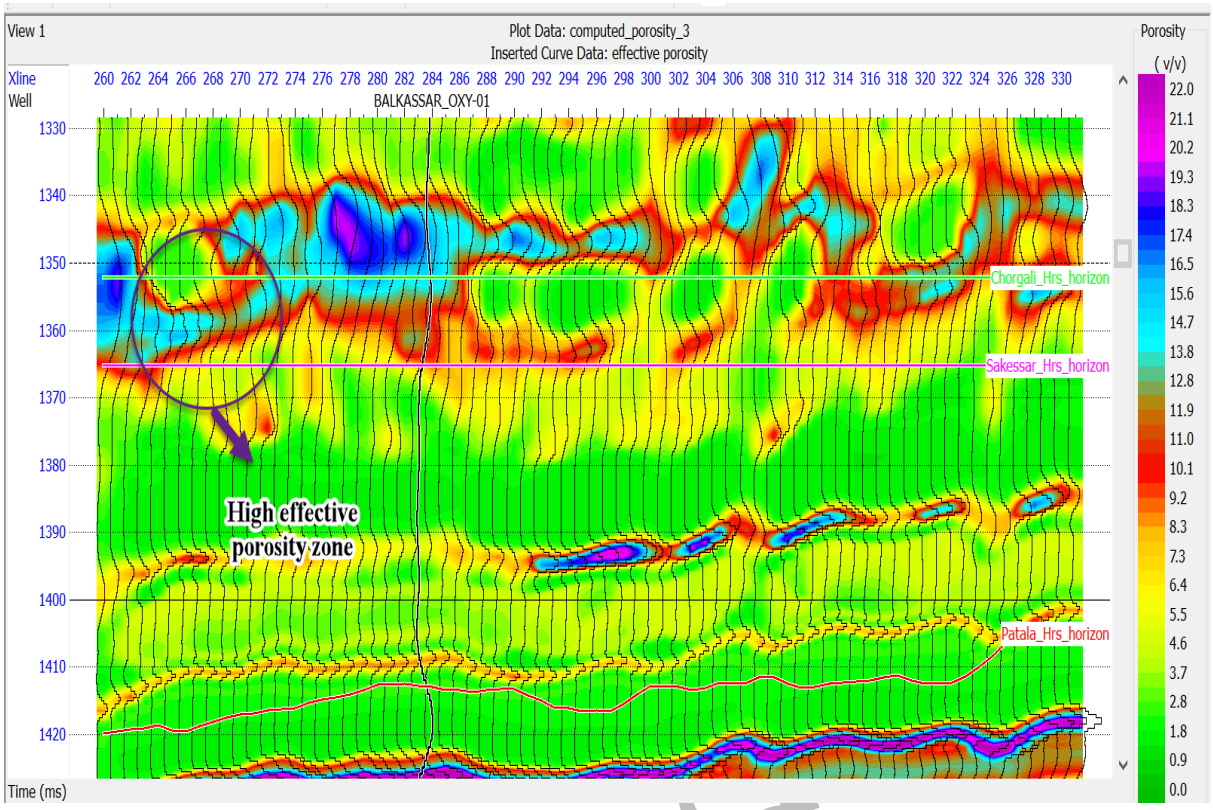

Figure 7.12 Predicted effective porosity from Sparse-spike inversions via Probabilistic Neural network.

The derived porosity from the petrophysical analysis and the predicted porosity from the seismic perfectly matched each other. According to petrophysical studies, the overall Chorgali formation has an average effective porosity of up to 9%. As a result, the Chorgali formation's calculated effective porosity from petrophysics and predicted effective porosity from seismic line up well.

In this section the Sakessar formation similarly follows the same pattern; here, the average effective porosity is 3%, compared to 2% from petrophysics. The high porosity zone is highlited with with a circle in this section.

Now, to strengthen the discussion and the suggest the location for the well OXY-1, I created the slices of spatially distributed porosity to enhance our understanding of the high porosity zone and to estimate the ideal location for the drilling of the Balkassar OXY-1 well.

7.3 Spatial distribution of porosity of Chorgali Formation

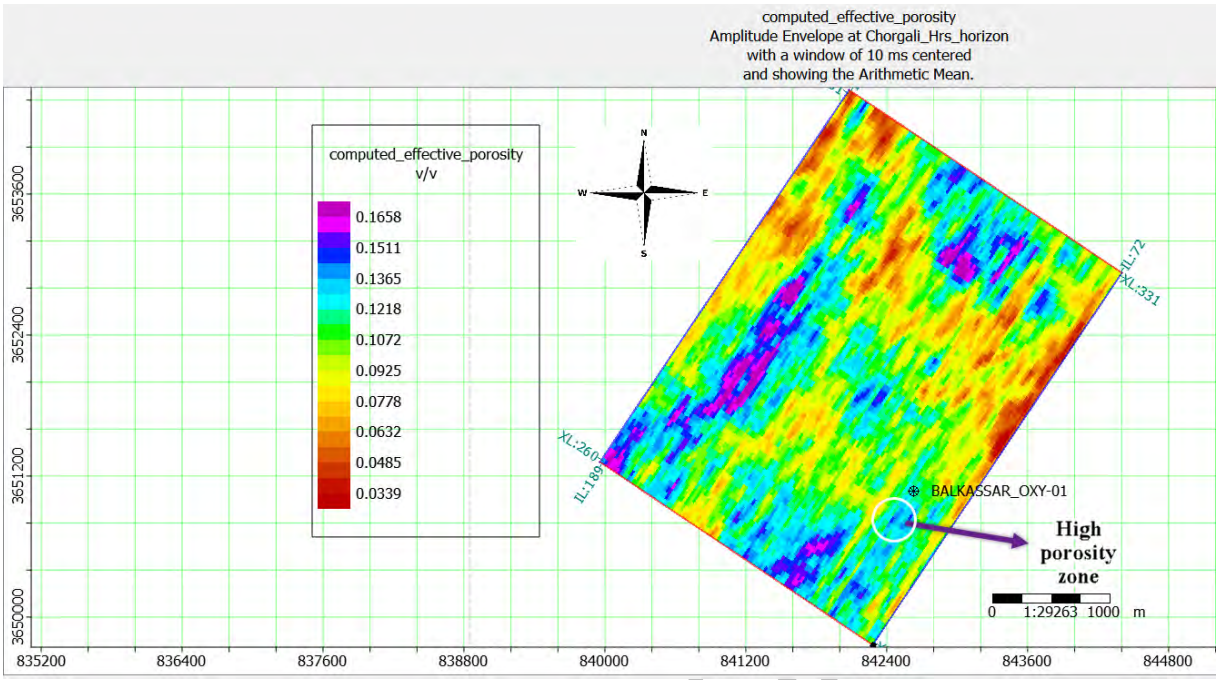

Figure 7.13 Spatially distributed effective porosity at Chorgali level from Model-based seismic inversion.

The high porosity zone is readily shown on the map by the spatial distribution of effective porosity at the Chorgali level. On the map, a white circle to the SW of the Balkassar OXY-1 well denotes a region with a 14% porosity.

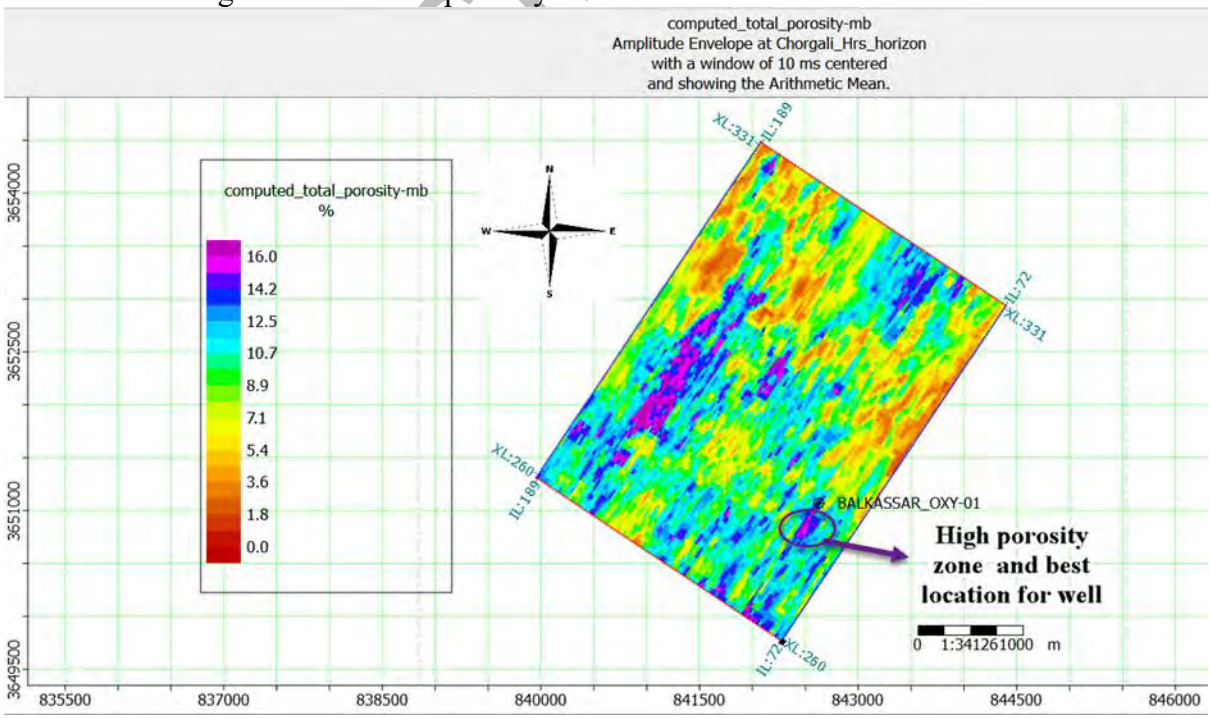

Figure 7.14 Spatially distributed total porosity at Chorgali level from Model-based seismic inversion.

High porosity zone shown in elipse. A very high porosity zone is visible to the southwest of the Balkassar OXY-1 well at cross line 266 in the spatial distribution of total porosity of 15% at the Chorgali level. This zone has also been indicated in the inverted seismic section.

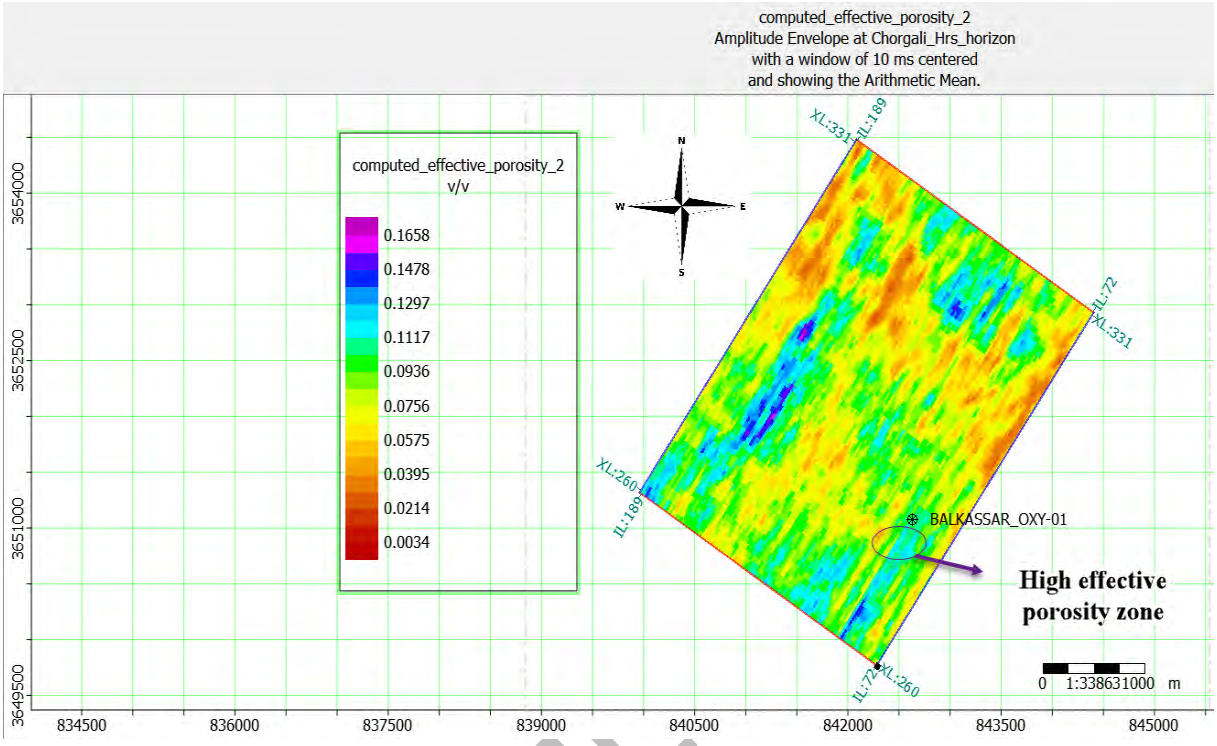

Figure 7.15 Spatially distributed effective porosity at Chorgali level from Sparse-spike seismic inversion.

This porosity slice has been extracted via Sparse-spike inversion, from this slice it is also evident that the SW side of the well Balkassar OXY-1 at the cross line 266 and inline 90 shows high effective porosity as compared to the zone where OXY-1 well is drilled .

The slice of total porosity has also been generated which also indicated that we have high porosity zone to the SW of Balkassar OXY-1 well at the cross line of 266 and inline 90 hence it is proved from the two different techniques of seismic inversion that the location for the Well OXY-1 is not suitable and the suitable location for the well OXY-1 was inline 90 but cross line 266.

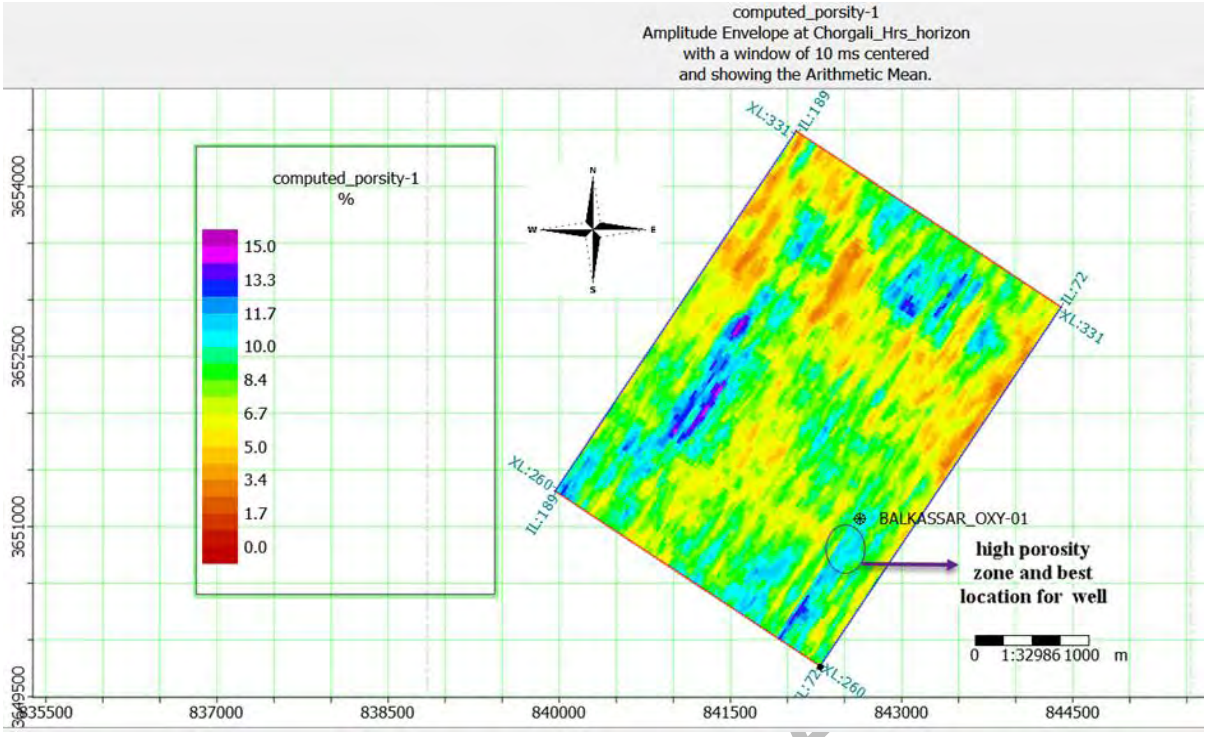

Figure 7.16 Spatially distributed total porosity at Chorgali level from Sparse-spike seismic inversion.

7.4 Spatial distribution of porosity of Sakessar Formation

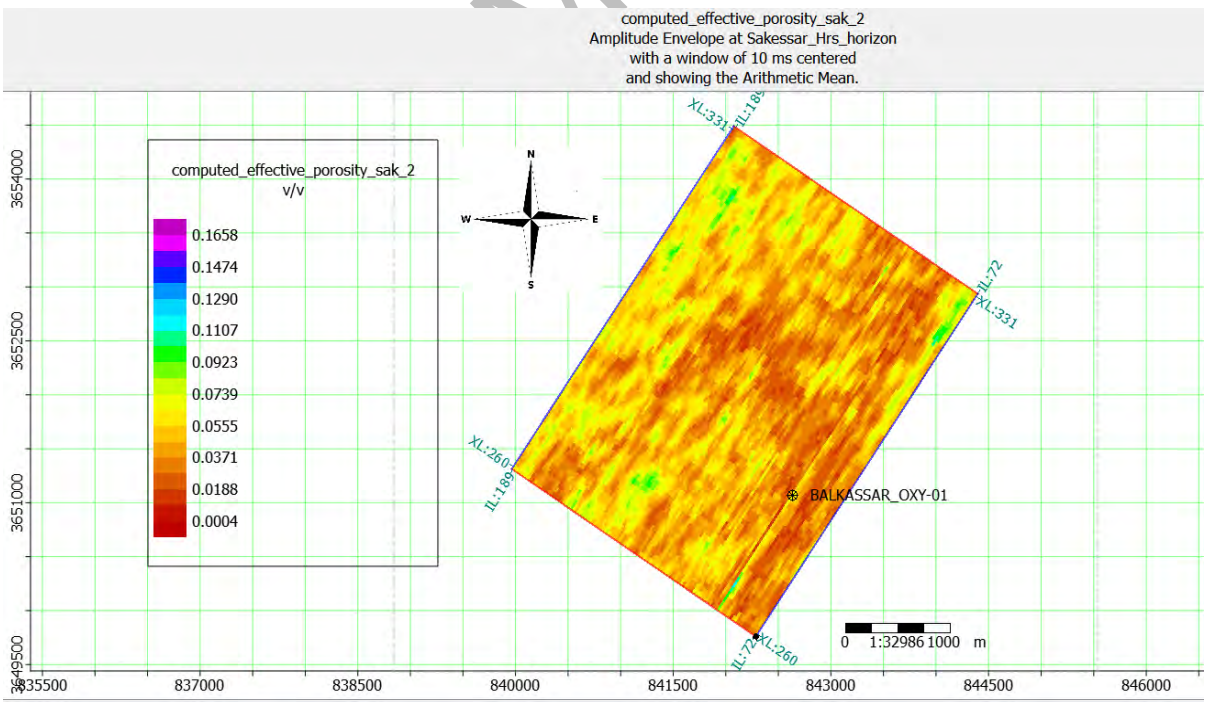

Figure 7.17 Spatially distributed effective porosity at Sakessar level from Sparse-spike inversion.

Figure 7.17 slice is nicely matches the result obtained from the petrophysical result but the effective porosity slice of the Sakessar formation shows very low porosity at this level hence no effective zone is seen at this level for hydrocarbon accumulation.

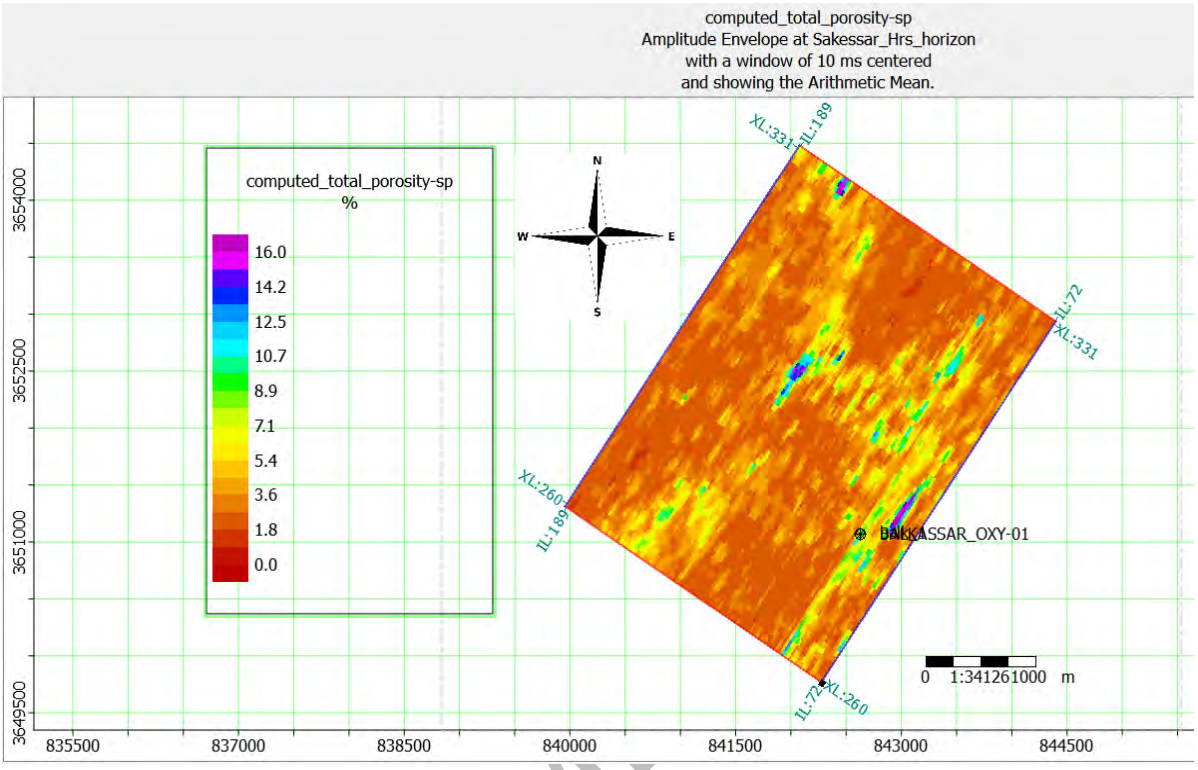

Figure 7.18 Spatially distributed total porosity at Sakessar level from Sparse-spike seismic inversion.

The result of this slice also matches the result of the porosity derived from the petrophysical result having very low porosity at Sakessar level hence no effective zone for the accumulation of hydrocarbon.

Slices of effective porosity of Sakessar has also been generated to check the spatial distribution of effective porosity at Sakessar level. The slice has been created from the predicted porosity derived from Model-based seismic section via geostatistical method as shown in figure 7.19. This slice also shows very less porosity at Sakessar level. Hence Sakessar is not effective reservoir for Hydrocarbon accumulation.

Slice of total porosity is also generated to check the spatial distribution of total porosity at Sakessar level as shown in figure 7.20. There is no effective zone for the storage of fluid. As it is evident from spatial distribution of porosity at Sakessar level, the region is dry and has very low porosity, as seen in these slices.

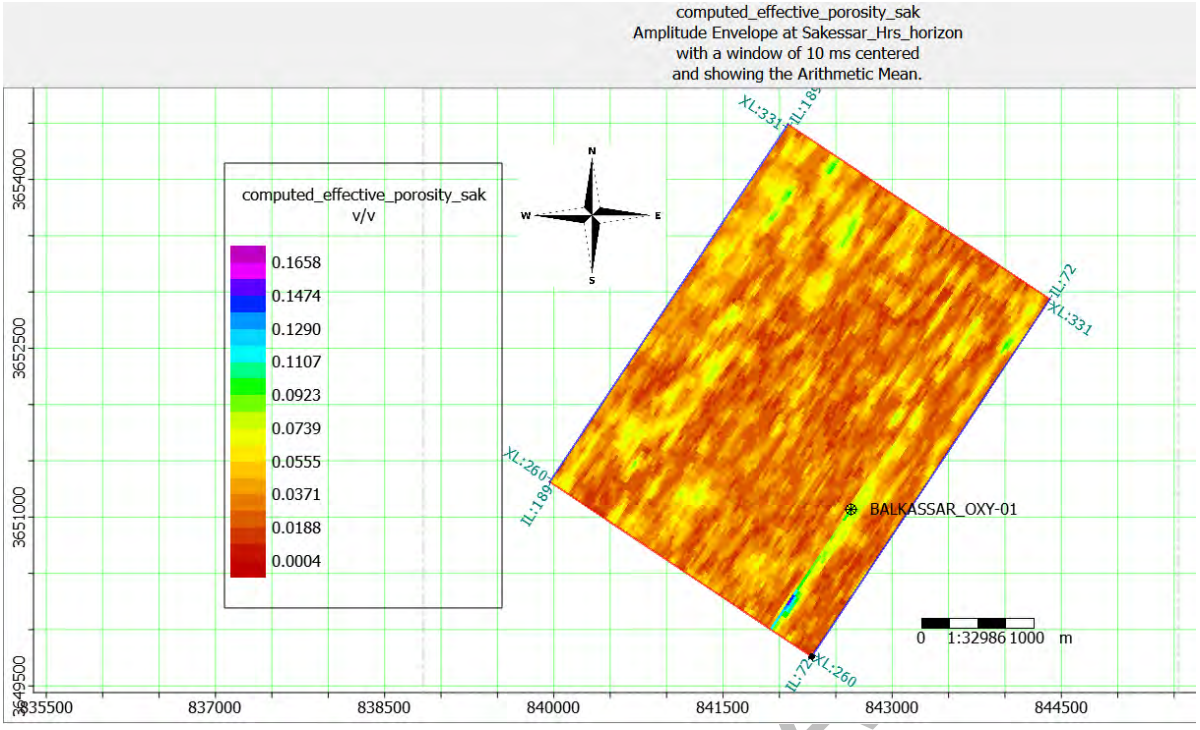

Figure 7.19 Spatially distributed effective porosity at Sakessar level from Model-based seismic inversion.

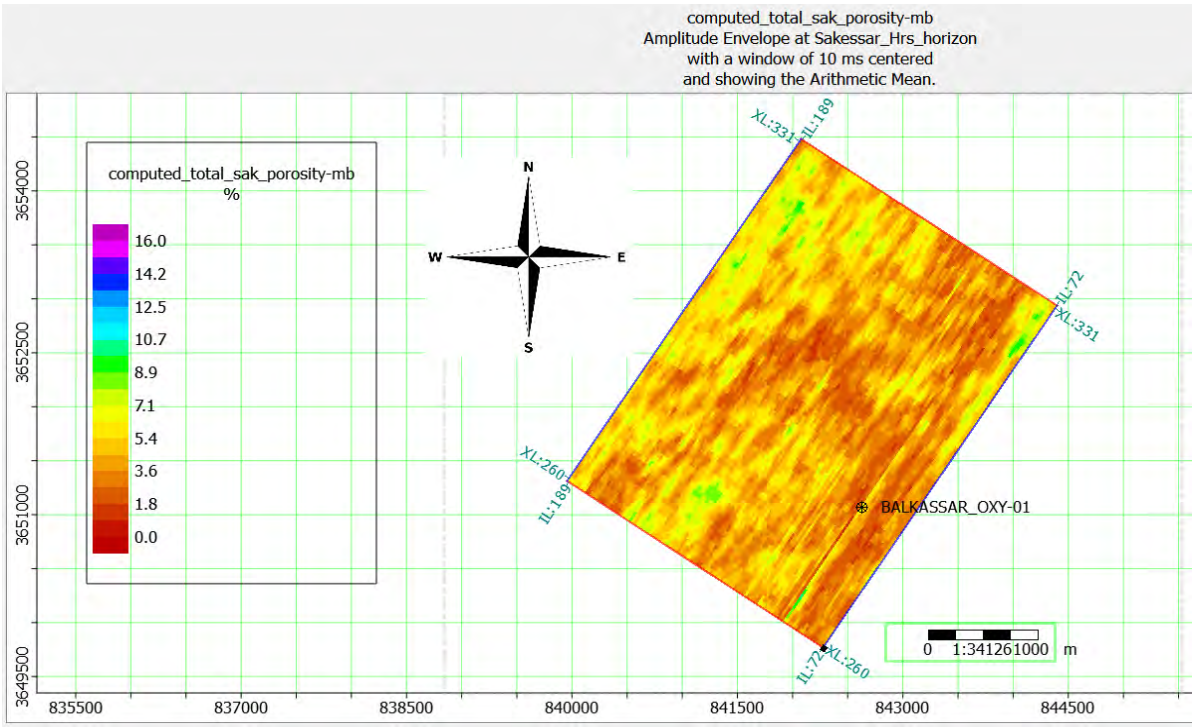

Figure 7.20 Spatially distributed total porosity at Sakessar level from Model-based seismic inversion.

8 Discussion and Conclusion

- The first step of extracting information from the seismic data is seismic interpretation. Structural and stratigraphic interpretation is very helpful for the identification of the favorable zone for hydrocarbon accumulation. The structural analysis and stratigraphic analysis are the two fundamental methods for interpreting seismic data. (Keary and Brooks, 1991). To perform the structural and stratigraphic interpretation you need to have a prior information as well as the well data of the research area (Telford et al, 1976)
- Although no structure has been marked on the seismic section because the 3D data that was provided to me only contains information below the crest of the Balkassar Anticline.
- The 3D seismic data used in this dissertation was stratigraphically interpreted using well data to mark horizons of the reservoirs of Chorgali and Sakessar limestone in the study area. Time and depth contour mapping of the Chorgali and Sakessar formation indicated that there was sufficient uplifting in the strata at the top of the Balkassar anticline because the research area is in the compressional regime. According to our map, the South-Eastern portion of the base map depicts a high topography region, whereas the north-western portion shows a low topographic zone. The well where Balkassar OXY-1 was dug is located in a low topographic area, according to the time and depth map.
- The fundamental method for calculating reservoir rocks properties at the well location is provided by petrophysics. Petrophysics relates the reservoir's fluid characteristics and matrix properties. Petrophysical analysis can be used to locate hydrocarbon-bearing zones. Well logs contain a lot of information about the reservoir and hence they are most useful tool for reservoir characterization (Cosgrove, J. W. et al., 1998).
- In order to determine the Hydrocarbon bearing zone and calculate the total and effective porosity of Eocene carbonate the OXY-1 well is now being used. Petrophysical analysis suggested that the OXY-1 well has no favorable zone in Eocene carbonates (Chorgali and Sakessar) for hydrocarbons accumulation and that the little zone of 3 meters between 2424 and 2427 meters of depth in the Chorgali formation has excellent porosity and Hydrocarbon saturation but this is very small zone which may not provide you enough Hydrocarbon and this small zone have total porosity of 27%, effective porosity 25% and contain 44% Hydrocarbon saturation and 56% water

saturation. However, the overall Hydrocarbon saturation and other petrophysical properties in Chorgali is quite low that is 12% total porosity, 9% effective porosity, 88% water saturation and 12% hydrocarbon saturation.

- Porosity, water saturation, and hydrocarbon saturation are all examined using a petrophysical interpretation of the Sakessar formation, but no favorable zones for hydrocarbon accumulation are identified because the calculated porosity is only 2%, the water saturation is 86%, and the hydrocarbon saturation is 14%. Due to the limitations of the data, no additional well's petrophysical analysis has been done.
- Fracture corridors are tabular areas with notably high fracture intensity or clusters of fractures that are closely spaced (usually joints, sheared joints, or veins) (Peacock et al., 2016), are common structural objects. More than 60% oil reserve of the world lie in the naturally fractured reservoir of carbonates rocks (Akbar et al., 2000) so the importance of fractures in carbonate rocks cannot be ignored because the presence of fractures in carbonate rocks is the primary cause of the secondary porosity. Applying attributes to identify fractures was therefore crucial. In carbonate rocks, the two most important effective reservoir parameters are fracture density and fracture orientation. The production from the fractured carbonate reservoir may be optimize with sufficient knowledge of these two parameters.
- The fracture attributes were applied to a Sakessar and Chorgali horizon to check the fractures density and orientation, The results of the attributes applied to a Chorgali level suggested that there is very low density at Chorgali level where the OXY-1 well is drilled and have high density towards the southeast of the OXY 1. The attributes were also applied to a Sakessar level to check the fracture density and orientation. Very low density of fracture was noted in Sakessar formation. The result derived from the attributes applied to a Chorgali and Sakessar level are in good agreement with the results derived from the petrophysical analysis performed at Chorgali and Sakessar level.
- A tool nowadays used for the extraction of rock's properties from the seismic data is the seismic inversion (Krebs et al., 2009). Seismic post stack inversion is the crucial technique used in exploration and production industries. In this technique the seismic poststack 3D data is converted into acoustic impedance volume to extract the important reservoir properties and to enhance the seismic resolution for better visualization of the subsurface.

- Two famous methods used to accomplish this research are Model-based and Sparse-spike inversion. further, the results of the two methods were compared. This two-inversion method were applied to a Chorgali and Sakessar level which suggested that there is very high impedance at Sakessar level as compared to Chorgali formation. The acoustic impedance is derived from both the Model-based and Sparse-spike inversion which confirm that the results of Model-based is far clearer than the result derived from the sparse spik inversion.
- The well where OXY-1 is drilled shows high impedance value at both Chorgali and Sakessar level which confirm that it was not the best place for digging well at this location. There is another zone on the same seismic inline 90 but cross line 266 to the southwest of the OXY-1 where there is very low impedance which can be clearly seen on both the Sparse-spike and Model-based p-impedance section. But it will be more clearly visualized on the Model-based acoustic impedance section than the Sparse-spike acoustic impedance section which confirm that Model-based is more reliable and have more realistic results than the Sparse-spike inversion method.
- The spatial distribution of porosity was essential for examining the porosity at a sparse well location to a complete seismic cube. In this research work firstly, I derived porosity from the borehole data then this derived porosity is integrated with seismic to see the spatial distribution of porosity at the whole seismic cube. The cross plots of porosities further enhanced my knowledge about the relation between reservoir actual porosities and the seismic predicted porosities by developing geostatistical relationship. The geostatistical approach is used to derives a surface by applying the values which are calculated from the specific location to assess the data points for each location between the data points (Ali et al., 2019).
- Slices were made for the representation of spatial distribution of porosity at the Chorgali and Sakessar levels which confirmed that there is a zone having high porosity very near to the OXY-1 well in the direction SW on the same inline 90 and cross line 266 and is the best place for drilling well at this location. So, the OXY-1 well's proposed placement i.e., cross line 284 was not viable, but crossline 266 on the same inline 90 was hypothesised to have a good total and effective porosity.

REFERENCES

- Ali, Aamir, Tiago M. Alves, Farhad Aslam Saad, Matee Ullah, Muhammad Toqeer, and Matloob Hussain. "Resource potential of gas reservoirs in South Pakistan and adjacent Indian subcontinent revealed by post-stack inversion techniques." Journal of Natural Gas Science and Engineering 49 (2018): 41-55.
- Ali, Aamir, Muhammad Younas, Matee Ullah, Matloob Hussain, Muhammad Toqeer, Asher Samuel Bhatti, and Azhar Khan. "Characterization of secondary reservoir potential via seismic inversion and attribute analysis: A case study." Journal of Petroleum Science and Engineering 178 (2019): 272-293.
- Toqeer, Muhammad, Aamir Ali, Tiago M. Alves, Ashar Khan, and Matloob Hussain. "Application of Model-based post-stack inversion in the characterization of reservoir sands containing porous, tight and mixed facies: A case study from the Central Indus Basin, Pakistan." Journal of Earth System Science 130, no. 2 (2021): 1-21.
- Shakir, Urooj, Aamir Ali, Muyyassar Hussain, Tahir Azeem, and Lamuail Bashir. "Selection of sensitive post-stack and pre-stack seismic inversion attributes for improved characterization of thin gas-bearing sands." Pure and Applied Geophysics 179, no. 1 (2022): 169-196.
- Maurya, S. P., N. P. Singh, and Kumar Hemant Singh. Seismic inversion methods: a practical approach. Berlin/Heidelberg, Germany: Springer, 2020.
- Pendrel, John. "Seismic inversion–still the best tool for reservoir characterization." CSEG Recorder 31, no. 1 (2006): 5-12.
- Kumar, Rajan, Baisakhi Das, Rima Chatterjee, and Kalachand Sain. "A methodology of porosity estimation from inversion of post-stack seismic data." Journal of Natural Gas Science and Engineering 28 (2016): 356-364.
- Russell, Brian H. Introduction to seismic inversion methods. No. 2. SEG Books, 1988.
- Erryansyah, M., T. B. Nainggolan, and H. M. Manik. "Acoustic impedance Model-based inversion to identify target reservoir: a case study Nias Waters." In IOP Conference Series: Earth and Environmental Science, vol. 429, no. 1, p. 012033. IOP Publishing, 2020.
- Alvarez, P., and B. Gebus. "Mapping Porosity in a Carbonate Reservoir Using Seismic Inversion and Integration of the Result into a Geocelullar Model." In 73rd EAGE

Conference and Exhibition incorporating SPE EUROPEC 2011, pp. cp-238. European Association of Geoscientists & Engineers, 2011.

- Prananda, Avishena, Mohammad Syamsu Rosid, and Robet Wahyu Widodo. "Pore Type and Porosity Distribution of Carbonate Reservoir Based on 3D Seismic Inversion in "P" Field Salawati Basin." In E3S Web of Conferences, vol. 125, p. 15002. EDP Sciences, 2019.
- Zemke, Kornelia, Axel Liebscher, and Maren Wandrey. "Petrophysical analysis to investigate the effects of carbon dioxide storage in a subsurface saline aquifer at Ketzin, Germany (CO2SINK)." International Journal of Greenhouse Gas Control 4, no. 6 (2010): 990-999.
- Datta Gupta, Saurabh, Sugata Kumar Sinha, and Raman Chahal. "Capture the variation of acoustic impedance property in the Jaisalmer Formation due to structural deformation based on post-stack seismic inversion study: a case study from Jaisalmer sub-basin, India." Journal of Petroleum Exploration and Production Technology (2022): 1-25.
- Abraham, Aidoo Borsah, Annan Boah Evans, and Brantson Eric Thompson. "Analysis of spatial distribution pattern of reservoir petrophysical properties for horizontal well performance evaluation-a case study of reservoir X." The Open Petroleum Engineering Journal 12, no. 1 (2019).
- Chopra, Satinder, and K. J. Marfurt. "Interpreting fractures through 3D seismic discontinuity attributes and their visualization." CSEG Recorder 34, no. 8 (2009): 5-14.
- Hossain, Shakhawat. "Application of seismic attribute analysis in fluvial seismic geomorphology." Journal of Petroleum Exploration and Production Technology 10, no. 3 (2020): 1009-1019.
- de Joussineau, Ghislain, and Jean-Pierre Petit. "Mechanical insights into the development of fracture corridors in layered rocks." Journal of Structural Geology 144 (2021): 104278.
- Hamidi, Rosita, Yasir Bashir, Deva Prasad Ghosh, Saeed Akhtar, and Manan Iqbal Sheikh. "Application of multi attributes for feasibility study of fractures and structural anomalies in Malaysian basin." International Journal of Engineering & Technology 7, no. 3.32 (2018): 84-87.
- Chopra, Satinder, and Kurt J. Marfurt. "Integration of coherence and volumetric curvature images." The Leading Edge 29, no. 9 (2010): 1092-1107.

- Kington, Joe. "Semblance, coherence, and other discontinuity attributes." The Leading Edge 34, no. 12 (2015): 1510-1512.
- Masood, Farhana, Zulfiqar Ahmad, and Muhammad Sohail Khan. "Moderate Interpretation with Attribute Analysis and 3d Visualization for Deeper Prospects of Balkassar Field, Central Potwar, Upper Indus Basin, Pakistan." International Journal of Geosciences 8, no. 05 (2017): 678.
- Shah, Syed Bilawal Ali, and Wan Hasiah Abdullah. "Structural interpretation and hydrocarbon potential of Balkassar oil field, eastern Potwar, Pakistan, using seismic 2D data and petrophysical analysis." Journal of the Geological Society of India 90, no. 3 (2017): 323-328.
- Iqbal, Shahid, Gulraiz Akhter, and Sehrish Bibi. "Structural model of the Balkassar area, Potwar Plateau, Pakistan." International Journal of Earth Sciences 104, no. 8 (2015): 2253-2272.
- Ahsan, Naveed, Muhammad Armghan Faisal, Tariq Mehmood, Nazir Ahmed, Zaffar Iqbal, and Shahid Jameel Sameeni. "3D Modeling of subsurface stratigraphy and structural evolution of Balkassar area, Eastern Potwar, Pakistan." Pakistan Journal of Hydrocarbon Research 22 (2012): 25-40.
- Mahmood, Muhammad Fahad, Urooj Shakir, Muhammad Khubaib Abuzar, Mumtaz Ali Khan, NimatUllah Khattak, Hafiz Shahid Hussain, and Abdul Rehman Tahir. "Probabilistic Neural network approach for porosity prediction in Balkassar area: a case study." Journal of Himalayan Earth Science 50, no. 1 (2017).
- Ashraf, Umar, Peimin Zhu, Aqsa Anees, Ayesha Abbas, and A. Talib. "Analysis of Balkassar area using velocity modeling and interpolation to affirm seismic interpretation, Upper Indus Basin." Geosciences 6, no. 3 (2016): 78-91.
- Shakir, U., M. Abbas, W. Ahmad, M. F. Mahmood, M. Hussain, M. Anwar, U. Sikandar, and T. Naseem. "Hydrocarbon Reservoir Evaluation and Fault Seal Analysis of Balkassar Area, Potwar Sub Basin, Pakistan." The Nucleus 56, no. 3 (2020): 96-104.
- Ushie, F. A. "Formation water resistivity (Rw) determination: the SP method." Journal of Applied Sciences and Environmental Management 5, no. 1 (2001).
- Khan, Umair, Baoyi Zhang, Jiangfeng Du, and Zhengwen Jiang. "3D structural modeling integrated with seismic attribute and petrophysical evaluation for hydrocarbon prospecting at the Dhulian Oilfield, Pakistan." Frontiers of Earth Science 15, no. 3 (2021): 649-675.

- Antonellini, Marco, and Atilla Aydin. "Effect of faulting on fluid flow in porous sandstones: petrophysical properties." AAPG bulletin 78, no. 3 (1994): 355-377.
- Rybach, Ladislaus, and Günter Buntebarth. "Relationships between the petrophysical properties density, seismic velocity, heat generation, and mineralogical constitution." Earth and Planetary Science Letters 57, no. 2 (1982): 367-376.
- Best, A. I., C. McCann, and J. Sothcott. "The relationships between the velocities, attenuations and petrophysical properties of reservoir sedimentary rocks 1." Geophysical Prospecting 42, no. 2 (1994): 151-178.
- Benavente, D., N. Cueto, J. Martínez-Martínez, M. A. García del Cura, and J. C. Cañaveras. "The influence of petrophysical properties on the salt weathering of porous building rocks." Environmental Geology 52, no. 2 (2007): 215-224.